Bruno Miguel Contente Rosa

Licenciado em Ciências de Engenharia Biomédica

A portable electroantennogram recorder for laboratory and field measurements of semiochemicals

Dissertação para obtenção do Grau de Mestre em

Engenharia Biomédica

Orientador: Paulo António Ribeiro, Professor Auxiliar, DF - FCT - Universidade Nova de Lisboa

Co-orientadores: Maria Rosa Paiva, Profª. Catedrática, DCEA FCT - Universidade Nova de Lisboa

Eduardo M. H. Pires Mateus, Investigador CENSE/FCT, DCEA FCT - Universidade Nova de Lisboa

Júri

Presidente: Prof. Doutora Carla Quintão Pereira
Arguente: Doutor José Luís Constantino Ferreira
Vogal: Doutor Paulo António Martins Ferreira Ribeiro

FACULDADE DE CIÊNCIAS E TECNOLOGIA
UNIVERSIDADE NOVA DE LISBOA

Maio, 2016

A portable electroantennogram recorder for laboratory and field measurements of semiochemicals

Este documento foi gerado utilizando o processador (pdf)LaTeX, com base no template "unlthesis" [1] desenvolvido no Dep. Informática da FCT-NOVA [2]. [1] https://github.com/joaomlourenco/unlthesis [2] http://www.di.fct.unl.pt

This page intentionally left blank.

Para a Alice
Que sempre quis ter um neto engenheiro

This page intentionally left blank.

Acknowledgements

I would first like to thank my supervisors Dr. Paulo Ribeiro for his support and guidance throughout this project. I would equally like to thank Dr. Maria Paiva and Dr. Eduardo Mateus for their insightful suggestions, enthusiasm and careful revision of my work. And also for introducing me to such an interesting field of science of which i had no previous knowledge. I would also like to express my sincere gratitude to Sofia Branco for her invaluable support and experience, and by providing me all the conditions and materials to demonstrate the capabilities of this device. The *G. Platensis* results would be impossible to obtain without her help. I would also like to thank Dr. Mário Secca for his support and confidence in me. A collective acknowledgment to all my colleagues at Lusospace for their support, useful remarks, the always fruitful technical discussions. A special acknowledgment to Nuno Franco for his under-pressure *Labview* support. And of course this thesis would not be possible without the support of Ivo Vieira to whom i express my sincere gratitude. I would also like to thank Brian Pisani from Texas Instruments for the support provided with their products. I would like to thank all my friends for their encouragement or indirect help. A special thanks to Sara Cavaco mostly for her friendship but secondly for her careful revision of my work.
Last but certainly not least, I would like to thank my mother Fátima for bearing with me all these years, for her unconditional support and words of encouragement. Not bearing with me for so long, but still as sportive and enthusiastic are my parents in law, Pilar and Eduardo to whom i have no means of expressing my gratitude. So thank you Pilar and Eduardo *Gracias por ser tan lindos como sois*. Lastly, a big, big thank you for my wife Pilar, for her confidence in me and for her love. *Te quiero.*

This page intentionally left blank.

Abstract

Electroantennography is a bioassay technique used to study the olfactory responses of insects. This technique allows for the identification of semiochemicals that mediate insect behavior and reproduction, thus making it one of the key research tools for environmentally friendly pest control methods. It is common practice to interface the insect antennae with micropipette Ag/AgCl electrodes supported on micro-manipulators and to amplify the signals resulting from the perception of the olfactory stimuli, through high gain differential amplifiers. This approach has been routinely used under laboratory conditions, yet the size and nature of the required apparatus and amplification equipment makes it impractical for field measurements. This project explores the use of modern *delta-sigma* analog to digital converters specifically designed for the measurement of biopotential signals, focusing on the miniaturization of the acquisition, processing and digitalization electronics. The design and a prototype of a device with autonomous air pumping, air distribution valve and a dual antenna support are presented, allowing for the simultaneous measurement of the signals of both insect antennae. The proposed antennae holder contains reservoirs for liquid or gel electrolytes and Ag/AgCl electrodes. The support is detachable, allowing easy insertion of excised antennae. 3D printed parts were used for the construction of the mechanical supports and insect antennae holder. The device has an envelope of 123x60.5x46.4 mm and is battery powered. The acquired antennal data is transmitted to a laptop computer via a USB connection. Applications of this device range from the identification of semiochemicals used in pest management programs to bio-sensor development and evaluation. Noise and linearity characterization of the device was performed and the olfactory responses of the eucalyptus weevil, *Gonipterus platensis* (Coleoptera curculionidae) to verbenone were successfully measured. The results obtained are discussed.

Keywords: Electroantennography; Portable EAG; VOC detection; VOC quantification; *Gonipterus platensis*.

This page intentionally left blank.

Resumo

A electroantenografia é uma técnica utilizada para estudo da resposta olfactiva dos insectos quando estimulados por substâncias semioquímicas. A sua utilização permitiu a identificação de semioquímicos que medeiam o comportamento e reprodução dos insectos, tornando-a assim numa das técnicas chave na investigação de métodos biotecnológicos para a monitorização e controlo de pragas, que não dão origem a impactes ambientais. É prática comum usar eléctrodos de Ag/AgCl em micro-pipetas suportados por micro-manipuladores e amplificar o sinal originado pela percepção do estímulo, através de amplificadores diferenciais de alto ganho. Esta metodologia produz resultados positivos em ambiente laboratorial mas o tamanho e natureza dos instrumentos e amplificadores necessários são pouco práticos para medições no exterior. Este projecto explora o uso de conversores analógico digitais *delta-sigma* desenhados especificamente para a medição de biopotenciais, focando-se nos aspectos da miniaturização da electrónica de aquisição e processamento. É apresentado o projecto e um protótipo de um aparelho com bombeamento de ar autónomo, válvula de distribuição de ar, e suporte duplo, permitindo a aquisição simultânea de ambas as antenas do insecto. O suporte de antenas proposto contêm reservatórios para electrólitos líquidos ou em gel, bem como eléctrodos de Ag/AgCl. O suporte é destacável, permitindo a fácil inserção das antenas excisadas. Na construção dos suportes mecânicos e suporte de antenas foram utilizadas peças feitas por impressão 3D. O aparelho tem dimensões globais de 123x60.5x46.4 mm, é alimentado por baterias e tem conexão USB. Este aparelho tem um campo de utilização muito amplo, que vai desde a identificação de semioquímicos, com aplicação em programas de protecção integrada, até ao desenvolvimento e avaliação de biosensores. A caracterização do aparelho em linearidade e ruído é efectuada, e a resposta olfactiva do gorgulho do eucalipto, *Gonipterus platensis* (Coleoptera curculionidae) à verbenona foi medida com sucesso. Os resultados são discutidos.

Palavras-chave: Electroantenografia; EAG portátil; detecção de COV; quantificação de COV; *Gonipterus platensis*.

This page intentionally left blank.

Contents

List of Figures

This page intentionally left blank.

List of Tables

This page intentionally left blank.

Glossary

CMRR Common-mode rejection ratio, is a measure of the ability of a device (a differential amplifier for example) to reject signals that appear simultaneously and in-phase on both inputs..

EPDM EPDM rubber (ethylene propylene diene monomer) is an elastomer used in a wide range of applications, as an example the manufacture of seals and gaskets.

I^2C (Inter-Integrated Circuit), pronounced I-squared-C, is a multi-master, multi-slave, single-ended, serial computer bus. It is typically used for attaching lower-speed peripherals to processors and microcontrollers..

mating disruption Mating disruption is a pest management technique that consists on the release of synthesized sex pheromones with the purpose of confusing the individuals and disrupt mate localization. The goal of this technique is the blocking of the reproductive cycle.

PTFE polytetrafluoroethylene is a synthetic polymer, widely known by its commercial name Teflon by DuPont.

Ringer solution Ringer solution is a solution of salts in water known to be isotonic to living organisms cells. It typically contains NaCl, KCl and NaHCO3, the latter used to balance pH.

RLD Right Leg Drive or Driven Right Leg is an electric feedback circuit used to actively cancel common-mode noise interference in biological signal amplifiers.

STL STL (STereoLithography), is a file format widely used for rapid prototyping, 3D printing and computer aided manufacturing.

This page intentionally left blank.

Acronyms

2EC two electrode configuration.

3EC three electrode configuration.

ADC analog to digital converter.

CENSE Center for environmental and sustainability research.

CFD computational fluid dynamics.

CMR common-mode rejection.

DSP digital signal processor.

EAD electroantennographic detection.

EAG electroantennography.

EEG electroencephalography.

EKG electrocardiography.

EMI electromagnetic interference.

EVM evaluation module.

FCT-UNL Faculdade de Ciências e Tecnologia - Universidade Nova de Lisboa.

FFT fast Fourier transform.

FID flame ionization detector.

GC gas chromatographer.

GC-EAD coupled gas chromatography - electroantennographic detection.

GPIO general-purpose input/output.

HID human interface device.

IC integrated circuit.

IPM integrated pest management.

MCU micro-controller unit.

OBPs odorant binding proteins.

ODP oviposition deterring pheromones.

ORNs olfactory receptor neurons.

ORs odorant receptors.

PCB printed circuit board.

PGA programmable gain amplifier.

PSU power supply unit.

PWM pulse width modulation.

SLA stereo-lithography.

SNR signal to noise ratio.

SPI serial peripheral interface.

sps samples per second.

USART universal synchronous asynchronous receiver transmitter.

USB universal serial bus.

UV ultraviolet.

VOCs volatile organic compounds.

Chapter 1

Introduction

Electroantennography is a bioassay technique used to study the olfactory responses of insects. This electrophysiological technique was initially developed in the 1950's and measures the electrical response of the antennae nerve cells that will be transmitted to the insect central nervous system. This technique allows for the identification of semiochemicals that mediate insect behavior and reproduction, thus making it one of the key research tools for environmentally friendly methods for pest control. It is common practice to interface the insect antennae with micropipette Ag/AgCl electrodes supported on micro-manipulators and to amplify the signals through high gain differential amplifiers. This approach has been proven to work well in the laboratory environment but the size and nature of the required apparatus and amplification equipment makes it impractical for field measurements. This project explores the use of modern *delta-sigma* analog to digital converters specifically designed for the measurement of biopotential signals, focusing on the miniaturization of the acquisition, processing and digitalization electronics, and the insect antennae interface. A dual antenna support is proposed, allowing the measurement of both insect antennae signals simultaneously to improve noise performance. The proposed antennae holder contains reservoirs for Ringer solution and Ag/AgCl electrodes. The use of conductive gel as electrolyte media was also evaluated. SLA printed parts were used whenever possible, namely for the mechanical supports and insect antennae holder. The device is battery powered and communicates through a USB connection to a laptop computer. The hand-held nature of the unit will allow researchers to perform *in situ* measurements of the insect responses which can be of particular interest in bio-sensor development, narcotic, explosives or disease detection. The complete development of this unit was initially thought possible within the available time frame. A time frame which proved to be too short given the challenges and multitude of fields involved in the design of such

an equipment (electronics, mechanical, firmware and software). Nevertheless a working prototype with representative electronics and acquisition software was developed. Laboratory tests were conducted to evaluate the performance of the prototype unit with an antenna simulator and with live insect antennae and the results are discussed.

1.1 Motivation

In Portugal eucalyptus is a culture with strong economic relevance, occupying 812 000 ha, that is the largest area of forest plantations (ICNF 2013). It is the major wood source for the pulp and paper industry. The introduction of the eucalyptus weevil *Gonipterus platensis* in the Iberian Peninsula seriously affected the wood production expectations for the near future (Reis et al. 2012). The method used to control the expansion of *G. platensis* is the seasonal release of the egg-parasitic wasp *Anaphes nitens*. However only limited results are achieved with this method in areas located above 400m of altitude, where most of the plantations in central and northern Portugal are located. The failure has been attributed to a mismatch between the origin of *G.platensis*, which comes from Tasmania and of the parasitoid, native from a warmer region in mainland Australia. The inefficient parasitism observed at higher altitudes indicates the urgent need to conduct research on alternative control methods (Reis et al. 2012). In 2012 another insect pest of the eucalyptus, the bronze bug *Thaumastocoris peregrinus*, which is also native from Australia was reported in Lisbon. *T. peregrinus* exhibits a strong aggregation behavior followed by dispersion when disturbed, an indication suggesting the release of an alarm pheromone Garcia et al. 2013. If confirmed, this fact could be exploited as a means of control.

The growing demand for the development of trapping methods based on the use of pheromones, attractants and repellents, for the control and monitoring of insect populations led to the development of portable EAG recorders as an attempt to provide an easy method of monitoring pheromone concentrations in the air (Van Der Pers and Minks 1998). The results achieved and ease of use of these devices evidenced a potential interest for this type of portable equipment even though better methodologies for the standardization of the measurements need to be developed. Electroantennography can be used both in the laboratory and in the field and is one of the simplest and cheapest research tools for measuring Volatile organic compounds (VOCs) in the air. Portable and easy to use devices thus constitute valuable tools to decode insect olfaction.

1.2 Objectives

The main goal of this project is the development and testing of a portable EAG recording apparatus. The device should be small in size and with a low production cost. The device should also be able to record to a computer the acquired data to allow further analysis. The quality of the acquired signal must be as good or better as commercially available

equipment. A compact and easy to use design is also desirable to allow easy insertion of the excised antennae without any special manipulating devices. This last objective is of special importance if the device is used in the field. A prototype will be designed, manufactured and tested. The performance of the recorder will be evaluated with signals simulating an insect antenna and with real antennal responses of an insect.

1.3 Related Work

The proposed portable EAG recorder is based on the work of Sauer et al. (1992) and Van Der Pers and Minks (1998). Sauer et al. (1992) presents a portable EAG apparatus for field measurement of synthetic pheromone release. The goal of the research was to evaluate the concentration, dispersion and propagation of artificial pheromones released in orchards treated with the mating disruption technique. A more refined approach was presented by Van der Pers and Minks (1998), who developed a more complete portable solution to achieve the same goal. This device is a truly portable apparatus with built in power source, autonomous air pump, and control and amplification electronics. Both devices will be further critically analyzed in section 2.4.2.

1.4 Structure of the report

This report is divided in to six chapters. The first chapter is an introduction to the theme of the project, the motivation behind the development of this equipment and the objectives initially set. The second chapter presents some background on the state of the art of the electroantennographic technique. The chapter also includes a small historical review focused on the major landmarks and breakthroughs. The following sub chapters detail some of the technical aspects of the electroantennographic technique itself and how it can be coupled to gas chromatography for the identification of bioactive VOCs. In order to better introduce the reader to the subject of this project, a brief overview on insect olfaction was also added, as well as applications of semiochemical methods of insect control in agriculture and silviculture. Chapter three details the design of the EAG recorder. The chapter includes the development methodology, the requirement gathering process and the testing and verification logic. The requirements are further analyzed and the decision processes involved in the design choices are further detailed. Chapter four describes the construction of a prototype of the EAG recorder along with the initial implementation of the final electronics. In chapter five the testing of the equipment is described, how the tests were conducted and the obtained results. These results are discussed in chapter six along with a final conclusion, lessons learned and future recommendations.

This page intentionally left blank.

CHAPTER 2

BACKGROUND

2.1 Introduction

Insect evolution has led to the development of specific organs for the detection of VOCs. These organs, located mainly in the insect's antennae have a wide variety of roles that go from communication to navigation and search for food sources (Hansson 1999). The production of communication volatiles by the insect is an energy-demanding process and therefore very small quantities are released. As a result, some of the sensory cells evolved to have the capability to detect these chemicals with high specificity and in very small concentrations (Schott et al. 2013). The discovery that insects could detect and respond to odors that modified their behavior not only allowed for the monitoring and control of insect populations using VOCs, but also opened the door to a range of biosensor applications (Myrick et al. 2008). The present technological applications of such biosensors already go from the detection of explosives,drugs, or diseases, to the detection of specific odors or taints in the food or wine industry (Baigrie 2003), yet their full potential remains to be explored.

2.2 An historical perspective

Published work on the topic of applied entomology was scarce up to the late 1800's. A major landmark for a turnaround were the economic losses in Europe due to the *Phylloxera* epidemic (Sarton 1931). In the 1870's the French entomologist Jean-Henri Fabre observed that a female great peacock moth enclosed in a jar, covered with a wire-gauze cloth attracted to his lab-study dozens of male peacock moth's. The male's ability to find the exact location of the female in the jar led him to investigate the means by which these insects find their counterpart. He conducted a series of experiments and concluded that

even if undetectable to the human nose, the female moth must release a potent odor that attracts the opposite sex (Fabre 1916). At the same time in the United States entomologist Joseph A. Lintner foresaw that the de-codification of these chemicals would allow the control of insect pests (Patlak et al. 2003). It was only in 1959 that Adolf Butenandt successfully isolated a silk moth's pheromone *bombykol*.

In 1957 Shneider pioneered the use of an insect antenna as an odor detector. Using electrophysiological techniques, he placed the antenna of a male silkworm *Bombix mori* on a pair of electrodes and amplified the signal to an oscilloscope. He expected to measure a depolarization of the receptor cells in the same way nerve cells depolarize. Upon stimulation with an extract obtained from a female lure gland puffed in a stream of air towards the antenna, he measured on the oscilloscope a rapid depolarization of the membrane of the sensory cells, followed by an exponential decay. He had successfully recorded the first "Electroantennogram" (Schneider 1999).

In 1969 J. E. Moorhouse and colleagues combined the electroantennogram with a gas chromatographer (Moorhouse 1969), and In 1975 Arn, Staedler and Rausher coined the technique "Electroantennographic detection (EAD)". The technique became the gold standard in identifying bioactive substances, allowing for the identification of a pheromone within days instead of years (Arn et al. 1975, Schneider 1999). It consists on evaluating the power of EAG responses to an extract of a pheromone gland exiting a Gas chromatographer (GC) column and correlating EAG peak responses to GC peaks (Arn et al. 1975). More details on this technique will be given on section 2.4.1.

2.3 Insect olfaction

Besides the capability of sensing tactile, visual and auditive stimuli, insects also use chemical signals for communication within the same species and with different species. Insects developed the ability to detect or respond to remarkably small concentrations of these substances. These chemicals are known as semiochemicals. Semiochemicals can be further subdivided in to pheromones and allelochemicals (Whittaker and Feeny 1971). The intraspecific chemical communication takes place via the release of volatile information-carrying "scent" chemicals, called pheromones. These semiochemicals can be further classified into several types depending on their function. Sexual pheromones are produced by one of the sexes, with the purpose of attracting individuals of the opposite sex for mating. A good example of this type of pheromone is the sexual pheromone of the silk moth *Bombykol*, mentioned in the previous section. Aggregation pheromones, which are also generally released by one of the sexes to attract both of them. Aggregation strategies are mostly used to overcome host resistance, by promoting a mass attack, yet these pheromones also play a role regarding defense against predators, as well as a mating role (Howse et al. 1998). Trail pheromones are produced by ants and termites, among other insects and form a chemical trail that can be followed by other individuals of the same species (Matsumura et al. 1968). Alarm pheromones have the

function of alerting other members of the species to the presence of a threat. In termites for example, the alarm reaction is characterized by rapid walking of activated termites and efforts to alert and activate other members of the group (Šobotník et al. 2008). Allelochemicals on the other hand act between different species and consist of four main groups: allomones, kairomones, synomones and apneumones (Nordlund and Lewis 1976, Brown et al. 1970). Allomones are chemical signals that give advantage to the emitting species (e.g. odorants repellent to other species) and kairomones give advantage to the receiving species (e.g. odorants that can be detected by a predator). Synomones are chemical signals that benefit both species. An example being floral scents, that benefit the insect by indicating a food source, and benefit the plant by ensuring pollination (Howse et al. 1998). Apneumones are defined as substances emitted from nonliving materials that evoke a behavioral or physiological reaction adaptively favorable to a receiving organism, but detrimental to an organism of another species, that may be found in or on the nonliving material (Nordlund and Lewis 1976). This nomenclature is context dependent i.e. a pheromone for one species can be a kairomone for a predator species. Even the characterization as sexual, alarm, etc. can be limiting in the sense that a pheromone is usually multi-component and can trigger a multitude of behaviors depending on the "blend". In other words, depending on the odorant elements relative concentrations, and other conditions, an alarm pheromone of a social insect can trigger different types of behavior, such as searching, approach, recruitment, alerting, attack or repellence (Howse et al. 1998).

2.3.1 Antennae and the ORNs

Although the decoding of chemical stimuli is processed by the central nervous system of the insect, the olfactory receptor neurons (ORNs) limit what exactly can be detected. The ORNs are therefore the sensory elements. The scope and accuracy of their sensing capability is limited by the number of sensors and their tuning to different chemicals (Bruyne and Baker 2008). Insect ORNs are not randomly distributed, they are housed in specific morphological units called olfactory sensilla. The olfactory sensilla have different shapes, appearing as long or short hairs, plates, pegs or cavities (Mucignat-Caretta 2014). Odor molecules penetrate the sensilla through pores of the cuticular wall. Insect ORNs are bipolar neurons that develop from epithelial cells. The dendrites of these cells extend into the lumen of the sensilla, and the axons project into the primary olfactory processing centers of the insect central nervous system (Keil 1997, see figure 3.8 B)). Olfactory sensilla are located primarily in the insect antennae, in quantities that can totalize several tens of thousands of ORNs. Olfactory sensilla can also be found in other body locations, such as the labial and maxillary palps, with various odor specificities depending on the insect orders (Mucignat-Caretta 2014). It is here that odorant binding proteins (OBPs) attach to the volatiles rendering them soluble and protecting them from odorant-degrading enzymes. OBPs carrying a volatile can either

bind to the membrane odorant receptors (ORs) or release the volatile so that it can bind to the receptor directly (Rützler and Zwiebel 2005). The ultimate result of this process is the opening of the ion channels or ion-channel-like chaperones. The number of open ion channels will depend on the amounts of odorant present, and if enough ion channels open simultaneously an action potential is sent along the dendrite, to the insect central nervous system (Schott et al. 2013). The next step in the chain of events is the release of the volatile to be degraded by a specific odorant-degrading enzyme. Degradation prevents the same volatile from re-triggering the neurons.

2.3.2 Intensity coding

ORNs are capable of coding the concentration of stimulus molecules into frequency of nerve pulses. This encoding covers a wide range of stimuli concentrations. The dose/response relationship is typically a sigmoid curve. Above a certain threshold ORNs firing frequency increases linearly as the log of the concentration, until it reaches a plateau (Mucignat-Caretta 2014). The frequency encoding however is a mix between specificity and intensity. These two figures are in fact interdependent, when stimuli intensity increases, chemical specificity decreases. High concentrations of an inefficient compound can produce the same ORNs firing activity as a low concentration highlly efficient compound (Mucignat-Caretta 2014).

2.3.3 Semiochemicals in agriculture and silviculture

The knowledge gathered from the identification of insect pheromones used for reproduction or other functions have been used for over 50 years to monitor and control pests (Cardé 1995). Several methods such as pheromone traps and plantation wide pheromone release to induce mating disruption are used with success (Ioriatti and Angeli 2002, Howell et al. 1992). Mating disruption relies on the use of sex pheromones to impair the male insects capability of finding females and mating. The method was implemented for the first time for the management of the Codling moth pest (*Cydia pomonella*), one of the main fruit-damaging insects in apple orchards (Damos et al. 2015). Chemical cues originated by conspecific insects can also affect the choice of oviposition site. These pheromones can have a stimulant effect or a deterrent effect, and are produced by the female or by conspecific larvae. Oviposition deterring pheromones can also influence behavior on competitor species, working as allomones to deter competitors (Pasteels and Daloze 2002). The use of oviposition deterring pheromones are also of special interest for pest control. For example, soon after the discovery of an oviposition deterring pheromones (ODP) of the tephritid fly *Rhagoletis cerasi* a collected sample was applied in the field with a 63 to 77% reduction in the infestation (Katsoyannos and Boller 1976). Sex pheromones can be used to control insects by interfering with mating, but are also a valuable tool for the monitoring of insect population numbers. A good example is the monitoring of the pine processionary moth (*Thaumetopoea pityocampa*) a

pest that frequently causes public health problems (Paiva et al. 2011). Pheromone baited trap catches correlate consistently with the number of *T. pityocampa* winter nests per hectare, however catch counts depend on pheromone concentration, trap maintenance and positioning. Standardization of these factors is mandatory in order to reliably use this methodology as part of an integrated pest management (IPM) (Jactel et al. 2006).

2.4 The electroantennographic technique

An electroantennogram measures the overall nerve response of all the odorant sensitive sensilla. The signal is acquired between the base and the tip of the antenna, while the antenna is being stimulated (Nagai 1981). The resultant signal typically consists of a temporary sharp depolarization followed by an exponential recovery (Cork et al. 1990). The measurement of this signal can either be made from live insects, or from freshly excised antennae (Beck et al. 2012). Even multiple antennae can be used to increase SNR (Park and Baker 2002). However, measurements performed using live insects can show responses from mechanoreceptor sensilla, due to movement, and therefore require restraining of the insect (Beck et al. 2012). In order to measure signals from live insects, the recording electrode is inserted through the tip of the antennae and the reference electrode placed either on the insect eye or head (Beck et al. 2012).

The contact between the electrode and the antenna is usually guaranteed by glass micro-pipette electrodes. The electrode is either made of a thin tungsten (D.S. et al. 1994) or Ag/AgCl wire (SYNTECH 2004) and a saline solution. Bare metal electrodes are not recommended because of the noise introduced by the electro-chemical potential developed (SYNTECH 2004). Ag/AgCl electrodes are the most commonly used electrode type because of their low electrochemical potential and the fact that they are non polarizable (SYNTECH 2004). The micro-pipettes are drawn to a fine point and then cut to an inner diameter wide enough to enable insertion of the excised antenna tip. Prior to the insertion of the antenna, the micro-pipettes are filled with a saline solution that can either be 0.1M KCl, 0.9% NaCl or Ringer solution. The micro-pipettes are assembled on micro-manipulators and the antenna tips are inserted. To facilitate the insertion process the operation is usually accomplished using a stereo microscope. The electrode wire can then be inserted into the micro-pippete and connected to the amplification system. The amplification systems are differential, and gain factors of 10 to 100 are normally used (Dickens 1984). Other alternative methods of antennae connection are also possible and are illustrated in figure 2.1.

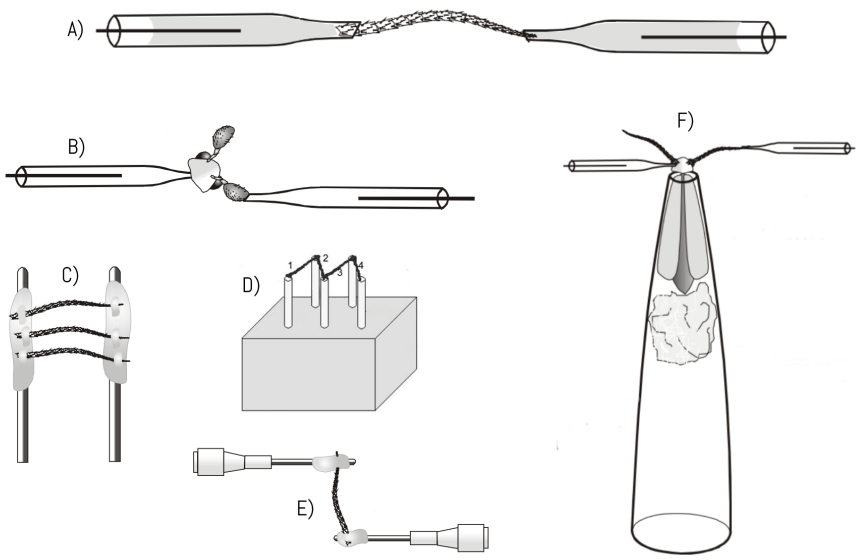

Figure 2.1: Antennae mounting methods for EAG recording. A) Excised antennae between two electrode micro-pipettes. B) Entire head mounting example, used for club-shaped antennae. C) Parallel mounting of antennae with electrode gel. D) Serial mounting of antennae to improve SNR. E) Mounting of antennae with electrode gel. F) Live insect antennal preparation. The insect is tethered inside a disposable plastic pipette. The bottom end of the pipette is closed with a cotton plug. A),B),C),F) images adapted from (SYNTECH 2004), image D) adapted from (Park and Baker 2002).

VOCs stimulus sources are generally prepared containing amounts of the test compound in decadic steps. The compounds can either be diluted in hexane or paraffin oil depending on their nature, and are applied to a piece of filter paper. The filter paper is inserted into a glass pipette or syringe, and puffs of the sample are mixed into a humidified stream of air. The odor is presented to the antenna through a stimulus delivery tube (SYNTECH 2004). The stimulus tube facilitates gentle stimulation in order to limit the triggering of mechanoreceptors and consequent noise. The air flow should be cleaned through a suitable air filter, or alternatively canned clean sources can be used (Bouwer 2010). Upon stimulation the tip of the antenna becomes negative with respect to the base, and the amplitude of this temporary depolarization can range from a few microvolts to several milivolts. The responses obtained can vary, depending on the insect species, mainly because of the antennae morphology. The sensitivity of the antennae to VOCs can be localized to a specific area of the antenna, and in the case of weevils (Coleoptera) the most sensitive area is located in the clava (Nagai 1981). However, other aspects can influence antennal response, or overall quality of the signal, namely:

- The nature of the stimulus
- The concentration of the stimulus
- The condition of the antenna

- The life-time of the preparation
- The number and strength of the previous stimulations
- The quality of the amplifier input
- Temperature and humidity

When measurements are performed using excised antennae, a decline in antennal sensitivity is observed due to drying. This decline is a downside of using excised antennae and makes the comparison of results more difficult between different recording sessions (Bouwer 2010). Normalization of acquisitions to a known response can be used to account for this effect (Bouwer 2010, White 1991). A recovery period between stimuli must also be observed, otherwise subsequent responses can be reduced due to a saturation effect. This period can range from 1 to 4 minutes (Bouwer 2010).

2.4.1 Coupled GC-EAG technique

The coupling of gas chromatography with electroantennography is known as "Coupled gas chromatography - electroantennographic detection (GC-EAD)". GC-EAD is a technique used to identify semiochemicals. In GC an inert carrier gas is used to "carry" the sample along a glass or metal tubing, the column. The inner walls of the GC are covered with a microscopic inert layer called the "stationary phase", with which the volatile compounds under analysis interact, separating in distance as they travel along the column, and thus eluting at different times. A detector at the end of the column detects the arrival of the separated components. Many types of detectors are available, the most commonly used in the identification of semiochemicals is the Flame ionization detector (FID). The time it takes for a specific compound to elute is called the retention time. The GC-EAD technique consists in collecting GC effluent, which is then vented over an antennal preparation. By synchronizing the response of the GC FID peaks (or other types of detector) with the electroantennogram and by measuring the retention times it is possible to determine the exact nature of the compounds eliciting an olfactory response.

2.4.2 Portable EAG equipment

The efficiency of mating disruption is affected by the initial insect population numbers, orchard isolation, temperature regimes and lure placement strategy (Cardé 1995), therefore a means for measuring the actual pheromone concentrations is highly desirable. A portable EAG recorder was developed for this purpose by U.T. Koch and co-workers in the 1990's and successfully measured concentration gradients and spatial distributions in vineyards (Sauer et al. 1992) and apple orchards (Suckling et al. 1994). A schematic view of the apparatus is presented in figure 2.2. This device presents some interesting features and ideas towards a portable EAG recorder solution, namely the use

of a separate antenna holder with two wells for the contact electrolyte, isolation of the insect's antenna from external air, the use of a charcoal filter to prevent undesired stimuli and the use of a suction pump instead of blowing air to the antenna. However, although having a usable design the equipment lacked compactness and required external electronics for signal acquisition. Another point worth mentioning is the lack of electromagnetic interference (EMI) shielding on the glass chamber.

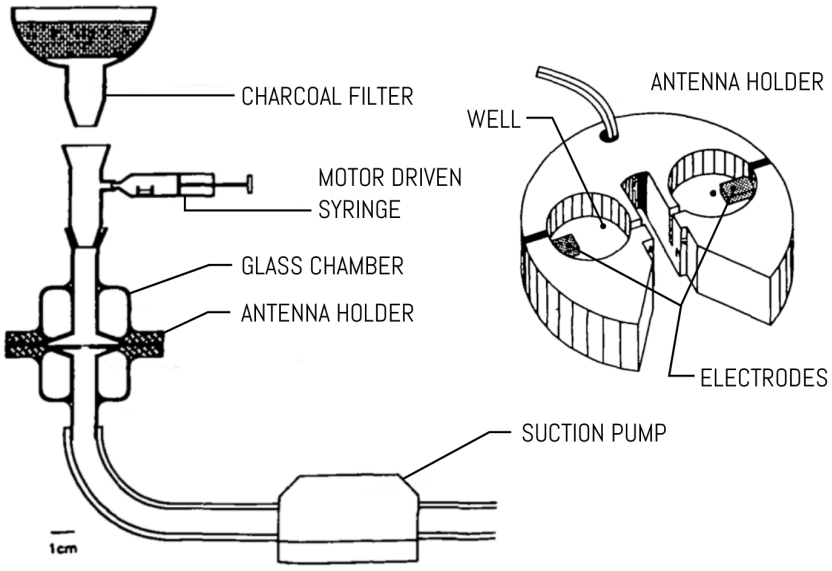

Figure 2.2: Schematic view of Sauer et al. 1992 portable EAG recording apparatus. Image adapted from (Sauer et al. 1992)

A commercial device was developed by Van der Pers (Van Der Pers and Minks 1998, see figure 2.3) also for the purpose of monitoring airborne pheromone concentrations in greenhouses practicing mating disruption methods of pest control. The equipment records responses from a single antenna and has a built in 3 way valve system to present the antenna with clean, reference and external air samples as a calibration method. The antenna holder follows the same principle idea of Sauer et. al. (1992), consisting of a PTFE interchangeable disk with reservoirs for the conductive electrolyte. The recorder amplifier has a selectable gain from x10 to x1000. The sampled data is recorded as a frequency modulated signal to an external audio tape recorder. The 1998 design has been updated to a new device by Syntech in the Netherlands, which seems to be the only portable EAG recording equipment commercially available. It is commercialized under the name of *PortEAG3* and includes new features not seen on the 1998 unit, namelly: an LCD screen to display recorded data in real-time, amplification gain from 50x to 1000X and a Universal serial bus (USB) data connection. It is powered by a lead-acid 12V 2.0Ah battery. The user manual for this device is available at Syntech website.

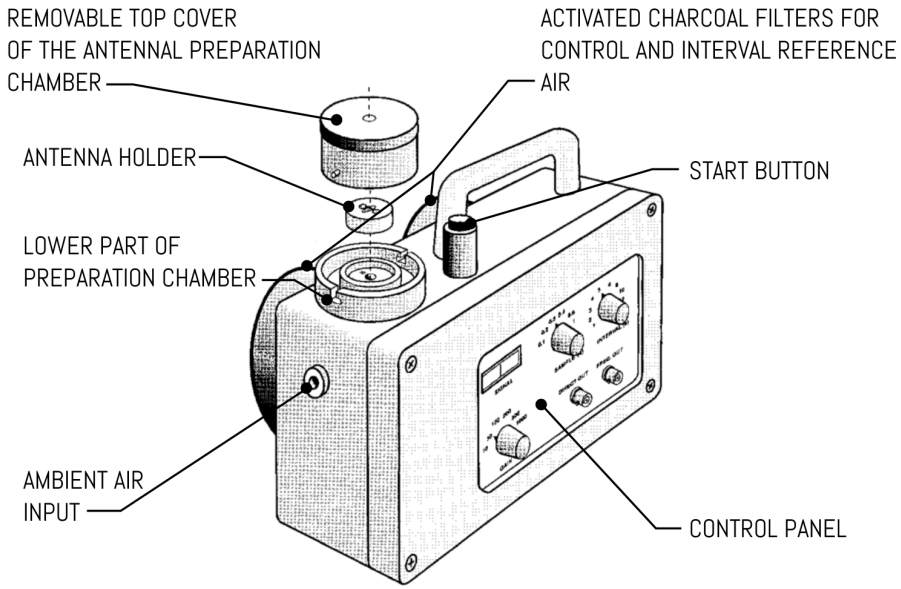

Figure 2.3: Schematic view of Van der Pers and Minks (1998) portable EAG recording apparatus. Image adapted from Van der Pers and Minks (1998).

This page intentionally left blank.

CHAPTER 3

DESIGN

3.1 Introduction

The task of creating an equipment of valuable practical use is an iterative process which spans through several areas of knowledge. These areas span from biology to mechanics, electronics and software. All of these fields come together in a final design, by providing a technical solution to the problem. This chapter will detail the process followed in the development of the EAG recorder. The chapter begins with a brief description of the methodology used, followed by the requirements specification and analysis. The verification philosophy is then presented, detailing the methods to evaluate the requirements. An overview of the chosen architecture is then summarized. The remaining of the chapter explains all the technical aspects, the challenges, and the solutions encountered.

3.2 Development methodology

The development methodology followed in the course of this project can be divided into five major blocks. The project began with an initial assessment phase. During this phase, the problem statement was refined to a set of functional and technical requirements and an early conceptual design was created. These early concepts were further detailed during the design phase. There was a strong design intent to re-use and adapt components in order to minimize the need for machining operations. With this idea in mind, a great deal of the design effort was dedicated to the search of off-the-shelf components that could fulfill the design intent, even if these components were originally designed for other purposes. An iterative approach was used in order to capture all the requirements defined in the previous phase. The outcomes of this phase were, a 3D model of the system

with all the required manufacturing data, a list of components to be acquired and a first draft of the electronics. During the late part of the design, when the definition of the major blocks of the electronics was concluded, demonstration cards for the most relevant electronic elements were acquired. These demonstration cards along with the designed or adapted remaining components formed the EAG recorder prototype. The prototype was built to represent the final design in form and function, as close as possible. The use and testing of the prototype proved that some adjustments were necessary in order to improve technical aspects or reliability, for this reason the prototyping and design phases are strongly interconnected. The prototype also served the purpose of verifying the EAG recorder's performance, in a series of tests. The last phase of the development was only partially concluded. The expected outputs from this phase were the final software and electronics. The development of the final software was set aside for schedule reasons. The work on the final electronics was initiated but set aside early on a board layout stage. The mechanical elements of the prototype are final and their assembly to a final circuit is possible. A schematic diagram of the development methodology is presented in figure 3.1.

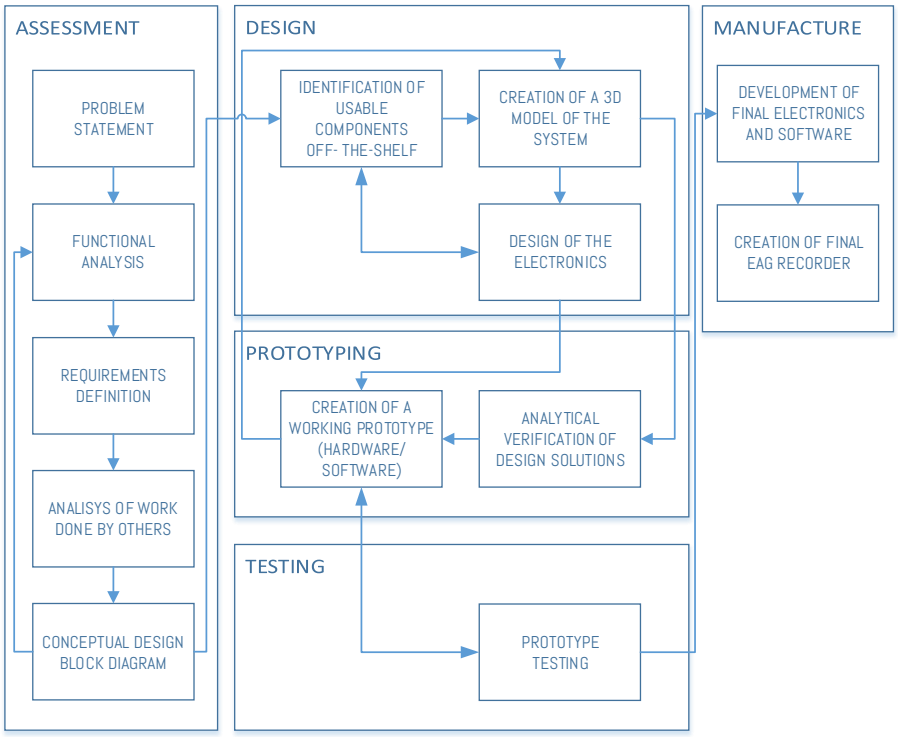

Figure 3.1: Development methodology.

3.3 Functional analysis and requirements specification

At the beginning of the project the requirements were not entirely specified. The only requirement was that the device should be able to record insect antennae olfactory responses. From that starting point a use-case of the equipment was drawn up. This use-case scenario is presented in figure 3.2. From this starting point and after evaluating the work done by other researchers, the requirements were further detailed. A mind-map of the thought process is depicted in figure 3.3. Most of the first level items are functional requirements. These requirements are very important because they reflect the expected functionality of the device. The functional requirements are listed in table 3.1. A functional tree of the device was drafted from this set of requirements. This tree is depicted in figure 3.4. This view is a design tool which helps to view the device not in terms of it's physical components, but in terms of it's functionality. The functional tree was then mapped to a set of technical solutions in a functions/components matrix. This matrix is presented in tables 3.2 and 3.3. The requirements associated with these components were then further detailed into a set of technical specifications, which are listed in table 3.4. The requirements were prioritized in a scale of 1 to 5 being priority 1 the most important level. The requirement list also contains the verification methods for the implementation of the feature or specification. The end goal of this analysis was the elaboration of a block diagram of the device. The block diagram of the EAG recorder is depicted in figure 3.4.

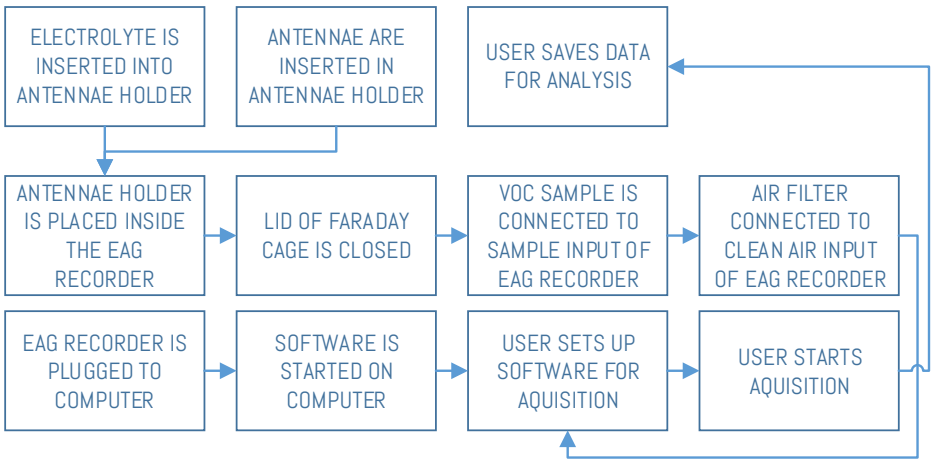

Figure 3.2: Simplified use-case of the EAG recorder.

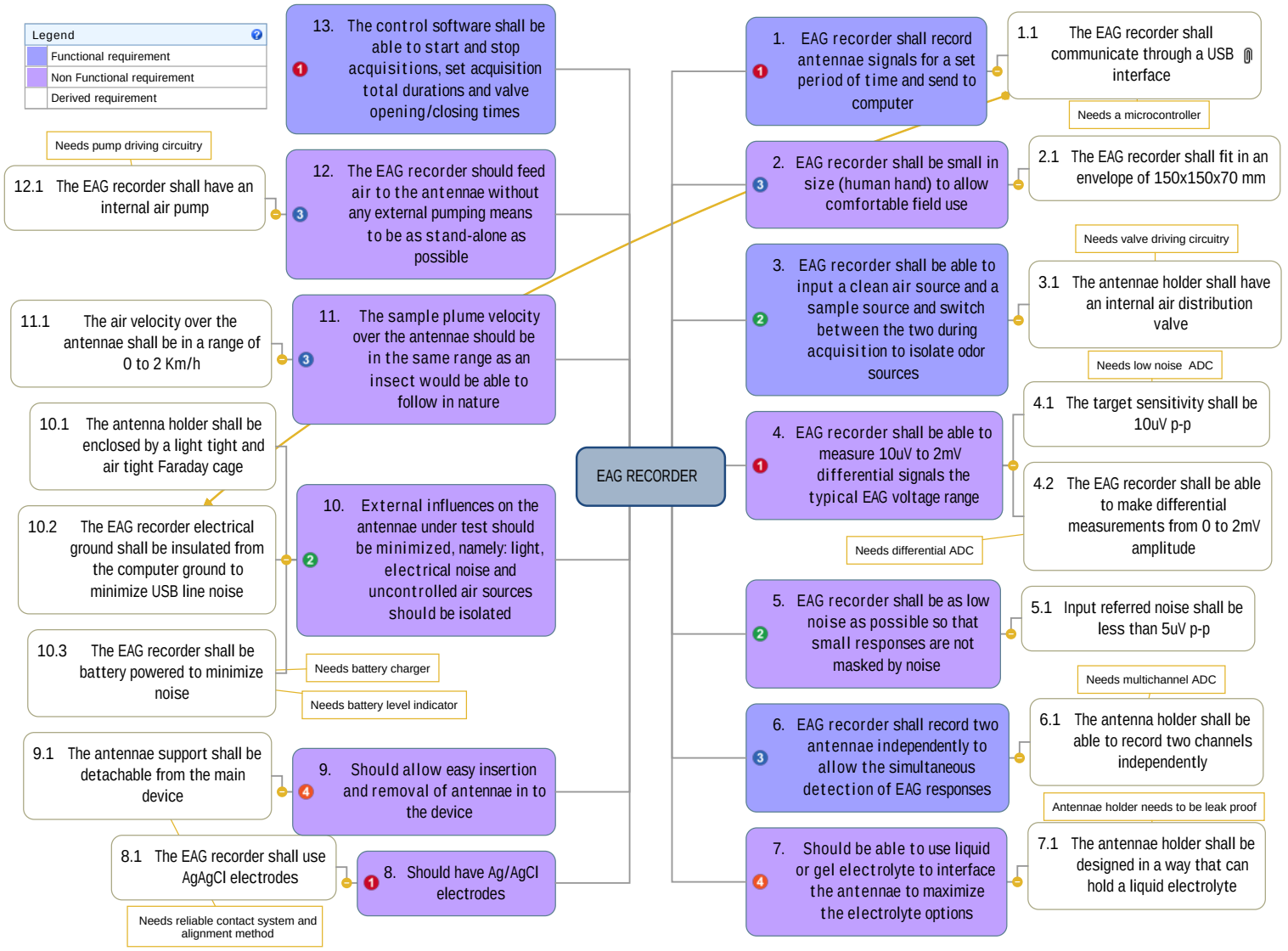

Figure 3.3: EAG recorder requirements mind-map obtained as part of the initial brainstorming process.

3.3.1 Functional analysis

A functional tree of the EAG recorder was drafted from the initial set of requirements listed on table 3.1. The functional tree represents the device in terms of a functional view, a complementary view of the more common physical view. The functional view is built by asking the question "what does it do?". It allows for the breaking up of the complex functions into smaller functions, and the creation of a function hierarchy. Each function on the tree is expressed in terms of a verb and a noun. The definition of each function should be as general as possible in order to stimulate the search for alternative ways of achieving the same functionality. Lower level functions are derived from higher level functions by asking the question "how?". Alternatively, moving from lower to higher level one should ask the question "why?". The functional tree for the EAG recorder is depicted in figure 3.4. The lower level functions that arise from the functional tree are called basic functions. These functions can then be mapped to specific physical solutions that implement them. The process is iterative and depending on the physical solutions encountered re-adjustment of the tree can be necessary to re-adapt it to the new physical solutions. In a further step, a matrix matching the technical solutions identified to the functions they implement is created. The purpose of this matrix is to ensure that all the functionality is covered by a physical solution, in this case a component of the EAG recording system. Another design characteristic that the matrix evidences is the coverage of multiple functions by a single design solution, which is in most cases highly desired.

Table 3.1: Functional requirements list.

Req. nº	**Requirement**	**Verification method**	**Priority**
1	The EAG recorder shall record antennae signals for a set period of time and send them to the computer	D	1
3	The EAG recorder shall be able to input a clean air source and a sample source and switch between the two during acquisition to isolate odor sources	D	2
6	The EAG recorder shall record two antennae independently to allow the simultaneous detection of EAG responses	D	3
13	The control software shall be able to start and stop acquisitions, set acquisition total durations and valve opening/closing times	D	1

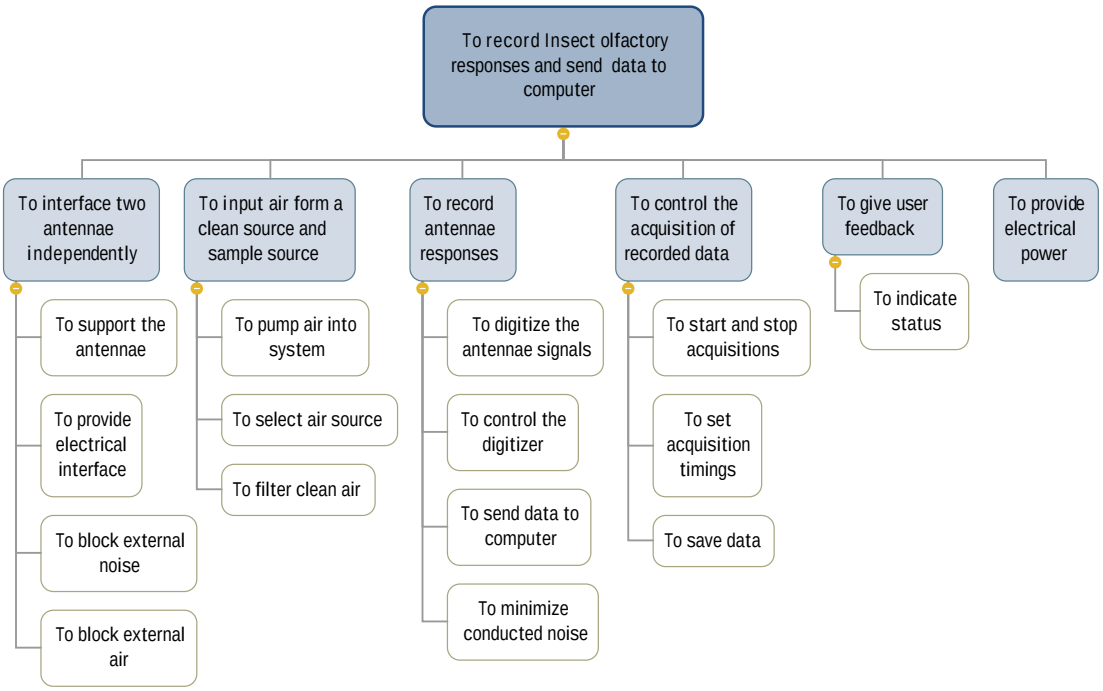

Figure 3.4: Functional tree the EAG recorder.

Table 3.2: Basic Components/Functions matrix (part 1).

Basic Components / Basic Functions	To support the antennae	To provide electrical interface	To block external noise	To block external air	To pump air into system	To select air source	To filter clean air	To digitize the antennae signals
Antennae Holder	×							
Faraday Cage			×	×				
Ag/AgCl Electrodes		×						
Pump and driver					×			
Valve and driver						×		
Air filter							×	
ADC								×

Table 3.3: Basic Components/Functions matrix (part 2).

Basic Components / Basic Functions	To control the digitizer	To send data to computer	To minimize conducted noise	To start and stop acquisitions	To set acquisition timings	To save data	To indicate status	To provide electrical power
MCU	×	×						
USB insulator			×					
Acquisition software				×	×	×		
Computer				×	×	×		
Indicator Leds							×	
Battery and PSU			×					×

3.3.2 Requirements specification

In order to further specify the EAG recorder a set of technical requirements had to be defined. The need for these requirements was already evident at the brainstorming level (see figure 3.3). But the consolidation of the requirements is the natural follow-up of the functional analysis process. After the identification of the main components of the system the performance of each individual component can be detailed. The requirements set the mark for performance, but were also a tool of creativity, stimulating the search for solutions that could cover the widest array of advantages. The technical requirements of the EAG recorder are listed in table 3.4. The table also includes the priority of the requirement. The priorities of every requirement were evaluated during the design, when solving trade-offs between different approaches. The priorities were also useful to guide the decision processes. Priority stimulates the concentration of design efforts on the essential aspects of the system. The verification method for the accomplishment of the requirement is also listed. The verification process is discussed in section 3.5.

Table 3.4: Technical specifications list.

Req. nº	Requirement	Verification method[1]	Priority
1.1	The EAG recorder shall communicate through a USB interface.	D	1
2.1	The EAG recorder shall fit in an envelope of 150x150x70 mm.	D	3
3.1	The EAG recorder shall have an internal air distribution valve.	D	2
4.1	The target sensitivity shall be 10 µV p-p.	T	1
4.2	The EAG recorder shall be able to make differential measurements from 0 to 2 mV amplitude.	T	1
5.1	Input referred noise shall be less than 5 µV p-p.	T	2
6.1	The antenna holder shall be able to record two channels independently.	D	3
7.1	The antennae holder shall be designed in a way that can hold a liquid electrolyte.	D	4
8.1	The EAG recorder shall use AgAgCl electrodes.	D	1
9.1	The antennae support shall be detachable from the main device.	D	4
10.1	The antenna holder shall be enclosed by a light tight and air-tight Faraday cage.	D	2
10.2	The EAG recorder electrical ground shall be insulated from the computer ground to minimize USB line noise.	D	2
10.3	The EAG recorder shall be battery powered to minimize noise.	D	2
11.1	The air velocity over the antennae shall be in a range of 0 to 2 Km/h.	A	3
12.1	The EAG recorder shall have an internal air pump.	D	3

3.4 EAG recorder architecture

The EAG recorder architecture can be divided in to five main blocks, namely: the antennae holder block, the Faraday cage block, the air delivery block, the electronics block and the EAG recorder enclosure block. The antennae holder is the block responsible for supporting and interfacing the insect antennae. The block consists on a SLA printed part containing the Ag/AgCl electrodes. The next block is the Faraday cage. The Faraday cage encloses the antennae holder and blocks it from external sources of

[1] D - Verification by design, T - Verification by test, A - Verification by analisys

electrical noise. Another function of the Faraday cage is to allow air to pass through to antennae. The electrode connections of the antennae holder pass through the Faraday cage. The physical implementation of the Faraday cage consists on a modified optical tube and accessories, and an SLA printed part. The next block of the system is the air delivery block. The air delivery block consists on a pump and a distributor valve and associated tubing and bulkheads. Its function is to supply clean air or VOCs sample to the antennae, through the Faraday cage. The next major block is the electronics block. This block contains all the necessary electronics to record the antennae signal and send it to the computer. The block also includes a battery and power supply as well as drivers for the pump and valve and a USB insulator. A block diagram of the EAG recorder is presented in 3.5.

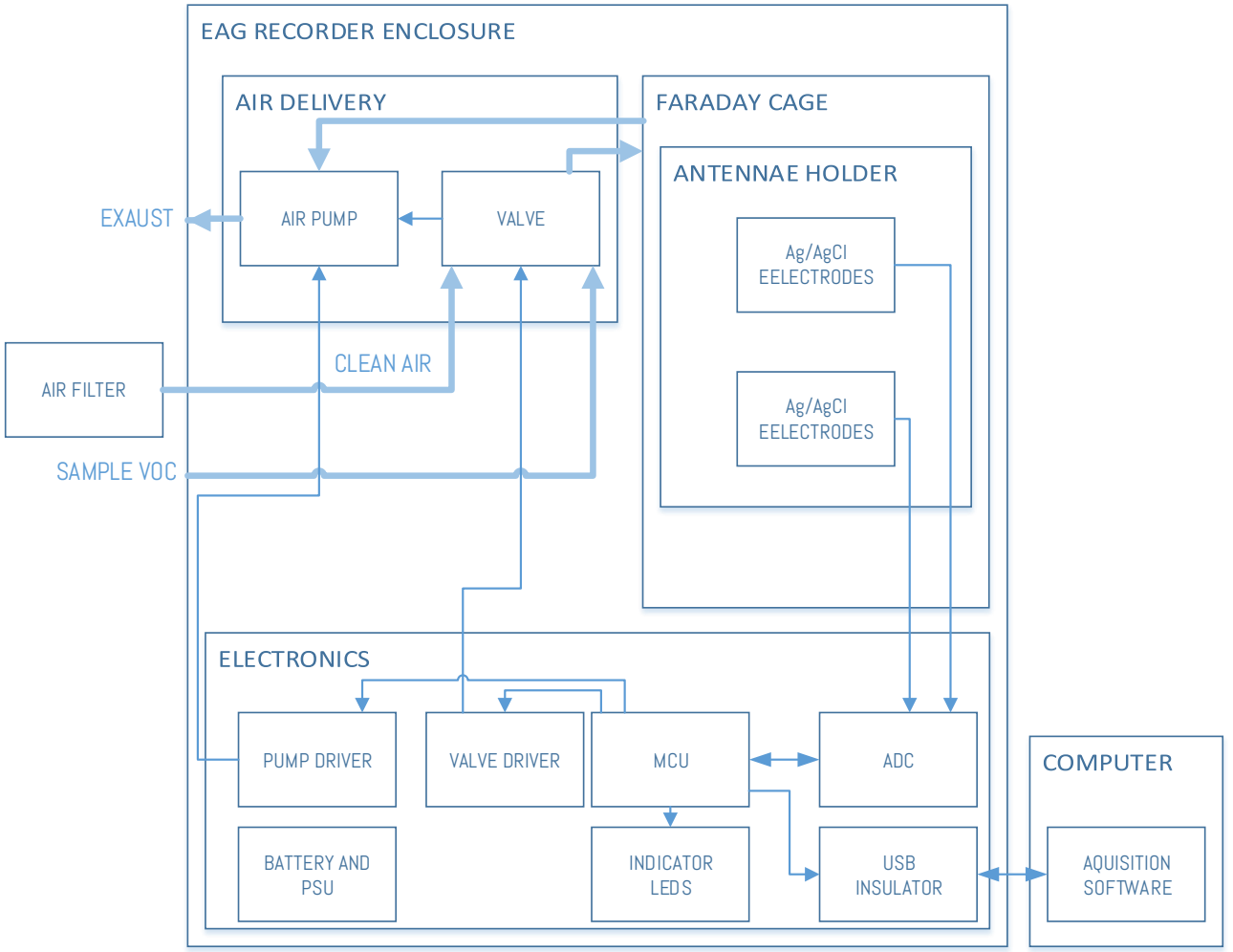

Figure 3.5: EAG Unit block diagram.

3.5 EAG recorder verification

The design requirements were evaluated according to the verification methods listed in table 3.5. Most of the requirements are verifiable by design. In order to verify requirement 11.1 a Computational fluid dynamics (CFD) analysis of the air flow inside the Faraday cage was performed. The results of this analysis are in section 3.6.3.3. For the verification of requirements 4.1, 4.2 and 5.1 on the electrical performance of the ADC, an antenna simulator was used. The simulator consists on a signal generator and an attenuator that is able to reproduce signals with the same amplitude as antennal responses. The antennae simulator is described in section 4.3.
Although electrical testing is a good indicator of the performance of the EAG recorder, measurements with an insect were also performed. Following up on the necessity to find other means of control for *G. platensis*, Center for environmental and sustainability research (CENSE) at Faculdade de Ciências e Tecnologia - Universidade Nova de Lisboa (FCT-UNL) is investigating the olfactory response of the insect. The objective of this research is to present an alternative control method where the parasitism by *A. nitens* lacks in effectiveness. The availability of specimens for testing and the added value the EAG recorder offers to this ongoing research justify this choice. The initial test plan logic is depicted in figure 3.6 and ore detail on the *G. platensis* tests is available in section 3.5.1. This test plan was not followed entirely in the systematic way it was devised as some of the test results were not in line with what was expected. The tests were adjusted in order cope with the findings, and to better understand the nature of the results. The results can be found in chapter 5.

Table 3.5: Methods for requirement verification.

Verification Method	Symbol	Description
Design	D	Verification by design, The item is verified if the design outputs meet the requested specifications.
Analysis	A	Verification by analysis, The item is verified if the analysis results predicted from the study of models or other calculations allow a good assumption that the requested specification will be met.
Test	T	Verification by test, the item is verified if the results of test, under a series of controlled inputs or stimuli ensure the required specification is met.

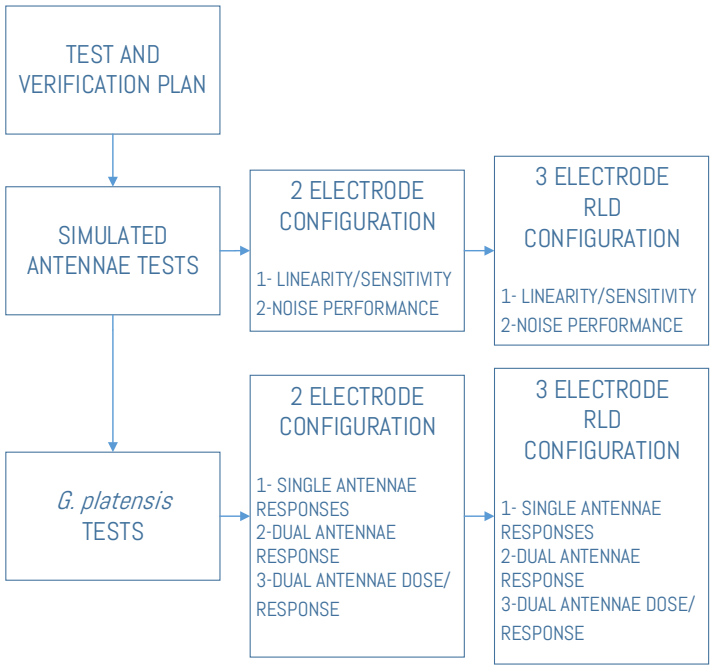

Figure 3.6: Initial test plan.

3.5.1 Measuring *G. platensis* olfactory response to verbenone

Gonipterus scutellatus Gyllenhal, commonly known as Eucalyptus weevil or Eucalyptus snout-beetle (figure 3.7), is an insect that belongs to the Australo-Pacific weevil tribe Gonipterini (*Coleoptera: Curculionidae*). The insect is a significant pest to eucalyptus species in Africa, America, Europe and New Zeland. Since the acceptance of *G. scutellatus* as the correct scientific designation for the species there has been some confusion in the identification of the individual species found in other countries to where in was introduced. (Mapondera et al. 2012). A genetic and morphologic study was conducted in 2012 by Mapondera and collaborators concluded that there are at least ten distinct taxonomic entities. Of these species formerly identified as *G. scutellatus* five have been described, one of them being *G. platensis* (Marelli 1926). *G. platensis* is the most commonly confused species with *G. scutellatus* because both are endemic to Tasmania although *G. platensis* is less common there (Mapondera et al. 2012). Outside of Australia *G. platensis* is the most widely distributed species of the *G. scutellatus* complex (Mapondera et al. 2012). The weevil has maximum dimensions 9.0×5.0 mm, being the males smaller than the females. Its coloration varies from a brown reddish to a dark brown and it was first identified in Portugal in 1995. In Portugal as well as in Galicia, Spain, *G. platensis* became a major limiting factor of eucalyptus wood production, prompting research on control methods such as tree resistance or chemical control, besides the classical biological control with the parasitoid *A. nitens*(Reis et al. 2012).

G. platensis has a club shaped antenna, common in *Coleoptera*. The antenna consists

on 3 parts: a proximal scape, a pedicel and a distal flagellum (see figure 3.8 A)). *G. platensis* antennae have a high density of mechanoreceptor sensilla and the majority of the chemoreceptors are located in the clava (S. Branco unpublished). The high density of mechanoreceptors makes *G. platensis* antennae especially sensitive to touch. This touch can either be direct contact pressure or, for example, air flow variation. Disturbance in the airflow can cause the stimulation of mechanoreceptors generating an unwanted response from the antenna. This response can mask the olfactory response (Bouwer 2010), adding an extra challenge to stimuli delivery. Traditionally, olfactory stimuli in EAG bioassays are puffed on to a stream of air flowing to the antennae. The length and shape of the stimuli delivery tube are used to dampen the sudden pressure variation generated by puffing. The EAG recorder is designed to use suction as a stimulus delivery strategy to minimize turbulence over the antennae and the stimulation of mechanoreceptors.

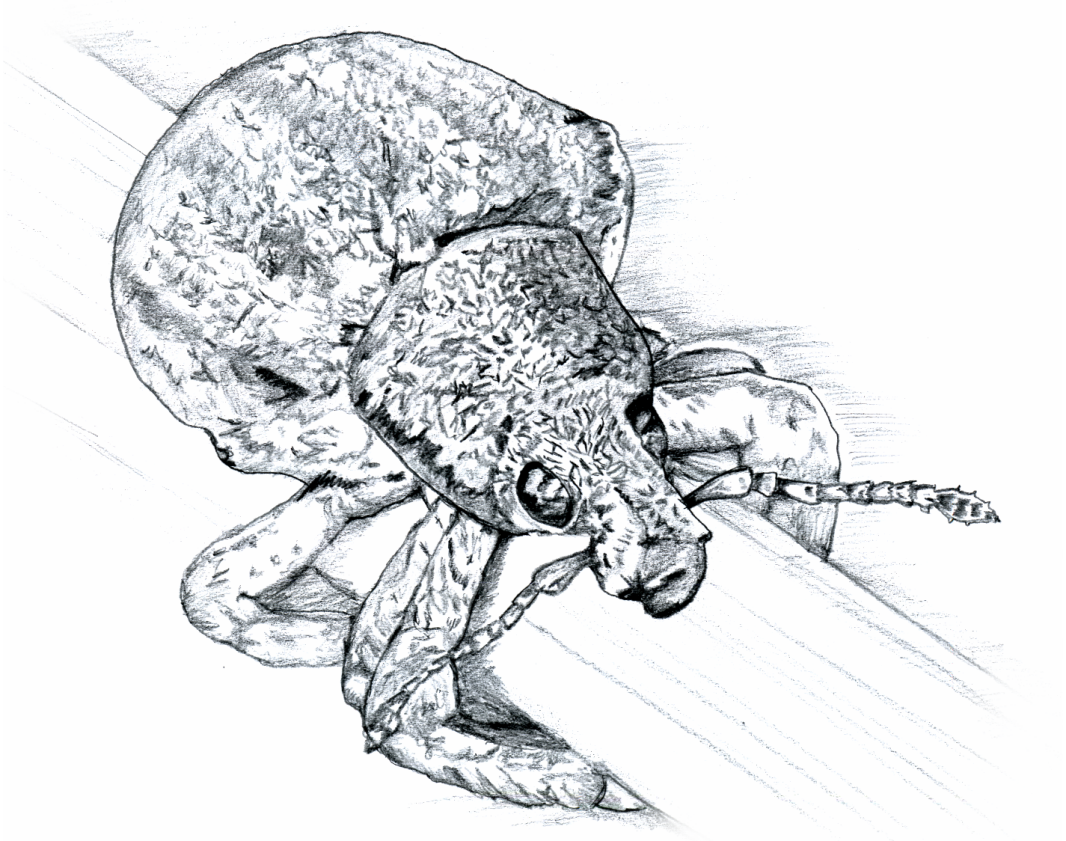

Figure 3.7: Eucalyptus weevil *(G. platensis)*

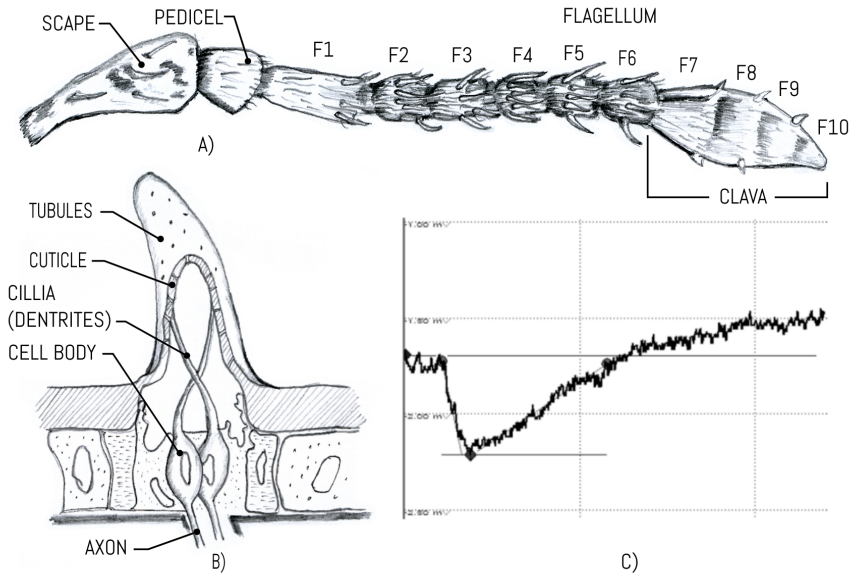

Figure 3.8: A) Female *G. platensis* antenna. B) Representation of an olfactory sensillum (Basiconica). C) Example of an olfactory response obtained from a *G. Scutellatus* (Bouwer 2010).

The ongoing study at CENSE identified dl-verbenone as a pheromone of *G. platensis*. The study also measured consistent olfactory responses to verbenone from *G. platensis* females. Although the tested specimens respond to the scent, the exact role played by verbenone is not known (S. Branco unpublished). Verbenone is an organic volatile classified as a terpene that is found naturally in a variety of plants. Besides being a constituent of plants, it and its analogs are insect pheromones. Dl-verbenone was used as stimuli to test the EAG recorder. The stimuli was prepared from a stock solution of 200 µL of dl-verbenone diluted in 1.8 mL of paraffin and then further diluted in decadic steps (please see table 3.6). To prepare the stimulus 50 µL of each step is applied to pieces of filter paper and inserted into a syringe (please see figure 3.9). The stimuli are applied in ascending concentration values, with a time interval to avoid saturation of the chemoreceptors. Spectra 360 conductive gel is added to the electrodes. The antennae are then removed from the insect with fine tweezers and placed in the antennae holder bridging across the recording and reference electrode. The clava of the antenna is placed on the recording electrode side. Since the majority of the chemoreceptors are located in the clava full wetting of this area was avoided. The expected olfactory response is a depolarization of the antenna, with an amplitude proportional to the logarithm of the concentration (see figure 3.8 C)).

Table 3.6: Verbenone stimulus steps (density of verbenone 0.978 g/cm^3).

Stimulus step	Concentration [g/µL]
10^{-1}	$9,78 * 10^{-2}$
10^{-2}	$9,78 * 10^{-3}$
10^{-3}	$9,78 * 10^{-4}$
10^{-4}	$9,78 * 10^{-5}$
10^{-5}	$9,78 * 10^{-6}$
10^{-6}	$9,78 * 10^{-7}$

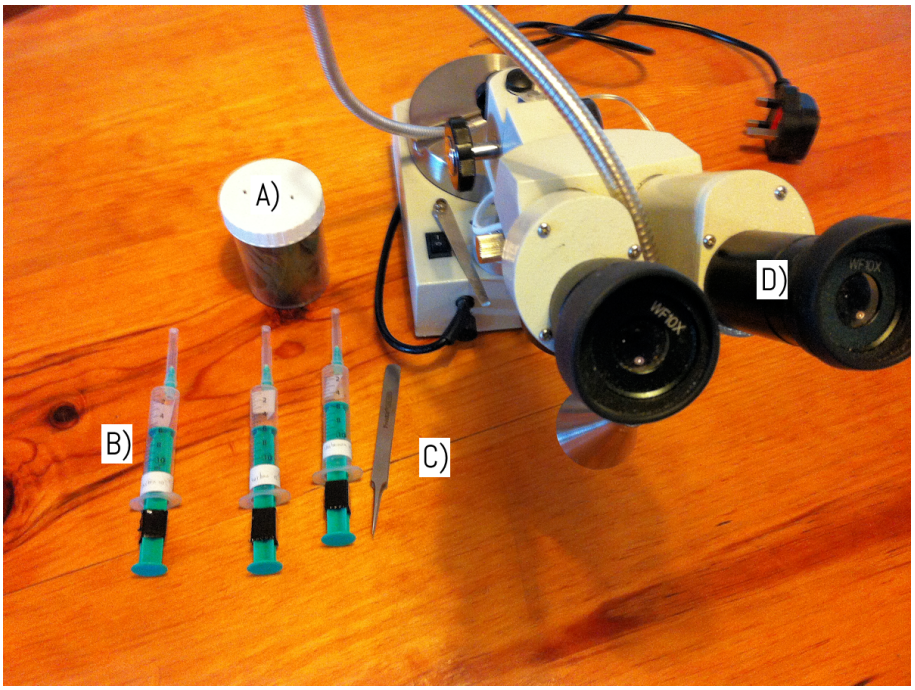

Figure 3.9: Test materials. A) *G. platensis* specimens. B) Stimulus steps syringes. C) Extra fine tweezers for antennae removal. D) 20X stereo microscope.

3.6 Mechanical design

The insect antenna holder concept of Arne E. Sauer et al. 1992 was the starting point of the EAG recorder design. This part could be modified in order to be detachable from the main device, facilitating the antenna insertion process (requirement 9.1). The part would be manufactured by SLA printing, taking advantage of the recent availability of SLA printers, and companies offering 3D printing services at a reasonable cost. The design freedom of 3D printing also meant that the size and shape of the part could be adjusted to be fitted into an already existing enclosure. This enclosure would work as a Faraday cage blocking the antenna from external electrical noise (requirement 10.1). The best candidate found for this task were lens tubes. Lens tubes are offered in a black anodization finish, they have 1" diameter and several lengths are available. Fittings and caps for these tubes are

also available. Resorting to the use of these standard parts would dramatically shorten development time as only small modifications to these parts would be necessary like, for example, drilling to allow electrical connections and air lines through. This design solution is fully compliant with requirement 9.1. Given the small dimensions of the Faraday cage a suitable housing for the electronics was chosen. The housing choice was based on an educated best guess on the size required to fit the electronics and battery. The enclosure chosen to contain the EAG recorder was a *Hammond Mfg.* 1590BBK. Openings were considered in order to fit the Faraday Cage, bulkheads, USB connector, and leds. Given that both the EAG enclosure and the Faraday cage are aluminum, EMI shielding is guaranteed (requirement 5.1). Built in pumping capability was not initially considered a requirement because of the extra complexity introduced. But after a more extensive analysis of the work of other authors, it was clear that without this feature it would not be possible to guarantee that the olfactory responses were not being induced by uncontrolled airborne volatiles, and thus requirement 12.1 was introduced. Along with internal pumping capability a way to select between "clean" air and air containing the VOCs sample was also introduced (requirement 3.1). A 3D model of the device was drawn with Solidworks. The antennae holder, antennae holder contacts support, air pump support and PCB support are SLA printed parts. The Solidworks modeled parts were converted to STL format for printing. The process of printing a part is straightforward and several iterations of the parts were made until a final design was reached. An external view of the device is shown in figure 3.10. Figure 3.11 depicts the final design with the main enclosure hidden.

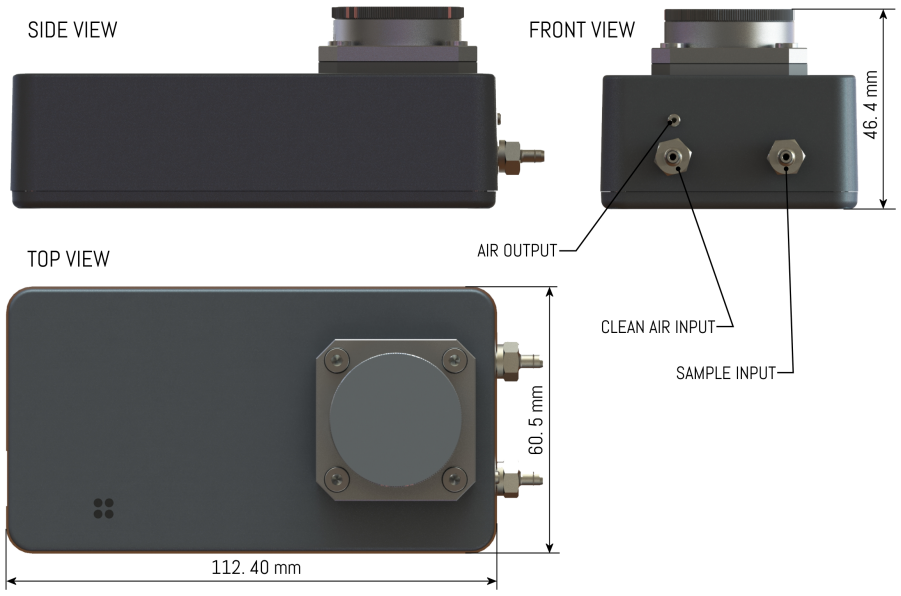

Figure 3.10: EAG recorder external views.

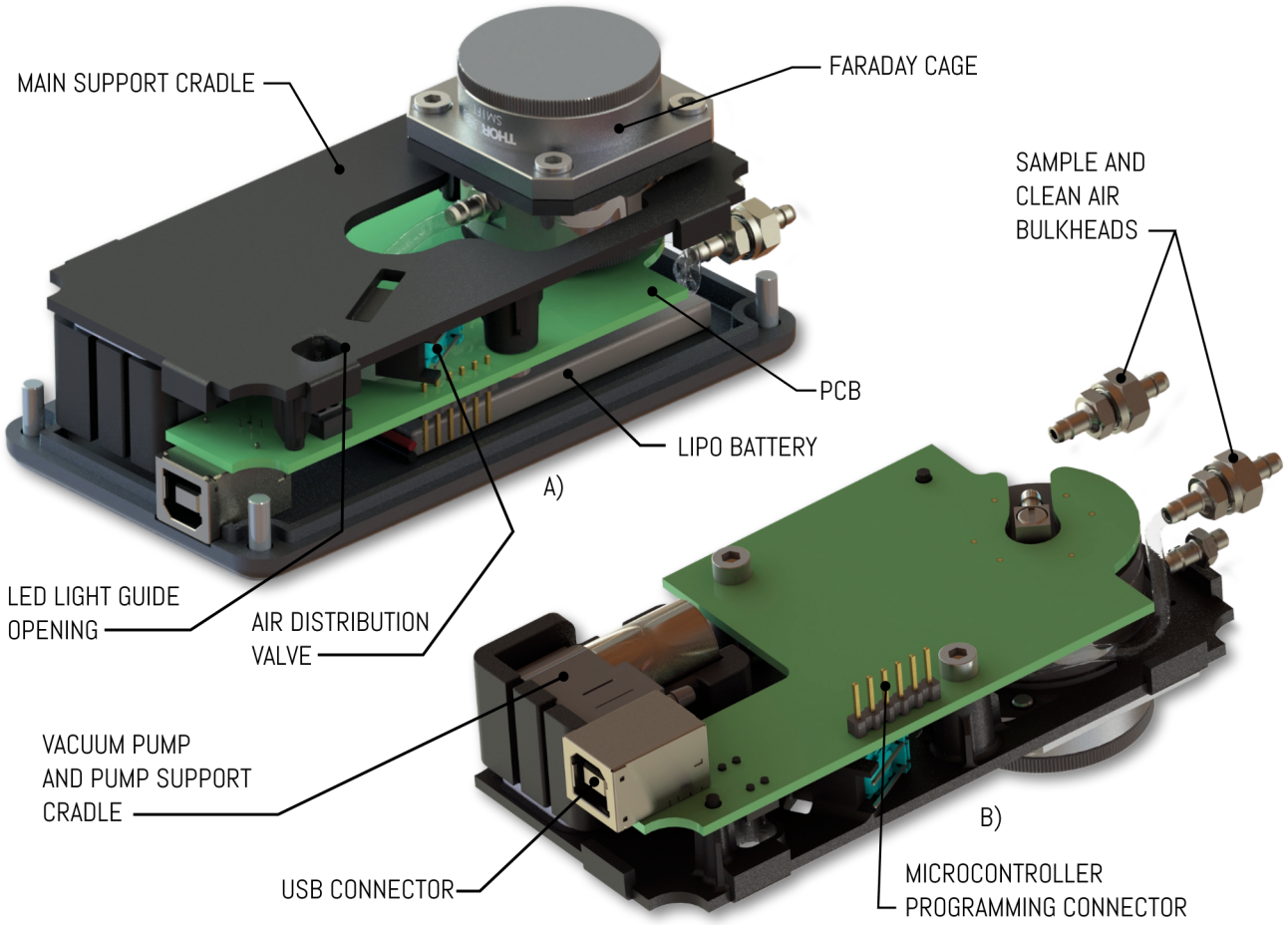

Figure 3.11: EAG recorder internals. A) Top view with enclosure hidden. B) Bottom view with bottom lid, battery and enclosure hidden.

3.6.1 Faraday cage

The antennae holder and the Faraday cage form the interface with the insect antennae. The sub-assembly, which can be seen in figure 3.12 consists on a SM1F1 flange, two SM1CP2 lids and an SM1L05 tube. These are standard parts from Thorlabs. The air input and output fittings are M3 threaded and attach to the side of the SM1L05 tube and bottom SM1L05 lid. The bottom SM1CP2 lid also has holes to allow the electrode contact saddles to reach the PCB. A custom SLA part was designed to support the base contact saddles. Actually besides this purpose the part has two other functions, support the antennae holder alignment magnets and provide a means to get the air suction nozzle close to the antennae. The Faraday cage has also a side thread for grounding purposes. The design complies with requirement 10.1 in a sense that once closed the Faraday cage is light and air tight. A set of O-rings on the top and bottom lids ensures hermeticity. The sample holder in inserted into the Faraday cage by removing the top lid and allowing it down with the help of tweezers. The magnets have their polarities aligned in a way to repel the antennae holder if positioned 180° from the correct position. This magnet polarity strategy ensures that the antennae holder cannot be inserted in reverse. During assembly the Faraday cage cannot be attached to the main enclosure totally assembled. The SM1F1 flange has to be detached from the tube and bolted first to the enclosure, and then the tube is screwed back on the flange.

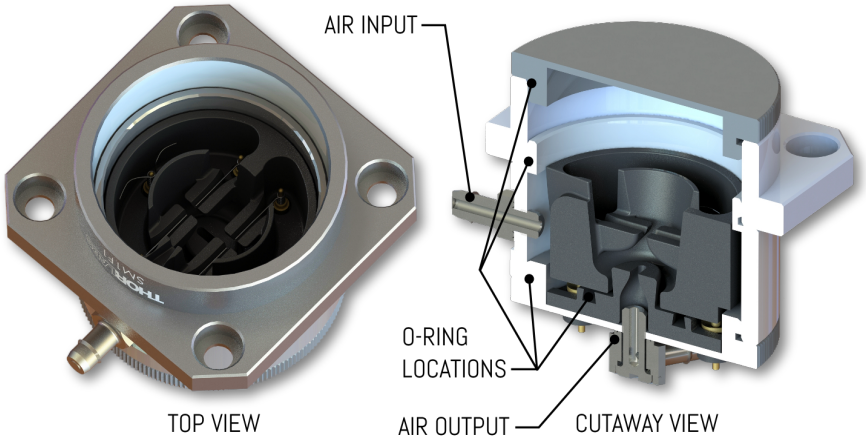

Figure 3.12: Faraday cage cutaway view.

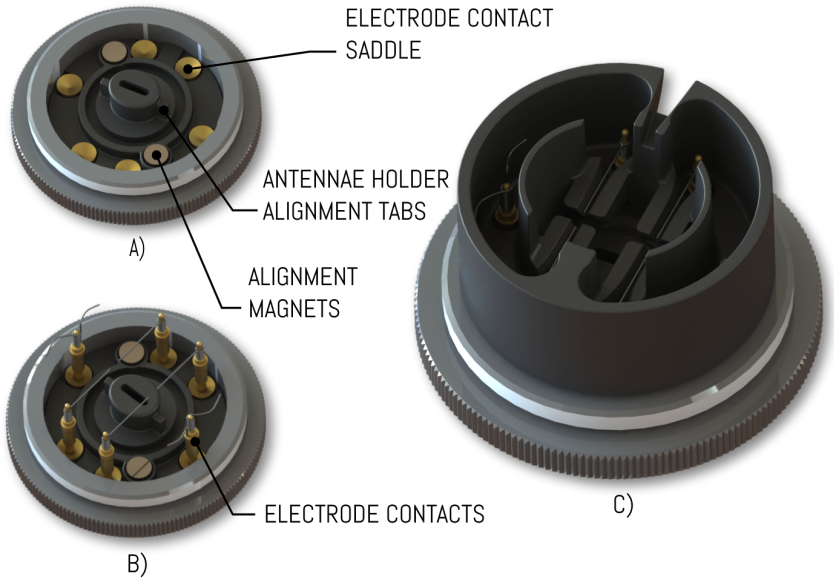

Figure 3.13: Faraday cage base SM1CP2 lid with SLA printed air insertion nozzle and electrode contact saddle support. A) Detail of the electrode contact saddle support showing the alignment magnets and contact saddles. B) Detail showing how the spring loaded electrode contacts connect with their saddles. D) Antennae holder attached to faraday cage base.

3.6.2 Antennae holder

The antennae holder is an SLA printed detachable part, allowing the fitting of the antennae under magnification. It is designed to support 3 electrodes for each antenna, allowing the measurement of two antennae simultaneously. Each electrode consists of an solid silver/silver chloride wire (Ag/AgCl) immersed in an electrically conductive solution. The antennae holder can be used with 0.1M KCl solution, Ringer solution or electrically conductive gel. Electrically conductive gels present several advantages, namely higher viscosity, similar electrical properties and better antennae wetting (Van Der Pers and Minks 1998). The use of a proper quality electrocardiography (EKG) gel does not yield significant measurement differences compared to a KCl solution and the longer drying times of gels also extend the lifetime of the antennal preparation (SYNTECH 2004). The simultaneous measurement of two antennae allows for the quantification of odor responses by comparing the responses antennae of different insect species to the same odor concentration. It also allows comparisons between left and right antennal responses when bilateral studies are required (Takasaki et al. 2012), or improve the signal to noise ratio (Park and Baker 2002). Figure 3.14 depicts the antennae holder. The electrode contacts are inserted into the part from the top and protrude through the bottom in order to make contact with the base. In the bottom of the antennae holder there are also two slots to fit NdFeB magnets. These magnets guarantee the correct

alignment of the electrodes with their saddle counterparts. The electrolyte wells are also liquid tight thus complying with requirement. 7.1. a lateral slot in the part allows the air to flow from the lateral air intake to the bottom of the part passing through both antennae. While working with liquid electrolytes the antenna is placed on the bridge making sure that both ends are touching the electrolyte media. If conductive gel is used, the antenna can be set on the gel, wetting on both ends, and thus guarantying electrical contact.

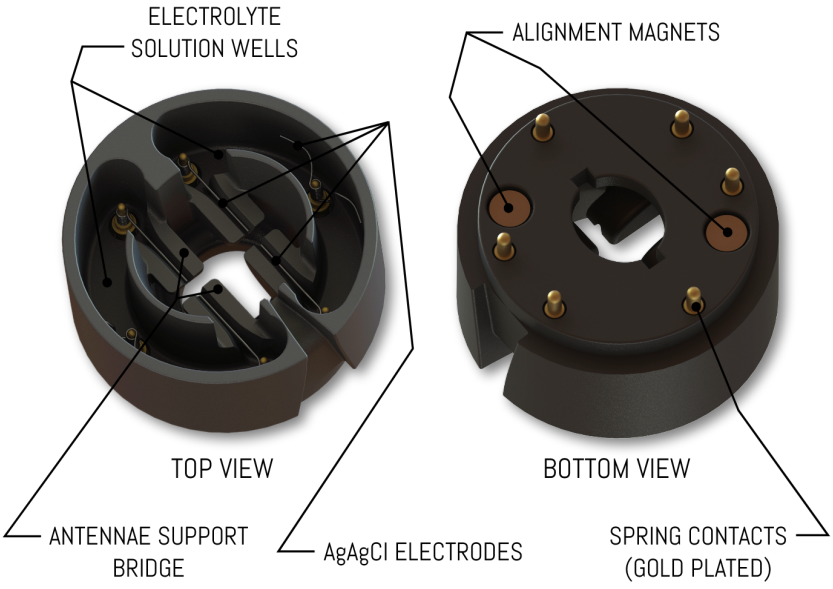

Figure 3.14: Antennae holder top and bottom view.

3.6.3 Sample delivery strategy

The sample delivery strategy is inspired by Guerrero et al. 1986 automatic sample injection system, but a different strategy was adopted. The sample delivery system's main components are the air pump and a distributor valve. The pump is set to produce vacuum, and intakes air from the bottom of the Faraday cage. A comparison study between using vacuum or positive pressure and their impact on air flow over the antennae was not studied in depth. But it was the author's understanding that vacuum would force the flow lines to converge at the intake nozzle thus making the flow as a whole behave in a more predictable way, eventually even being less turbulent. A flow simulation was conducted to determine the optimum chamber geometry and to validate requirement 11.1 on air velocity over the antennae (section 3.6.3.3). The distributor valve selects between to inputs. In one of these inputs an activated charcoal air filter is fitted, in the other input the samples with the VOCs are inserted. The air tubes have a 2.5 mm inner diameter which allow insertion on the 3/32" bulkheads. The valve barbs are smaller in diameter (5/32") but the difference was accommodated by heat-shrinking

the tube. The sample delivery system is depicted in figure 3.15.

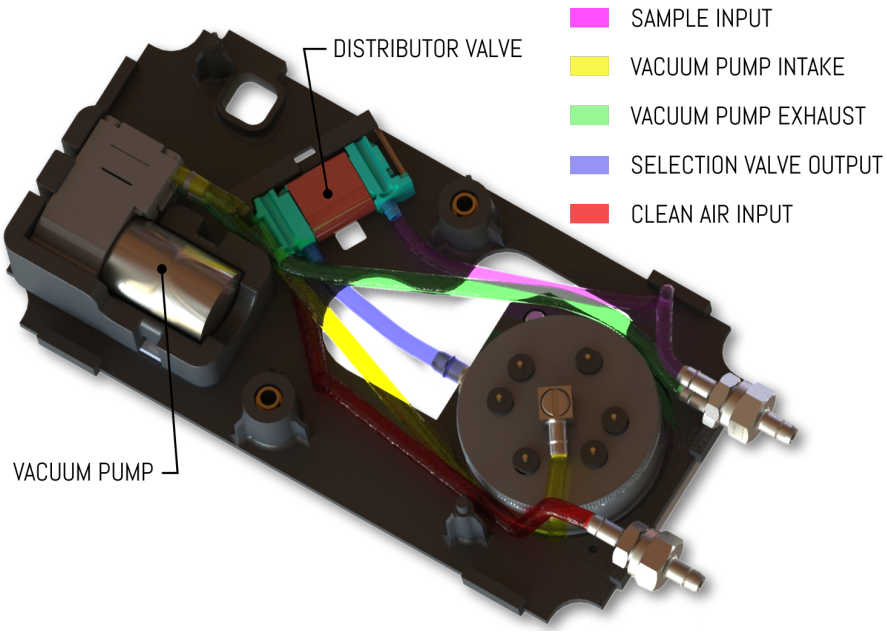

Figure 3.15: Sample delivery pumping system.

3.6.3.1 Air pump

Requirement 2.1 size restriction also poses a limitation on the availability of parts, like pumps and valves. The pumps considered had to be of a miniaturized nature. Air pumps used for automatic blood pressure measurement apparatus were considered, as well as pumps for microfluidic equipment. One pump was identified as having a good balance between size, and generated vacuum that could be used to attain enough air flow. Researchers report using volumetric air flows in the order of 2.5 L/min (Suckling et al. 1994, Sauer et al. 1992) 400 mL/min (Takasaki et al. 2012) and 500 mL/min (Weissbecker et al. 2004). In order to minimize disturbance to the G. platensis mechanoreceptors M. Bouwer used 30 mL/min (Bouwer 2010). The chosen pump has a volumetric flow rate of 300-400 mL/min. The pump's performance chart is depicted in figure 3.17, and the more relevant specifications are listed on table 3.7. A support cradle was designed in order to mechanically decouple the pump vibration from the rest of the assembly, specially the Faraday cage and antennae support. The pump is tied to the support cradle with a cable tie, this simple method proved to be sufficient. Figure 3.16 depicts the air pump support method.

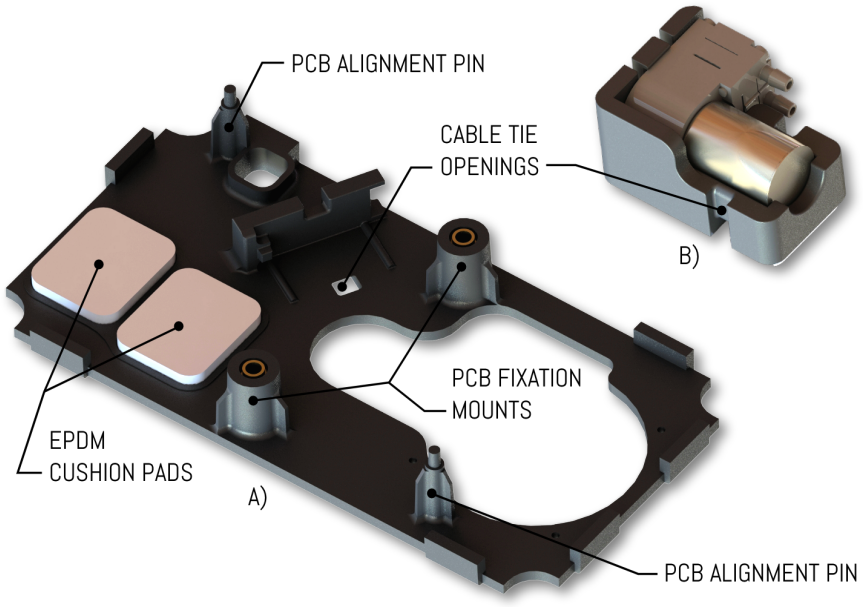

Figure 3.16: Air pump cradle.

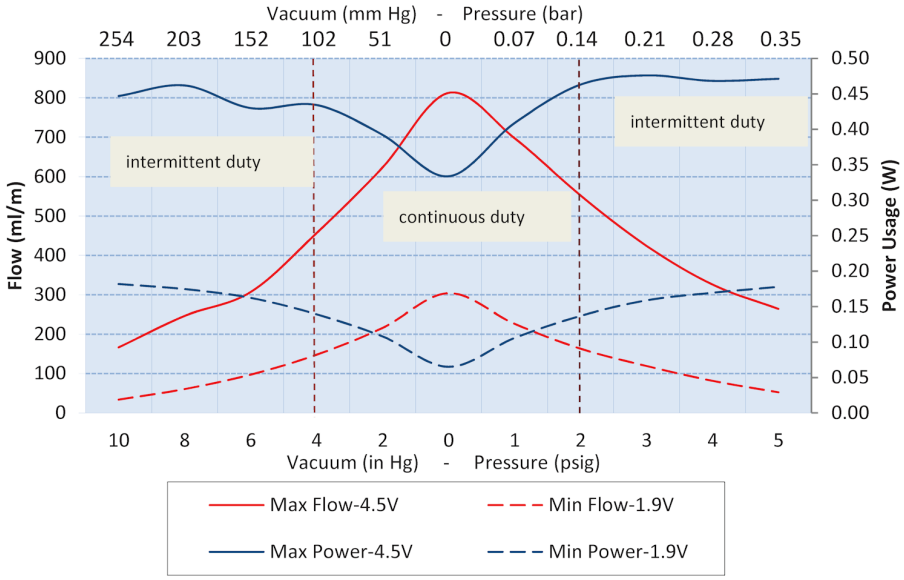

Figure 3.17: Air pump performance. Specifications taken from the manufacturer datasheet.

3.6.3.2 Air distribution valve

The air distribution valve is a miniaturized tree way distributor. It has one output and two inputs and can either work with positive pressure or vacuum. The valve is a poppet style actuated by a solenoid. In the EAG recorder it is used under vacuum. The solenoid actuation voltage is 3 V and the power consumption 0.5 W.

Table 3.7: Air pump specifications

Physical Properties	Electrical	Pneumatic
Op. Environment :	**Motor Type (DC):**	**Head Configuration:**
-20 to 50°C	Low Inductance Coreless Brush	Single head
Media:	**Nominal Motor Voltage (DC) :**	**Maximum Flow:**
Air, Argon, Helium, Nitrogen, Oxygen,	3.3 VDC	800 smlpm
and other non-reacting gases	**Max Power at Nominal Voltage:**	**Maximum Intermittent Pressure:**
Humidity:	0.36 Watts	430 mbar
Most non-condensing gases	**Current Range:**	**Maximum Continuous Pressure:**
5-95% Relative Humidity	34 - 105 mA	138 mbar
Noise Level:	**Inductance:**	**Maximum Intermittent Vacuum:**
As low as 45dB	0.05 mH maximum @ 1kHz/50mV	274 mm Hg
Pump Assembly Rated Life:		**Maximum Continuous Vacuum:**
Up to 6,000 hours		104 mm Hg
Weight:		**Efficiency at Free Flow:**
14g		LPM/Watt: 4.08 @ 1.9 VDC

3.6.3.3 Air velocity simulation

In order to verify requirement 11.1 a CFD analysis was performed in Solidworks. The simulation considered only the Faraday cage and its inputs and outputs. The pressure losses on the air pump, valve and associated tubing were not considered. The initial assumption was that the internal geometry of the Faraday cage with the antenna holder inserted would cause a pressure loss. The analysis used two boundary conditions: The intake of the Faraday cage is at ambient pressure (760 mmHg), the output flow-rate was then iterated using the fit of the pump performance curve and the simulated pressure drop. The iteration process is stopped when the simulated pressure and flow-rate drop lay on the pump performance curve. The iteration process data is presented in figure 3.18. The units of mmHg and mL/min were preferred to SI units because they allow a better feel for the obtained results. The final velocity simulation plot obtained is depicted in figure 3.19. From this plot we can verify the distribution of flow velocities inside the Faraday cage, and are in accordance with requirement 11.1.

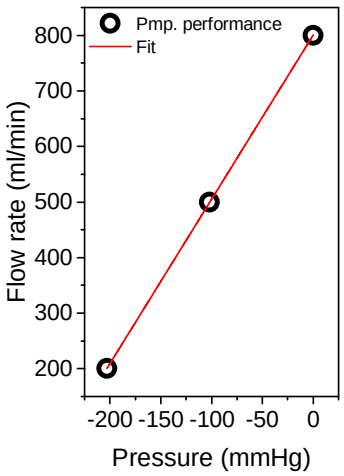

Equation	y = a + b*x		
Weight	No Weighting		
Residual Sum of Squares	1,45598		
Pearson's r	1		
Adj. R-Square	0,99998		
		Value	Standard Error
Flow rate	Intercept	800,49018	1,10259
	Slope	2,95564	0,00841

Flowrate iteration			
IT	Input flowrate [ml/min]	Pressure drop [mmHg]	Calc. Flowrate [ml/min]
1	800,00	-4,04	788,55
2	788,55	-3,96	788,79
3	788,79	-3,96	788,79

Figure 3.18: Air pump performance. Left) Pump flow-rate vs pressure. Top right) Linear fit of the pump performance. Bottom right) Simulated flowrates. Boundary condition at the Faraday cage input considered ambient pressure (760 mmHg), iteration of the flow-rate value based on the pump performance curve and the pressure drop calculated by simulation.

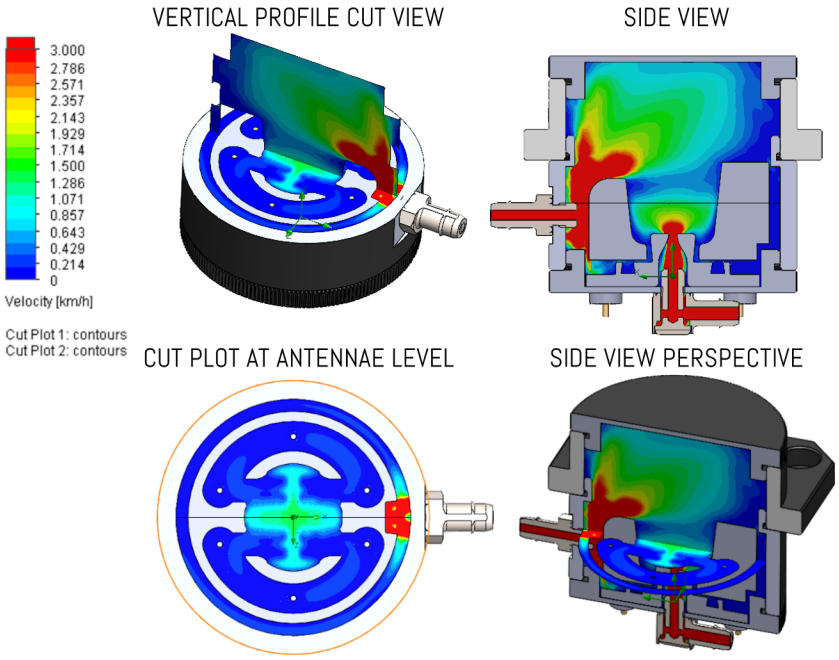

Figure 3.19: Faraday cage and antennae holder flow velocity simulation plot.

3.7 Electronics design

An initial evaluation of the characteristics of the EAG signal showed that it was in the same range as other commonly measured biopotentials. This fact led to the

consideration of using integrated ADCs designed for EKG or electroencephalography (EEG). A survey identified ADS1299 a 24 bit biopotential ADC with 8 channels and with 1 µV p-p input referred noise (Texas Instruments 2012). The multichannel capability of the ADC also introduced requirement 6.1, given the available space in the antenna holder. The simultaneous recording of two antennae also opened the possibility of being able to correlate antennae data or sum both signals to improve SNR. Two solenoid driving circuits were also necessary for the driving of the air pump and valve. The devices chosen were DRV8830 and DRV8832 also from Texas Instruments. A micro-controller was also necessary to control the ADC and handle the USB data transfer. A PIC32 family device with USB capability was chosen for the task. Electrical noise is a concern in this design, for this reason a USB insulator was also added. This device has the function of electrically insulating the EAG recorder from the computer and still be able to send data. The block diagram of the EAG recorder is depicted in figure 3.20. The pump and valve drivers are controlled by the micro-controller. The micro-controller also handles the data acquisition from the ADS1299 via a Serial peripheral interface (SPI) interface. The data is then sent to the computer via USB. After the first successful tests with the prototype it was concluded no extra front-end amplification would be necessary so it was not considered on the final circuit. The EAG recorder unit will be powered from a 3.7 V single cell Lithium polymer battery.

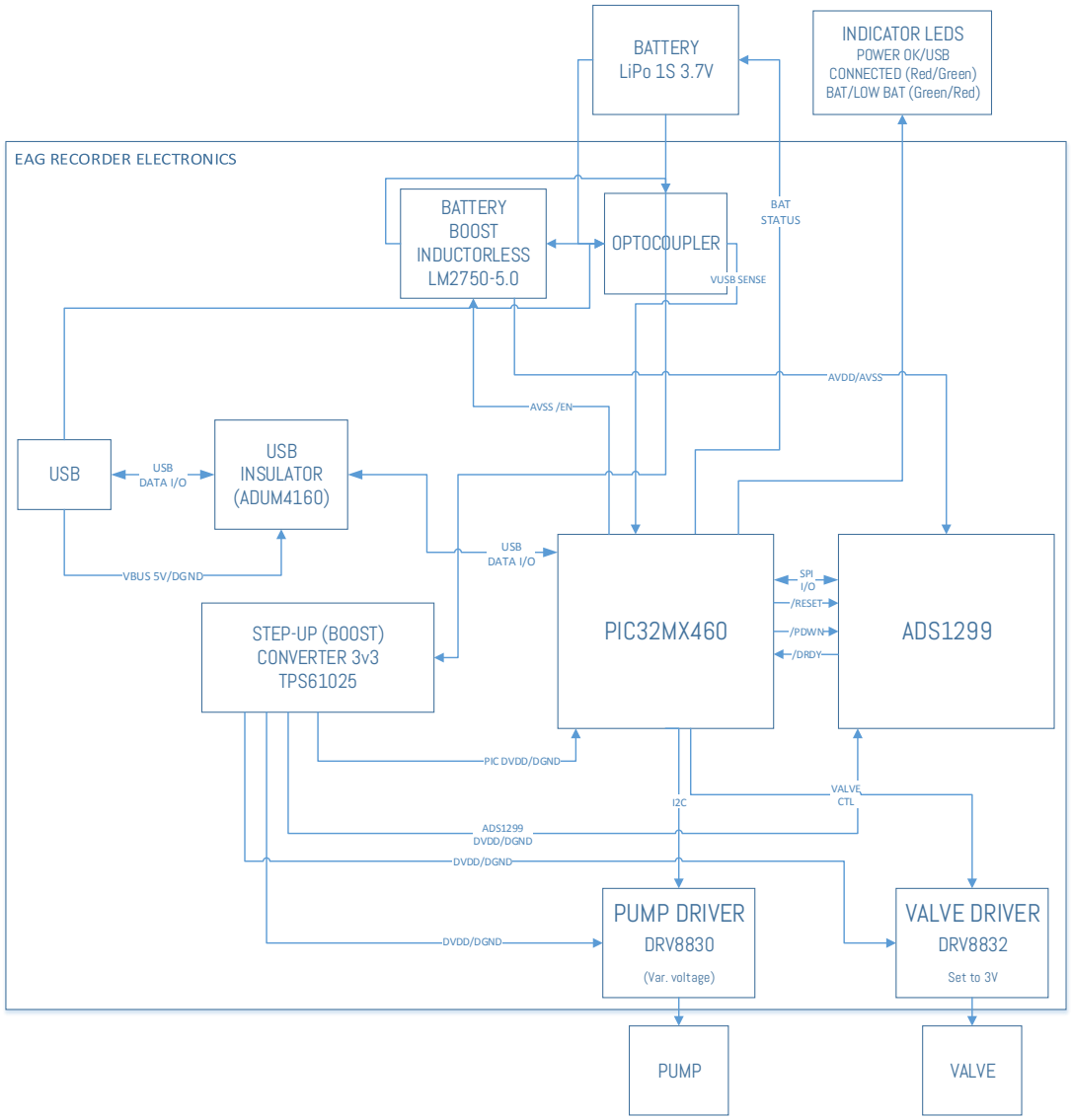

Figure 3.20: EAG Unit electronics block diagram.

3.7.1 Noise considerations

CMR is one of the most important performance parameters for micro-volt level biopotential amplifiers (Acharya 2011). As an example, in EKG systems large amounts of electromagnetic interference (EMI) is coupled to the patient's body. Interference can also couple to the subject under measurement through the power supply coupling capacitors, ground coupled, or from earth coupling. The usage of long leads for measurement is also another source for this undesired interference. It is then desirable to have a system as close as possible to being truly isolated to have high CMR. The most common source of interference is the AC mains at a frequency of 50 Hz (Europe and Asia), or 60 Hz (United States).

3.7.1.1 Common-Mode to differential signal translation

Common-mode to differential signal translation is an undesired effect caused by the mismatch in electrode, cables and input circuitry impedances. If we consider the circuit of figure 3.21 with a simple input RC filter and non-insulated (AC ground shared with system ground), for an interfering AC signal, the voltage seen by the antenna is given by:

$$V_p = \frac{Z_g}{Z_g + \frac{1}{sC_2}} \cdot V_s \tag{3.1}$$

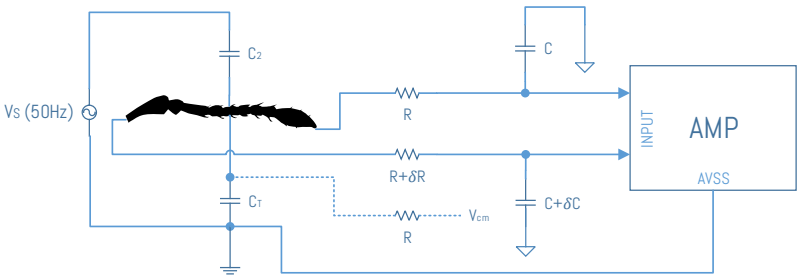

Figure 3.21: Common mode rejection and component mismatch. Figure adapted from (Acharya 2011).

Where Z_G is the impedance from the insect antenna to ground. Z_G is approximately:

$$Z_g \approx \left[\left(\frac{1}{sC_T}\right) \| \left(\frac{1+sRC}{s2C}\right)\right] \tag{3.2}$$

V_P is a common-mode signal to the system. If the filter components, electrodes and electrode to antenna contact are perfectly matched then CMR is very high. If there is a mismatch of δR or δC then the CMR of the the system can be approximated by equation (3.3). Where F_C is the -3 dB frequency of the filter. As an example if 1% tolerance components are used and the filter has a 5 kHz bandwidth, the system only has -74 dB

of CMR. This value does not account for electrode impedance mismatch, cabling, etc. Therefore other techniques are necessary to improve CMR.

$$CMR = 20Log\left(\frac{\delta R}{R} + \frac{\delta C}{C}\right) + 20Log\left(\frac{f}{f_c}\right) \tag{3.3}$$

3.7.1.2 Techniques to improve CMR

Given that the component mismatch on the input stage is unavoidable a few other techniques to improve CMR are commonly used.

1. **Faraday shield**
   A Faraday shield covering the input electronics, and the antennae reduces the level of internal and external interference.

2. **Isolation Capacitance**
   Improving the insulation between the device ground and the antennae AC ground improves the CMR. The use of batteries and insulation from the computer power supply are means of achieving a better CMR figure.

3. **Signal post-processing**
   The use of digital filtering, can help on removing the undesired common mode signals. Finite impulse-response digital (FIR) filters can be used, or even digital notch filters set to specifically remove the 50 Hz frequency component. However filters affect the phase information of the signal and should be used with care in order to minimize phase distortion.

4. **Driving the common-mode voltage through a resistor**
   A resistor that drives the common-mode potential appears in parallel with Z_G (see figure 3.21), generating a larger attenuation.

5. **Driving the common-mode voltage in closed loop RLD**
   Further improvement in CMR can be obtained by sensing the common-mode voltage at the differential amplifier outputs and feeding back the amplified difference. This method uses the RLD amplifier (see figure 3.22). This loop improves CMR by $(1 + A)$ where A is the amount of the closed-loop gain of the feedback loop. The real gain depends on the values of the feedback resistor, capacitance and output common-mode sensing resistor. The value of the closed-loop gain is given by equation (3.5).

   $$A = 2 * \frac{Z_F}{R_{CM}} \tag{3.4}$$

   Z_F being:

$$Z_F = \frac{R_F}{1 + sR_F C_F} \tag{3.5}$$

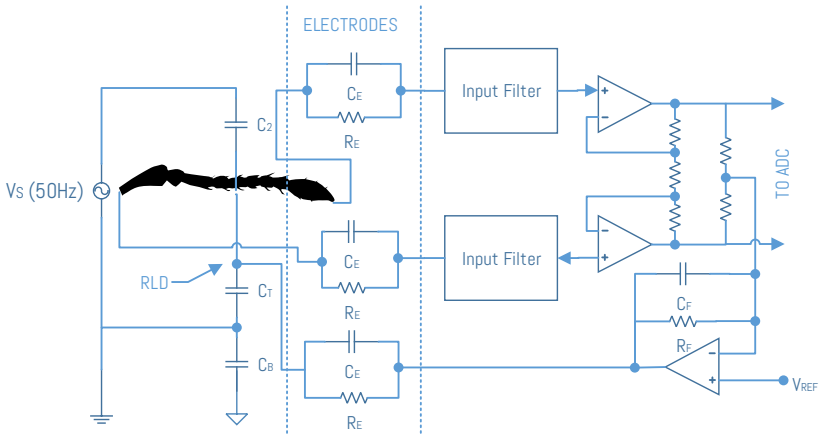

Figure 3.22: Improving CMR with closed-loop feedback (RLD). Figure adapted from (Acharya 2011).

3.7.2 Analog to digital converter

The ADS1299 is a low-noise, 8-channel, 24-bit analog front-end for bio-potential measurements (Texas Instruments 2012). The ADS1299 has a low-noise multichannel 24-bit delta-sigma ADC and also includes a built in PGA, internal voltage reference, and on board oscillator. The data rate of the ADC can vary from 250 Samples per second (sps) to 16 KSps depending on the internal decimation filter options. The digital filter cutoff frequency is tied to the ADS1299 data rate. In this particular application where the bandwidth is below 50 Hz, a data rate of 250 Sps is sufficient. At this data-rate the input referred noise of the ADC is below 1 µV. The ADS1299 also has some special built in features specifically designed for EEG applications. The most interesting of these features is the built in RLD feedback amplifier. The sensing of the common-mode signal can be turned on or off in the case RLD is not used. The RLD is the feedback signal (already mentioned in section 3.7.1.2) of the measured common-mode voltage taken at the positive and negative output of the PGA. The common-mode noise is typically dominated by the 50 Hz interference from mains AC. The gain and bandwidth of the the feedback loop can be adjusted with external resistor and capacitor. The feedback signal is then connected to the electrolyte pool through the third electrode, effectively reducing this kind of periodical noise. Using RLD more than 120 dB of CMRR can be achieved.

3.7.2.1 Analog input

The analog input of the ADS1299 is fully differential. If the PGA gain is 1, the input voltage ($IN_P - IN_N$) swings between $-V_{REF}$ and $+V_{REF}$. There are two methods of driving the analog inputs, single-ended or differential (figure 3.23 A) and figure 3.23 B) , respectively). When the input is used in single-ended mode IN_N is held at a common-mode voltage (typically mid-supply voltage) and IN_P swings around the common-mode voltage. The amplitude of the signal swings between ($Commonmode + 1/2V_{REF}$ and $Commonmode - 1/2V_{REF}$). When inputs are in differential mode the common-mode is given by $(IN_P + IN_N)/2$. In this mode both input signals swing from $Commonmode + 1/2V_{REF}$ and $Commonmode - 1/2V_{REF}$. The input stage of the ADS1299 is differential input and output amplifier (figure3.24). The PGA has seven gain settings. The gain setting can be changed by an internal register. The inputs of the PGA are CMOS so current noise is negligible. In the EAG recorder the gain setting used is 24, yielding a bandwidth of 27 Khz.

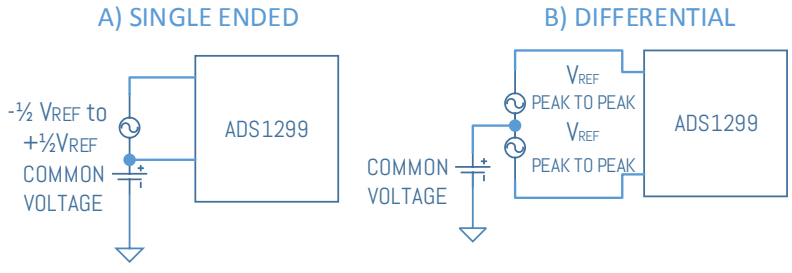

Figure 3.23: ADS1299 Analog input driving methods. A) Single-ended. B) Differential.

3.7.3 PGA settings and input range

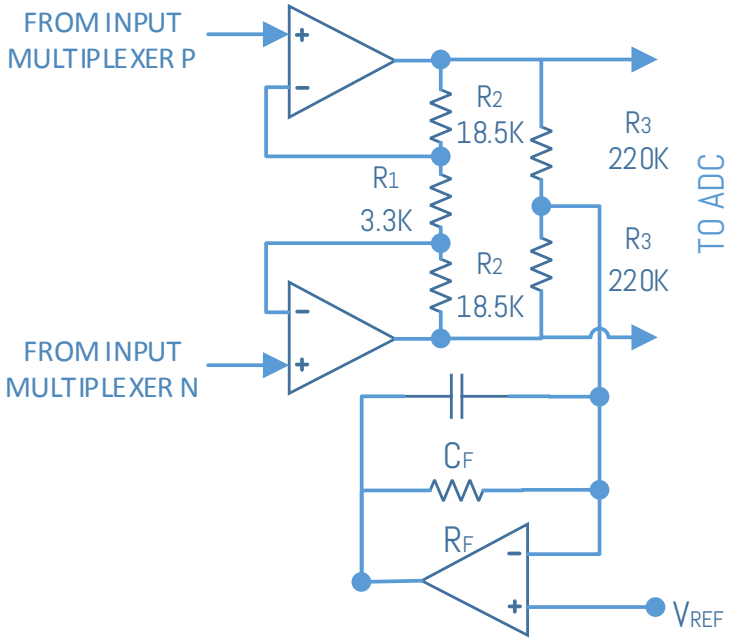

Figure 3.24: ADS1299 PGA block, shown with gain of 12x configuration.

3.7.4 Voltage reference

The ADS1299 has a built in bandgap 4.5 V voltage reference. This reference is generated with respect to $AVSS$. When in use V_{REFN} must be connected to $AVSS$. Two input channels out of the eight available will be used, at a sample-rate of 250 Sps. Typically EAG amplifiers use a gain setting of 100 or more (Van Der Pers and Minks 1998, Page and Koelling 2003). In this application the gain setting is 24. The high resolution given by the 24 bits is expected to compensate for the lack of gain. With careful PCB layout and shielding the 1 µV input-referred noise can be achieved yielding 66 dB of SNR.

3.7.5 MCU

PIC32MX460 was the chosen micro-controller. This MCU operates at a clock speed of 80 MHz, and has the necessary peripherals built in (e.g. SPI,USB, Universal synchronous asynchronous receiver transmitter (USART), General-purpose input/output (GPIO) and I^2C). This particular device was chosen because it has all the necessary peripherals and a demonstration card was available. PIC32MX460 has more than one SPI channel, which

opens the possibility of future upgrading with a memory device or wireless transmitter. The addition of memory would allow the local storage of acquired data, removing the need of a computer for data storage. An initial draft of the firmware flowchart was elaborated and is depicted in figure 3.25. The MCU implements the following functionality: configuration of the ADC, sending of data to computer VIA USB, starting and stopping the pump, switching the distribution valve, waking up the system from sleep upon USB connection and measuring the battery status.

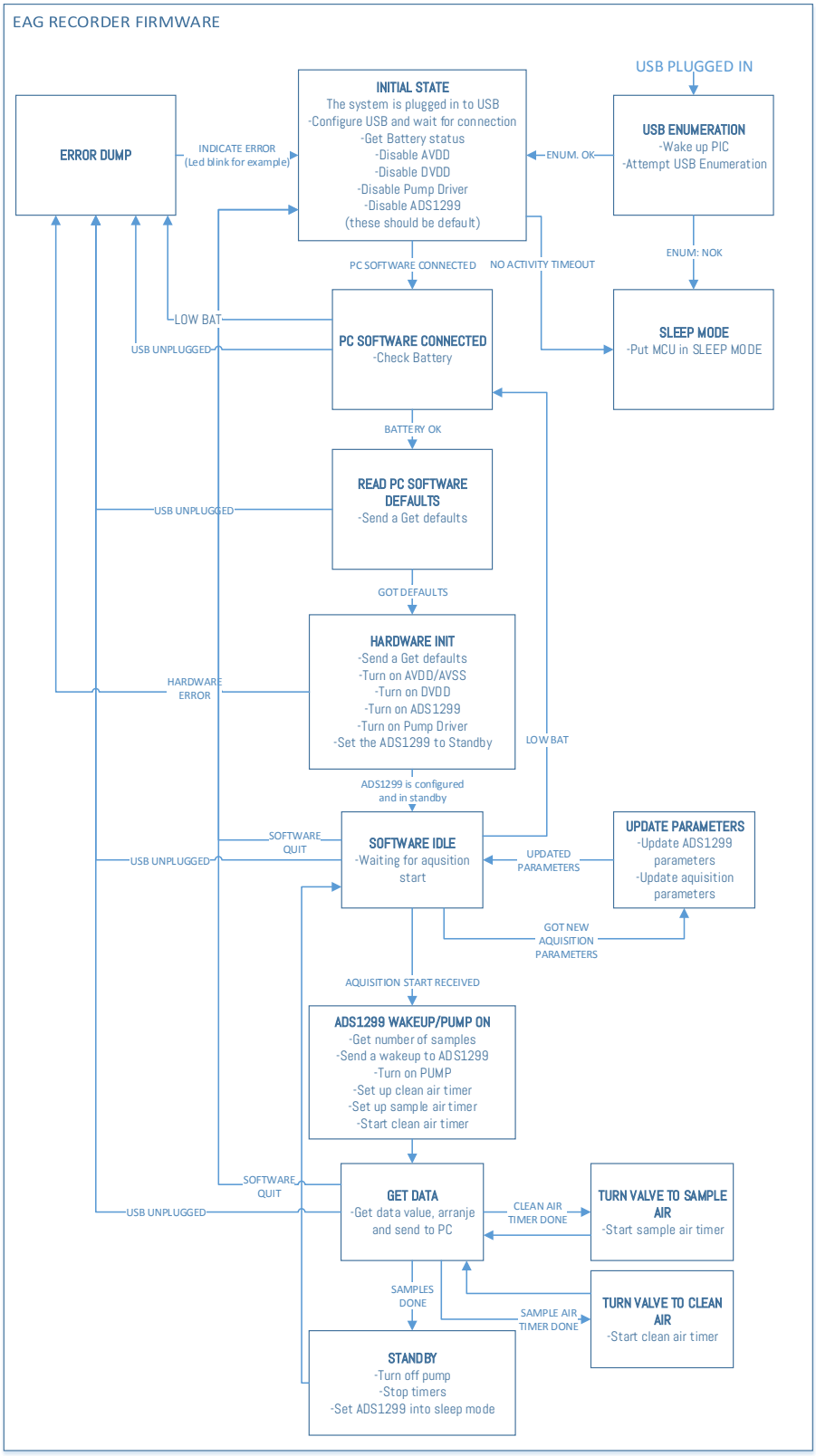

Figure 3.25: MCU firmware logic flowchart.

3.7.6 Air pump and valve drivers

DRV8830 and DRV8832 are very similar versions of the same integrated circuit (IC). Although the valve throttling could have been achieved using a simple pulse width modulation (PWM) driver controlled by the MCU, the integrated driver was preferred for the following reasons: Ease of use, using this device shortens the development time and, minimizes the risk of developing a discrete component solution; Rich set of useful features, DRV8830/32 has very useful features, like for example the capability to maintain pump speed independently of the battery voltage; Small size, the package of the device is only 3x3 mm. Two other features of these drivers that are interesting are the over-current protection, and the I^2C interface. The latter adding the capability of controlling the air pump speed.

3.7.7 PSU

The main power source of the EAG recorder is a 3.7 V lithium polymer battery. Battery power was chosen because of is inherent low noise nature. This battery in particular was chosen because of the small mass to capacity ratio. The battery voltage is monitored by the MCU, and the battery should be recharged when device indicates a low battery condition. TPS61025 was the chosen IC to power the final board of the EAG recorder. The IC is a 96% efficiency synchronous boost converter. The IC is designed to operate from a battery power supply and has a wide range of input voltages, from 0.9 V TO 6.5 V. This DC-DC converter has a nominal switch current of 1.5 A for a 3.3 V output, allowing to accommodate worst case scenario current demand (see table 3.8). The power budget, table 3.8 lists the larger power consumers of the EAG recorder. In order to generate the analog voltage required by the ADS1299 another 5 V DC-DC converter is also present. This second DC-DC converter is a low noise inductor-less type, in order not to introduce excessive noise in the ADC analog supply.

Table 3.8: Power budget of the major consumers. Power value is calculated for an absolute worst-case scenario.

Component	**3v3 Power** [mW]	**Peak current** [mA]	**Nominal Current** [mA]	**Notes**
Pump	475	438	150	
Valve	500	180	80	50ms Max cycle time
ADS1299	330	100	10	+10 mA on analog voltage
PIC32MX460	247.5	75	55	Current varies depending on too many factors
Total	**1552.5**	**793**	**295**	

3.7.8 USB insulator

Computers and specially computer power supplies are noisy elements. This noise is generated by the switching elements of the power supply but can also be generated by the internal clock ICs. The sudden turning on or off of loads in a computer is also a source ou noise in a computer. This noise can be present not only on the USB supply voltage, but it can also show up in the ground. The EAG recorder is battery powered but in order to communicate via USB the computer ground and the apparatus ground must be connected. In order to avoid this extra source of conducted noise the EAG recorder has the ADUM4160 from Analog Devices. This IC insulates the USB connection to +5 kV while allowing data to go through.

3.7.9 Printed circuit board design

The PCB is a 4 layer board using the top and bottom layers for signal and the inner layers for power and ground planes. Ground separation was also considered, and there are 3 separate grounds on this board, a USB ground, a digital ground and an analog ground. The USB ground is located in a small area near the USB connector. It is separated from the main digital ground by the USB insulator circuit. The analog ground is used for $AVDD/AVSS$ of the ADS1299. The separation of analog and digital grounds has the purpose of providing the ADC with a reference free of switching noise, both from the power supply DC-DC converters as well as the MCU.

This page intentionally left blank.

Chapter 4

Implementation

The implementation of the EAG recorder was also an iterative process. The developments in the early stages were focused on the validation of some of the design ideas, namely if the micro-controller would be adequate for simultaneously handling the data acquisition and the USB transfer. After these initial developments of a firmware nature, the activities were focused on the procurement and development of the 3D model. As the design concepts settled and the mechanical parts were available the construction of the device began. The quality of the ADS1299 acquisition with bleach chlorined electrodes gave positive indications that the overall design was feasible. The Faraday cage and the rest of the parts were ready for testing soon after. The final circuit was designed in parallel to these developments, but at a certain stage the time investment diverged towards a working prototype. The prototype had the possibility of proving the overall concept, with a shorter development time. The prototype would provide a similar performance since it contained the same electronics, and tests results could obtained with live insects. Another important part of the EAG recording system developed at this stage was the insect antenna simulator. This simulator consists on a signal generator and a voltage attenuator with an adapter to facilitate the connection of electrodes to the antennae holder. The simulator, already mentioned in section 3.5, allows the electrical verification of the EAG recorder by providing signals of the same magnitude of the insect antennal responses.

4.1 Initial firmware developments

In the beginning of this project the only hardware available for development was a CHIPKITpro MX4 board. This is a generic hardware platform for prototyping PIC32 projects. The initial developments with this board focused on several objectives. The first objective to achieve proficiency with the development tools and on the new it

MPLAB Harmony integrated software framework. The second objective was to get the PIC32 to send and receive commands through the SPI interface. The third and final objective was to get the PIC32 communicating with the PC through USB. At the time there was no possibility of communicating with an ADS1299 so the Digilent Analog Discovery was used to intercept SPI messages. The same Analog Discovery was used as a signal generator for the testing of the EAG recorder. The SPI messaging was successfully implemented, and the next step would be USB. USB is a complex BUS protocol where the host is the master and devices are set up as slaves. The EAG recorder would be set up as a device with a series of interfaces and endpoints. These parameters are read by the host controller on the PC and they tell the PC what kind of device has been plugged in. Initially it was not clear what would be the most suitable device type for the EAG recorder. It could either be a Human interface device (HID) or set up as an audio device. Given the complexity of setting up as an audio device and the fact that the data rate of the ADS1299 is 250 Sps the best candidate was HID. A good example of a HID device is a computer mouse. The two advantages of HID are simplicity of use on the micro-controller side and the fact that Windows and other operative systems have built-in drivers to handle HID devices, so no drivers were necessary on the PC side. During these initial developments a HID device was also implemented in the CHIPKITpro MX4 board.

4.2 Prototyping the EAG recorder

The prototype of the EAG recorder was built as designed with the exception of the electronics. An effort was made to use the same electronic components as the ones chosen for the final circuit. The core of the prototype electronics is the evaluation board ADS1299EEGFE-PDK which sits on top of the Texas instruments MMB0 modular evaluation motherboard. A ChipKit Pro-MX4 board with a PIC32MX460F512L was also included. This board is representative of the micro-controller solution of the final design and it was planned as the hardware platform for the development of the micro-controller firmware. Although the prototype data extraction is done through the MMB0 board USB connection, the SPI bus connection from the ADS1299 is made allowing an easy switchover to the PIC as the main micro-controller of the prototype. This configuration was planned to a later stage where the prototype would be used as a firmware development platform and used the pic's own USB output. The valve and air pump are driven with DRV8832 chips from Texas Instruments. A development kit is also available for this chip and two were included in the prototype. The prototype connects to a laptop computer and data is acquired to a modified version of Texas Instruments EVM software. The prototype is powered from a 6 Volt battery pack to improve the noise performance. In order to facilitate transportation and to improve the general reliability of the prototype all the components were assembled on a plywood board. Figure 4.1 depicts the EAG recorder prototype.

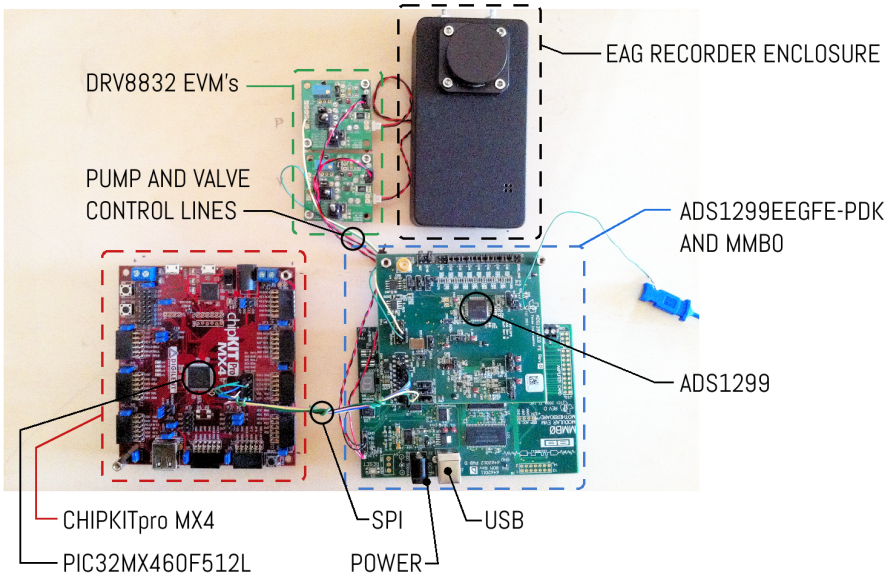

Figure 4.1: EAG recorder prototype. Electrode connections from the main enclosure to the ADS1299 EVM were not soldered when the photo was taken.

4.2.1 Faraday cage

The Faraday cage was built according to the design described in section 3.6.1. In order to drill the lateral air output threaded hole and bottom cap holes for the electrode contacts, a drill guide was SLA printed and used on the drill press. After the assembly of the bottom cap to the Faraday cage tube, the drill guide is inserted thus guaranteeing perfect alignment of the six bottom holes and lateral hole. Following the drilling of these holes the lateral and central bottom hole were threaded. The bottom cap was disassembled and the antenna tube electrode base could be assembled. This base is a SLA printed part to which the electrode contact bases are attached, as well as the alignment magnets. Both the electrode base contacts and alignment magnets were glued with two part epoxy. The part with the electrode contact bases already glued in place was then assembled on the bottom metallic cap of the Faraday cage and also glued with two-part epoxy. The last step was the assembly of the tube bulkhead fittings, these bulkheads are threaded (M3) and therefore the process of assembly is straightforward.

4.2.2 Electrodes and antennae holder

The electrodes were manufactured from 99.9% silver 0.2 mm wire. The process of manufacture consists on cleaning the wire with isopropyl alcohol and then wrapping the wire to the head of the spring terminal. Sn96Ag4 solder is then applied to the wire wrap. The wire is trimmed to length and cleaned in isopropyl alcohol in order to remove solder flux residues. The finished electrodes are driven into a piece of *Styrofoam* leaving the

wrap area and the silver wire protruding in order to be chlorided. The chloriding method used was bleach immersion for 30 minutes. Chloriding all electrodes simultaneously is a better approach as it improves the consistency of results. The end result is a dull dark gray coating on the wire surface instead of the silver metallic shine. The antennae holder was SLA printed. The parts were wet-sanded with 600 grit followed by 1000 grit in order to improve the surface finish. The electrodes are then assembled on to the antennae holder and glued to their cavities with Permabond UV6302 UV curable adhesive. The advantage of the UV curable adhesive is that a mild fixation can be achieved on all electrodes for positioning, followed by the application of a thicker layer to bury the contacts bases in the glue. However, the quality of the results obtained with UV6302 were not entirely satisfactory. Although the handling characteristics are good and the adhesive has the low viscosity required, this particular glue tended not to fully cure with the UV illumination system used. Another idea was to use the same resin used for the printing of the part itself as an adhesive but the option was not evaluated. Figure 4.2 depicts the manufacture process.

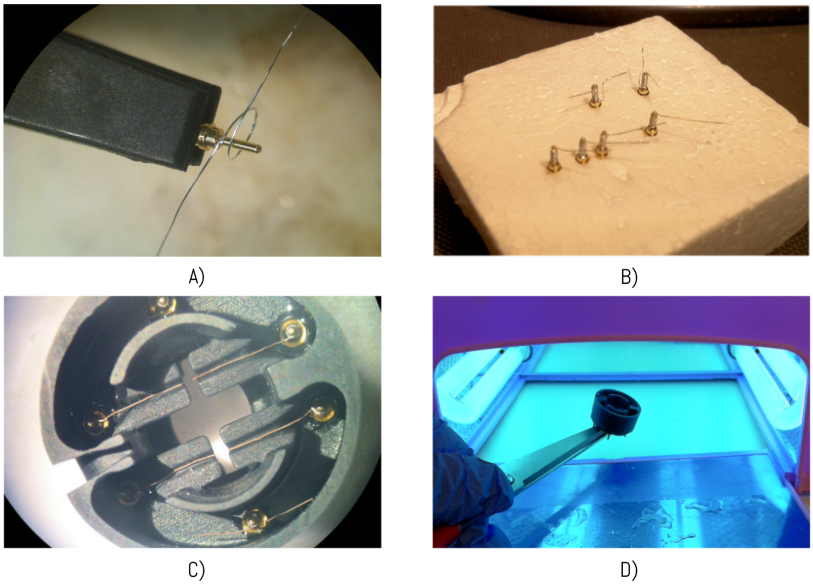

Figure 4.2: Antennae holder manufacture. A) Wrapping of the siver wire to the terminal. B) Finished electrodes attached to *Styrofoam* block ready for chloriding. C) Electrodes assembled in antennae holder ready for glue application. D) UV exposure of Permabond glue

4.2.3 EAG recorder enclosure

The EAG recorder enclosure was manufactured from a Hammond Mfg. 1590BBK metal case. The holes on the enclosure and the top opening for the Faraday cage tube were drilled with the help of two SLA printed drill guides. The first guide for the top and frontal openings, the second guide for the light guide and USB connector area. The USB

drill guide is depicted in figure 4.3. The top opening was then filed to final shape using a Dremel tool with a sandpaper disk, and the squared shape of the USB connector hand filed. The SLA printed guide was used a reference for final size. The end result proved to be very accurate and involved only the use of a drill press and manual tools.

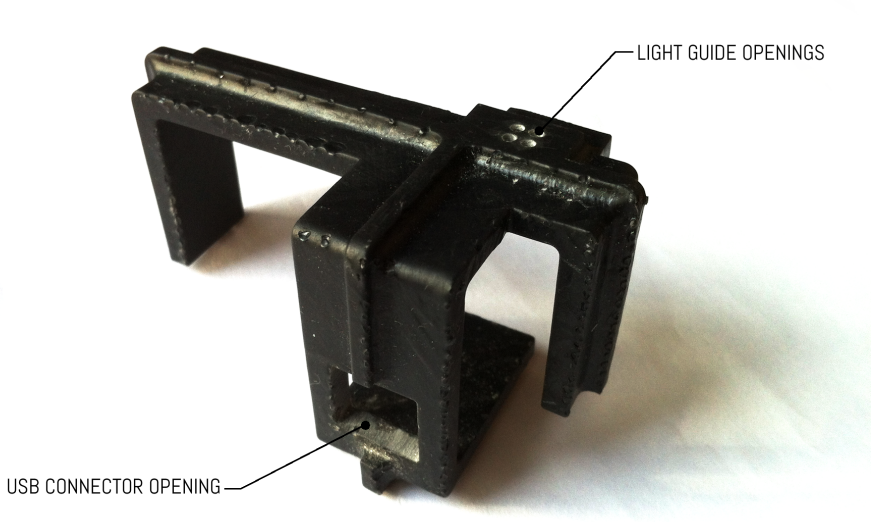

Figure 4.3: EAG recorder enclosure drill guide. The drill guide is an SLA printed part. The part allowed the drilling of the enclosure to a tight tolerance without the use of positioning stages.

After sanding of the remaining SLA printed parts to remove print marks, the air pump is assembled to it's support cradle. The pump is attached with a cable tie, and a pair of EPDM dampers are glued to the base with two-part epoxy glue. The whole block is then glued to the PCB support cradle. The next step is the assembly of the valve, which is also attached with a cable tie. The whole assembly can then be fitted in to the metal enclosure. There are eight extensions of the PCB cradle that stand against the sides of the enclosure, these extensions already mentioned in section 3.6 were thought as tensioners against the metal case, and in a final assembly glue spots would be applied to permanently hold the cradle inside the metal enclosure. These glue spots were not applied to allow a possible disassembly without damaging the parts. M3 threaded inserts were also pressed on the PCB standoff posts and can be seen in figure 4.4. The bulkheads were fitted and the Faraday cage assembly mounted to the main enclosure. The air pump and valve were fitted with JST GHR-02V-S miniature connectors, and allowed enough cable length to reach the external drivers. The last step of the assembly was the fitting of the air tubes. The tubes were formed from polyolefin heat-shrink tubing material. Given their elastomer nature it is not possible to perform tight bends without creasing the tube, therefore a bending strategy had to be devised. The tubes were processed as follows, first the bend location was determined and marked on the tube. A section of 10 cm of 0.5

mm solder wire was wrapped around a piece of piano wire forming a solder spring. This spring was then inserted in the tube leaving a straight length of solder wire extending to the outside. Heat was applied while simultaneously bending the tube. The heat was then removed without relieving the bend. The tube shrinks around the bend and by the time it cools off the bend is formed permanently. The solder wire is soft enough to allow being pulled out. This procedure was performed to form all the bends, and the tubes were fitted in their respective locations. The last step was to apply heat to the bulkheads to shrink the tube around the nozzles in order to form an air-tight connection.

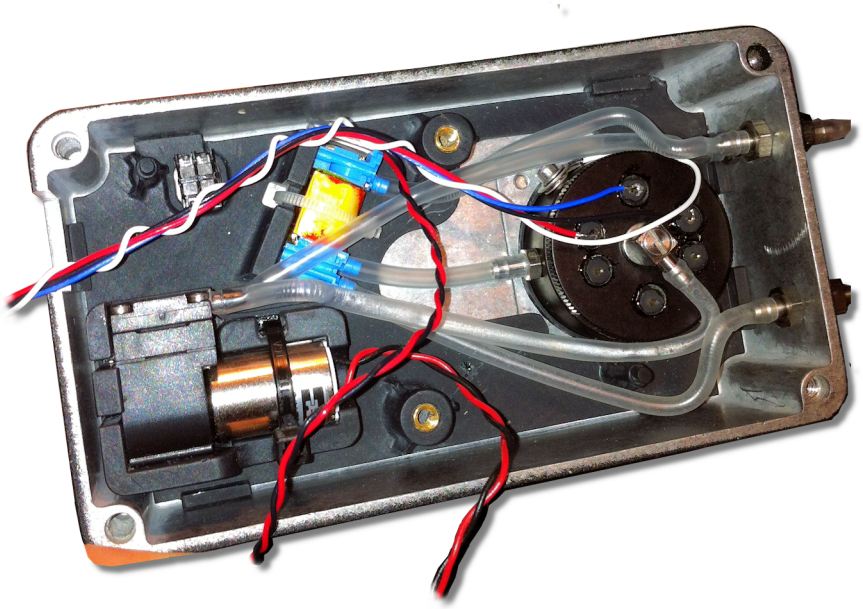

Figure 4.4: EAG recorder enclosure. The air pump and cradle can be seen on the left as well as the valve just above it. The Faraday cage to the right is already assembled with an electrode pair wired. White wire is the case ground connection, this connection is screwed to the outside of the Faraday cage tube.

4.2.4 Prototype electronics

The MMB0 motherboard is equipped with a TMS320VC5509APGE Digital signal processor (DSP) and is able to acquire data from the ADS1299 and send it to the computer via USB. Texas Instruments provides a Labview software to interface with the ADS1299, which the author modified to perform the extra actions of turning on the pump and switching the air valve, from clean air to sample. The MMB0 board is a generic board Texas Instruments uses for demonstration purposes and therefore contains a series of features which will not be necessary for this project. The board also includes a powerful DSP chip, which in this application is merely handling the task of data retrieval from the ADS1299. The board to the left on figure 4.1 is the Digilent CHIPKITpro MX4 board. This is the same board mentioned at the beginning of this chapter. The CHIPKITpro board has its SPI bus connected to the ADS1299 SPI data port.

The board was included in the prototype in order to allow the development and debugging of the firmware. The remaining boards included in the prototype are the air pump and valve drivers. These boards are DRV8832 EVM's, the same chip planned on the final electronics design (see section 3.7.6). For simplicity, the GPIO ports of the ADS1299 were used to trigger the pump and valve controls. These registers are available on an one of the headers of the ADS1299 EVM and can be controlled by the software.

4.2.5 Prototype acquisition software

The acquisition software of the prototype was adapted from Texas Instruments own demonstration software for the ADS1299. This software is written in Labview. Labview programming strategies vary, and in this specific case the software is event driven. The software establishes an event queue and processes those events sequentially depending on its state and user inputs. The event-driven nature of the software blocks the sending of commands to the ADC during acquisitions. A workaround for this problem was to switch the distributor valve to the correct air input before beginning the acquisitions, but during the tests there was no possibility of switching the valve back to a clean air source. This shortcoming led to a more careful presentation and handling of the stimuli. The software allows the setting of all of the ADC internal parameters, number of samples to acquire and also allows export of the data to Microsoft Excel. A bug in the original version from Texas Instruments prevented the individual setting of the RLD positive input sensing switches. This bug made the sensing of the positive input side of the input amplifier impossible. The bug was fixed and the software now has the capability of individually setting the positive and negative inputs as sources for RLD feedback.

4.3 Insect antennae simulator

The insect signal simulator consists on a signal generator capable of delivering voltage signals in the 10 to 1000 µV range. The signal generator is a Digilent Analog Discovery. The signal is delivered through a pair of AgAgCl electrodes immersed in the antennae holder electrolyte. The attenuator resistors are soldered on this part. To connect the signal generator to the antennae a 30cm section of coaxial cable was used. Figure 4.5 depicts the antennae simulator. The signal generator connects to the computer via USB, this allows the simultaneous use of the computer for antennae simulation and data acquisition. The ground on the signal generator side was not connected to the ground of the EAG recorder to avoid creating a ground loop. The generator is capable of generating signals in the 1 mV to 5 V range, but use of the lower end of the range was avoided because of crossover artifacts on the signal. In order to minimize these artifacts the range used was 100 mV to 1 V before attenuation. The attenuator was calculated with a simple voltage divider (See equation 4.1) and no buffering was added as the ADS1299 has very high input impedance.

The resistors used were 909 kΩ and 1 kΩ precision 1% tolerance. These values were chosen in a great part by availability reasons. The attenuator has a 1:1.1E^{-3} ratio.

$$Ratio_{ATT} = \frac{R2}{R1 + R2} \tag{4.1}$$

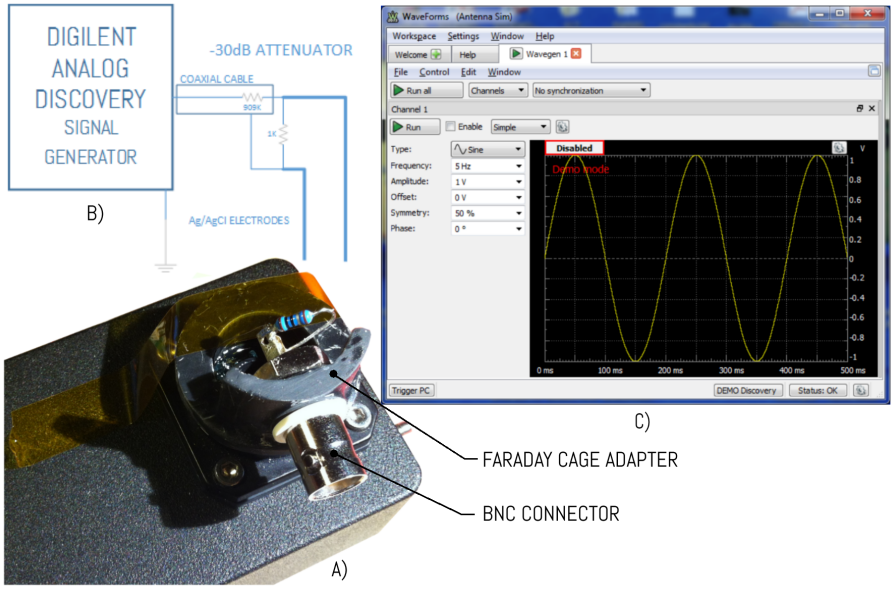

Figure 4.5: Insect signal simulator. A) Faraday cage adapter inserted. B) Block diagram of the simulator. C) Screenshot of the PC side control software.

4.4 Printed circuit board Layout

The software used for the circuit board layout and schematic was Altium Designer. This software allows the representation of the board in 3D, a feature that is of special interest in compact designs, alerting the designer for collisions between the electronic components and the mechanical elements. Figure 4.6 shows the designer view of the board. Work on the PCB was not completed within the project time-frame, a view of the board layout and layer stack-up is shown in 4.7.

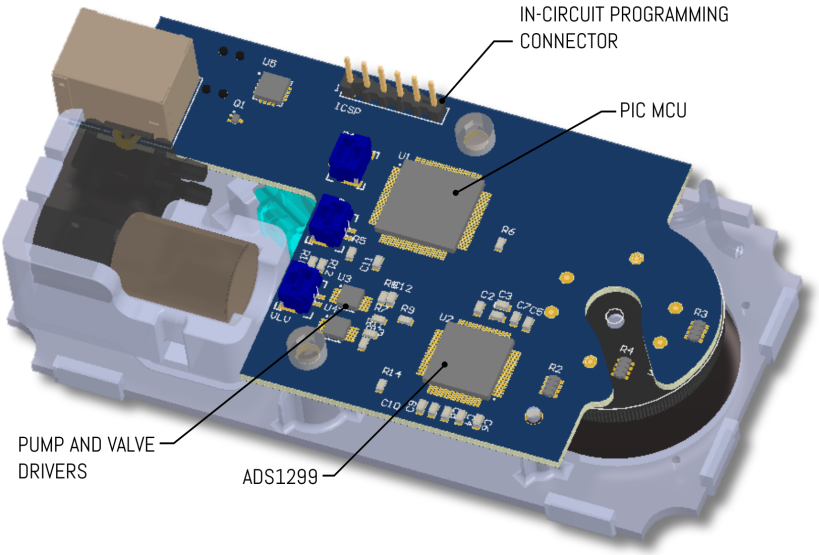

Figure 4.6: 3D view mode of the EAG PCB in Altium Designer

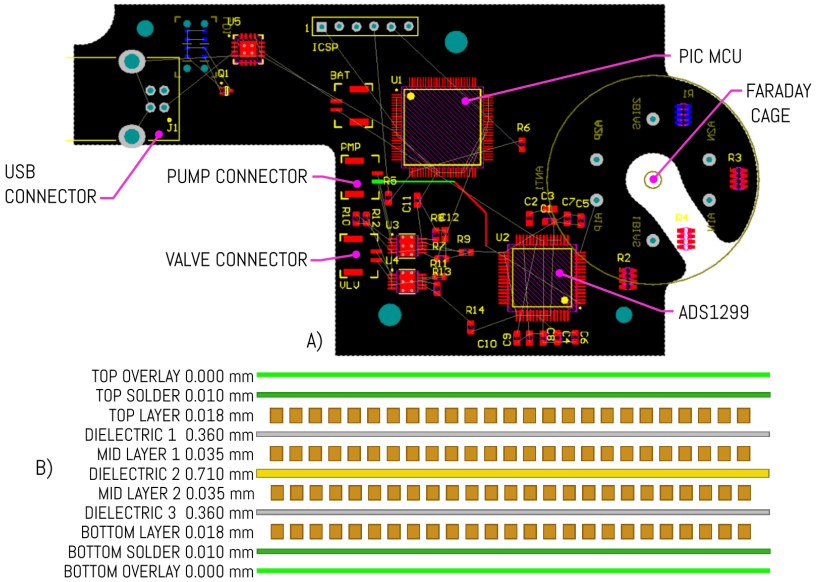

Figure 4.7: EAG PCB top layer and layer stack-up A) Top copper layer of PCB with main components identified. B) PCB layer stack-up details.

This page intentionally left blank.

Chapter 5

Test results and discussion

5.1 Introduction

A series of tests were conducted in order to evaluate the performance of the prototype. These tests followed the logic sequence previously presented in section 3.5. As results were gathered the test sequence was adjusted in line with the findings. The objective of these tests was the evaluation of the concepts chosen during the design stage, namely:

1. Verify if the antennae holder design would be practical and robust.
2. Verify if the electrode construction method would give reliable measurements.
3. Verify if the air pump performance would allow the precise measurement of the antennae responses.
4. Verify if ADS1299 would have the sensitivity and gain expected to allow the measurement responses of the antennae.
5. Test the noise performance with no active feedback versus RLD.
6. Evaluate the simultaneous acquisition of antennal responses.

5.2 Prototype electrical tests

In order to test the prototype a special test setup was created using the insect antennae simulator, already mentioned in section 4.3. The antennae simulator was connected to the antennae holder with conductive gel. The general test setup for the electrical tests is depicted in figure A.1. In order to evaluate the performance with and without RLD this setup was connected with two configurations. The naming convention used for

these two configurations are "two electrode configuration" (2EC) depicted in figure A.2 and the "three electrode configuration" (3EC) depicted in figure A.3. The tests attended requirements 4.1, 4.2 and 5.1. Linearity was not covered by the requirements but its an important parameter to be verified when it comes to measuring real antennal responses. All the measurements were made with the same ADC settings except where noted, these settings are listed in table 5.1. The tests were conducted with the prototype powered by batteries and the computer disconnected from the mains.

Table 5.1: ADS1299 parameters used during the prototype tests.

Setting	Value	Notes
Output data rate	f(MOD)/64 (250 sps)	
Reference buffer	enabled	
Bias measurement	open	
Bias ref signal source	(AVDD-AVSS)/2	internal mid-supply voltage
AVDD	+2.5 V	
AVSS	-2.5 V	
Channel 1 settings	enabled, PGA gain 24	
Channel 2 settings	enabled, PGA gain 24	during two channel acquisitions
Lead off detection	Not used	
Bias sense	Ch1-P,Ch1-N,Ch2-P,Ch2-N	used in RLD mode
GPIO4	Pump on/off	
GPIO3	Valve clean air/ Sample air	used by software

5.2.1 Linearity test

The linearity of the EAG recorder was measured by generating sinusoidal signal with 0.1 to 1 V amplitude and a frequency of 5 Hz, and then attenuating the signal. The signal was recorded for a period of 5 seconds. The initial objective was to verify only the 100 µV to 1 mV range, since this is the amplitude range of the antennae signal. But for completeness the 10 µV to 100 µV was also measured by replacing the 1 kΩ resistor of the attenuator with 100 Ω. Measuring the lower range also allowed to verify the sensitivity of the device (requirement 4.1). The maximum of 2 mV input of requirement 4.2 was not verified. The setup used for the linearity test was the 3EC (figure A.3). The resulting plot is depicted in figure 5.1. The methodology of analysis was to filter the acquired signal with a high pass filter with a F_C of 0.2 Hz to remove signal drift, and then perform a sinusoidal fit. The amplitude of the fit was used as measured amplitude and the error of the fit as Y error on the plot. The X values were calculated with the ratio of the resistors and the error used the maximum mismatch of tolerances. Altough the ADC has good linearity characteristics the slope of the the two ranges does not match. This leads to the conclusion that the assumption that the loading of the attenuator with the input impedance of the ADC would not interfere with the amplitude measured was wrong. The resistor change did affect the amplitudes measured, and although linearity is demonstrated, the method is not recommended to obtain calibration values.

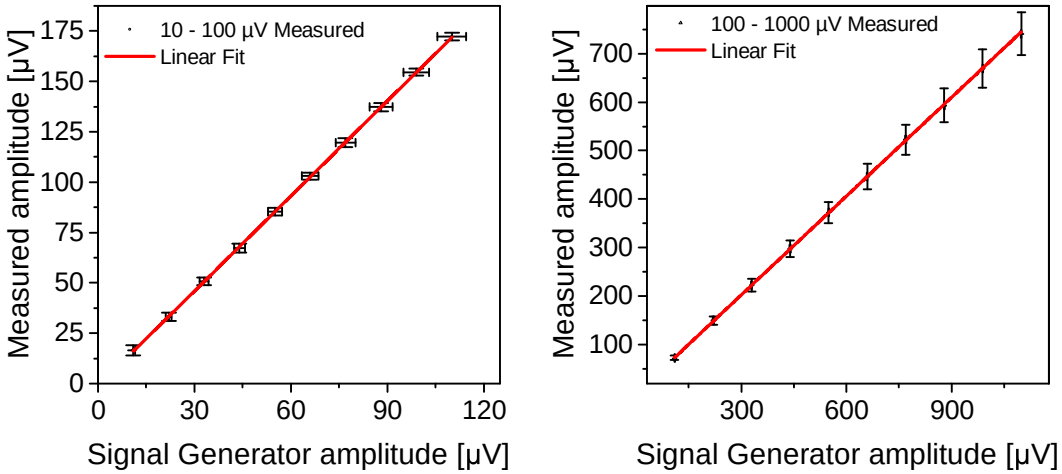

		Value	Standard Error
Fit Amplitude 10-100	Intercept	-1,26733E-6	2,09801E-6
Fit Amplitude 10-100	Slope	1,57351	0,04366

		Value	Standard Error
Fit Amplitude 100-1000	Intercept	-1,6554E-6	5,33863E-6
Fit Amplitude 100-1000	Slope	0,67941	0,01897

Figure 5.1: Linearity plot. Left) 10 µV to 100 µV range. Right) 100 µV to 1 mV range.

5.2.2 Noise

The main reason behind the inclusion of a third electrode was noise reduction. This third electrode would set the common-mode voltage of the electrolyte and would re-adjust this voltage actively to counteract the external periodical noise (RLD technique). In order to evaluate noise, the 2EC and 3EC were tested in the same conditions. Clearly the 3EC with RLD has less noise (figure 5.2). In order to get more insight into the nature of this noise a fast Fourier transform (FFT) of the signal is presented in figure 5.3. The signal analyzed is a 5 Hz 100 µV sinusoidal with 5 seconds of duration. As expected the signal with no RLD has a higher content of 50 Hz noise. Figure 5.4 depicts the a signal histogram of a 5 second acquisition with the ADC inputs shorted. The noise histogram fits a gaussian distribution. The measured 3 σ error is below 1 µV complying with req. 5.1.

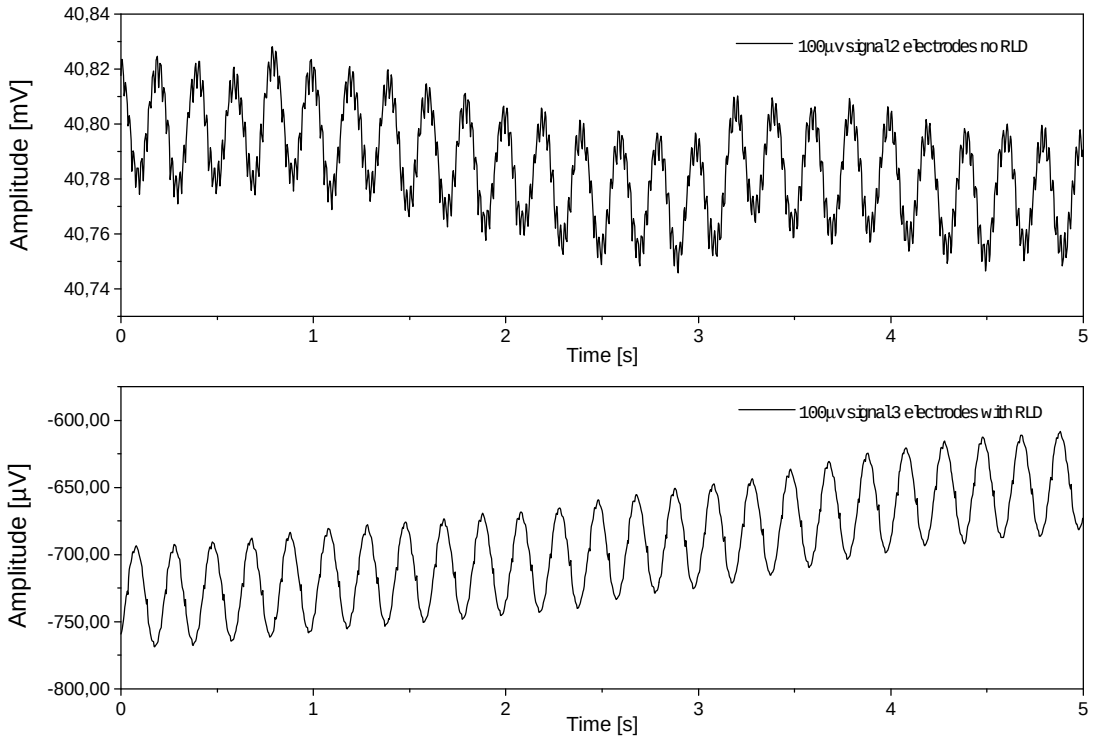

Figure 5.2: A comparison of the signal obtained with 2EC and 3ECs. Top) 100 µV 2EC. Bottom) 100 µV 3EC.

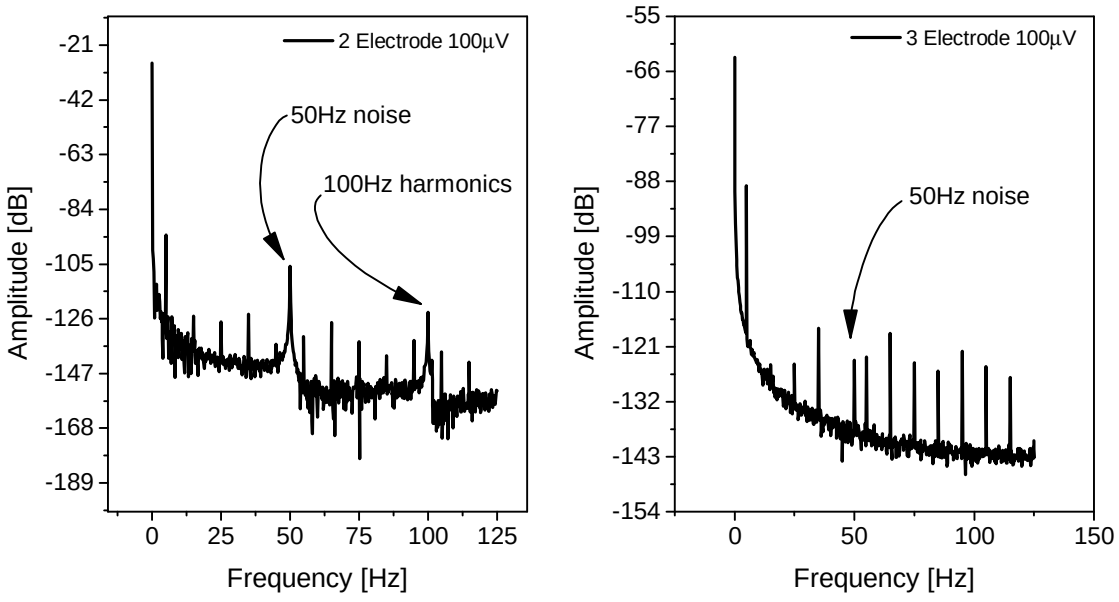

Figure 5.3: A comparison of the FFT of the signal of figure 5.2. Left) 2EC. Right) 3EC.

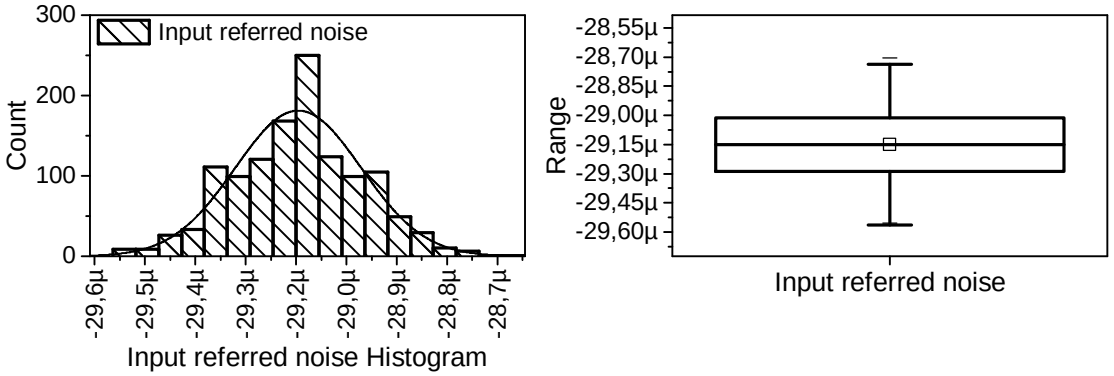

Figure 5.4: Noise histogram. Right) Box diagram showing 1σ and 3σ values. Left) Histogram of the measured system noise with the inputs shorted.

5.2.3 Sensitivity

The sensitivity of the EAG recorder was measured with the antennae simulator. Using the data acquired for the evaluation of linearity the sensitivity value is shown as the minimum distinguishable signal, in this case the 10 µV step. Figure 5.5 depicts a 10 µV signal, the superimposed noise is significant but the 5 Hz sinusoid is still measurable, complying with requirement 4.1.

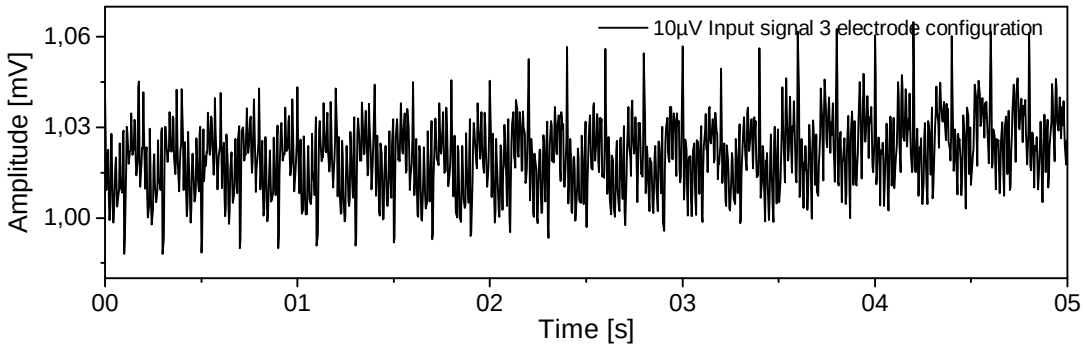

Figure 5.5: 10 µV Signal measured with the 3EC.

5.3 *G. platensis* tests

G. platensis tests started as soon as the antennae holder was finished. Only female specimens were used for olfactory response measurement. The first tests were conducted without the third electrode, in the 2EC. Only one channel was available so two simultaneous channel measurements were not possible to obtain. The protocol used is listed in table 5.2. The 100% paraffin stimulus was used as a control for mechanoresponse and a control for the olfactory response to paraffin itself, which was

expected to be close to zero. A dose-response curve of the obtained responses is depicted in figure 5.9. The second run of tests were conducted with the 3EC configuration and with two simultaneous antennae. Although better noise performance was obtained with the 3EC configuration, no consistent insect olfactory responses were obtained. The protocol used is listed in table 5.3. A test result with one insect is presented in figure 5.10. Dose-response was not evaluated. Literature often recommends the use of humidified air to perform EAG recordings (Qiu 2005, Park and Baker 2002, SYNTECH 2004). In order to investigate if the difficulty of detecting olfactory responses was due to humidity, a humidifier was built and adapted to the recorder input. The humidifier is depicted in figure 5.6. It consists on a distilled water container with an input tube immersed in water and an output tube above the water level. The container is air tight except in the input and output connections. The air intake line is fitted with an activated charcoal filter to filter airborne odors. Embedded in the output tube is a syringe needle used to introduce the stimuli. After a series of tests with no responses with humidified air, the prototype was reset to 2EC configuration with simultaneous antennae acquisition. Measurements with the humidifier used the same protocol as the previous tests (see table 5.3). This protocol did not involve a control stimuli because evaluation of the control stimuli used in the first 2EC tests revealed no response to the control. However the responses obtained injecting the sample through the syringe needle of the input tube revealed a substantial EAG response that was independent of the odor concentration. In order to investigate if these responses were due to the disturbance of the *G. platensis* mechanoreceptors a test was run without stimuli. The test consisted on squashing the air delivery tube at 1 minute intervals. The result obtained is plotted in figure 5.11. The conclusion was that the injection of the stimuli in the air delivery tube was causing a pressure variation or air-flow disturbance that was effectively being sensed by the mechanoreceptor sensilla. To counteract this undesired response the humidifier was removed and another strategy was adopted. The new strategy consisted on increasing the pump speed in order to get more aspiration. The reasoning behind this strategy was that instead of injecting the stimuli, the delivery should be done by aspiration. The syringe piston would be removed and the back of the syringe would be exposed to the intake tube. This strategy would deliver the sample without any disturbance to the air flow. An acquisition with this strategy revealed antennal response to stimuli, Figures 5.12 and 5.13. A dose-response was plotted (figure 5.14) revealing a positive dose-response curve, but with a higher average as the one measured in the first tests with the 2EC configuration.

Table 5.2: Protocol used for first 2EC configuration tests.

step	time	stimulus [Vol/Vol]
1	10s	Paraffin 100%
2	1m10s	Verbenone 10^{-6}
3	2m10s	Verbenone 10^{-4}
4	3m10s	Verbenone 10^{-2}

Table 5.3: Protocol used for 3EC configuration tests.

step	time	stimulus [Vol/Vol]
1	10s	Verbenone 10^{-5}
2	1m10s	Verbenone 10^{-3}
3	2m10s	Verbenone 10^{-1}

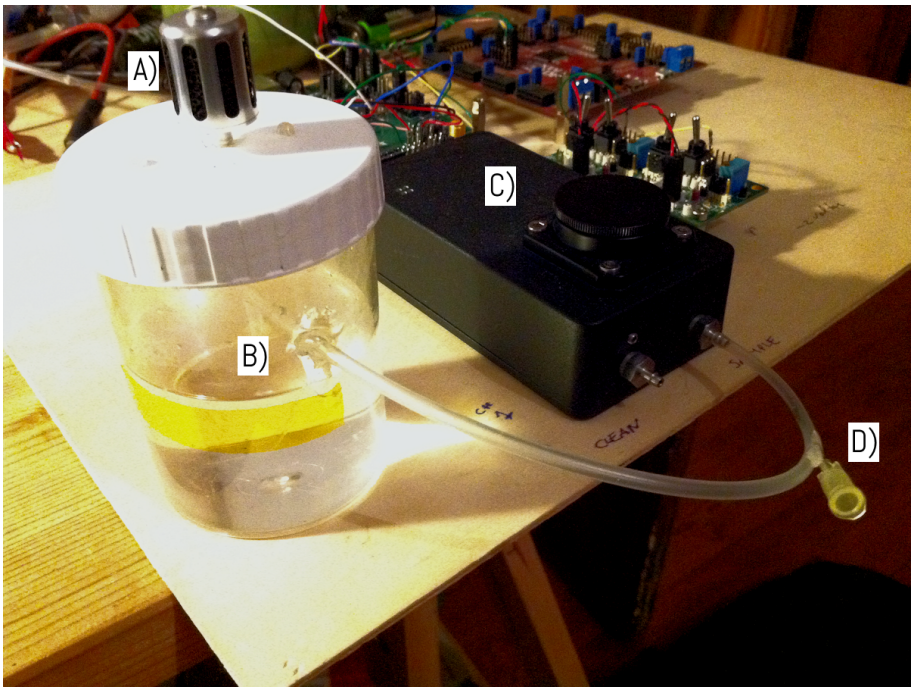

Figure 5.6: Humidifier. A) Air intake, activated charcoal filter. B) Humidifier vessel, C) EAG recorder, D) Stimuli injection needle.

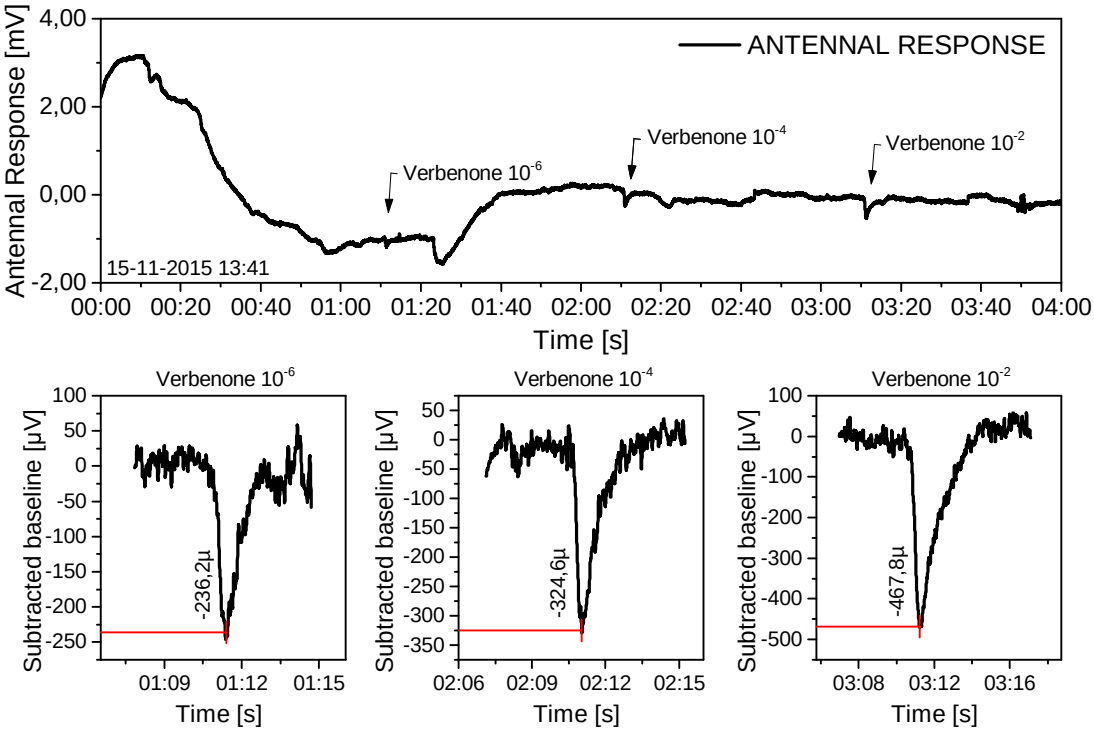

Figure 5.7: Insect 1, 2EC configuration, single electrode acquisition with verbenone stimuli. 10^{-6} puff at 1:10m, 10^{-4} puff at 2:10m and 10^{-2} puff at 3:10m

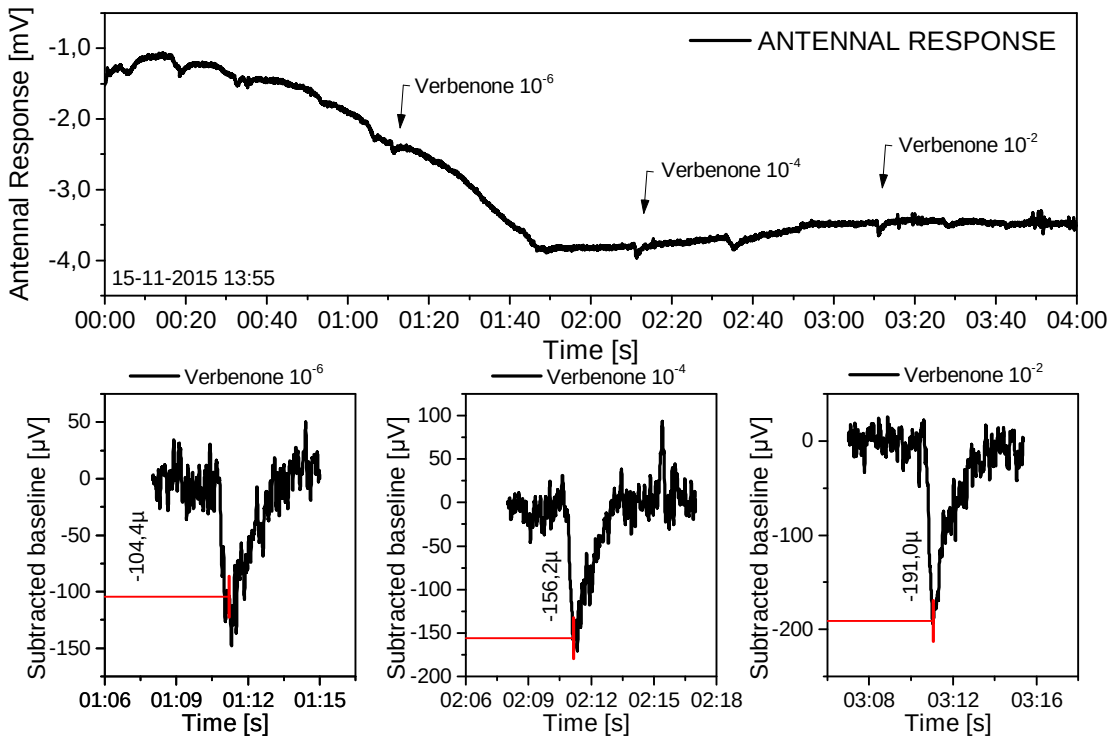

Figure 5.8: Insect 2, 2EC configuration, single electrode acquisition with verbenone stimuli. 10^{-6} puff at 1:10m, 10^{-4} puff at 2:10m and 10^{-2} puff at 3:10m

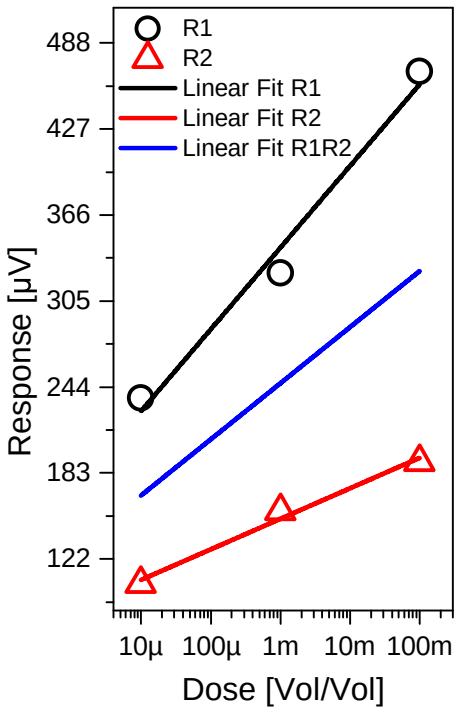

Equation	y = a + b*x		
Weight	No Weighting		
Residual Sum of Squares	4,8143E-11	4,99191E-10	
Pearson's r	0,99363	0,99082	
Adj. R-Square	0,97461	0,96346	
		Value	Standard Error
Run 2	Intercept	2,1542E-4	8,37906E-6
	Slope	2,16319E-5	2,45314E-6
Run 1	Intercept	5,16568E-4	2,69812E-5
	Slope	5,79059E-5	7,8993E-6

Equation	y = a + b*x		
Weight	No Weighting		
Residual Sum of Squares	6,1294E-8		
Pearson's r	0,54056		
Adj. R-Square	0,11526		
		Value	Standard Error
Concatenated Data	Intercept	3,65994E-4	1,05704E-4
	Slope	3,97689E-5	3,0947E-5

Figure 5.9: Dose-response for verbenone. Run 1 corresponds to the data obtained from figure 5.7 and Run 2 corresponds the data from figure 5.8.

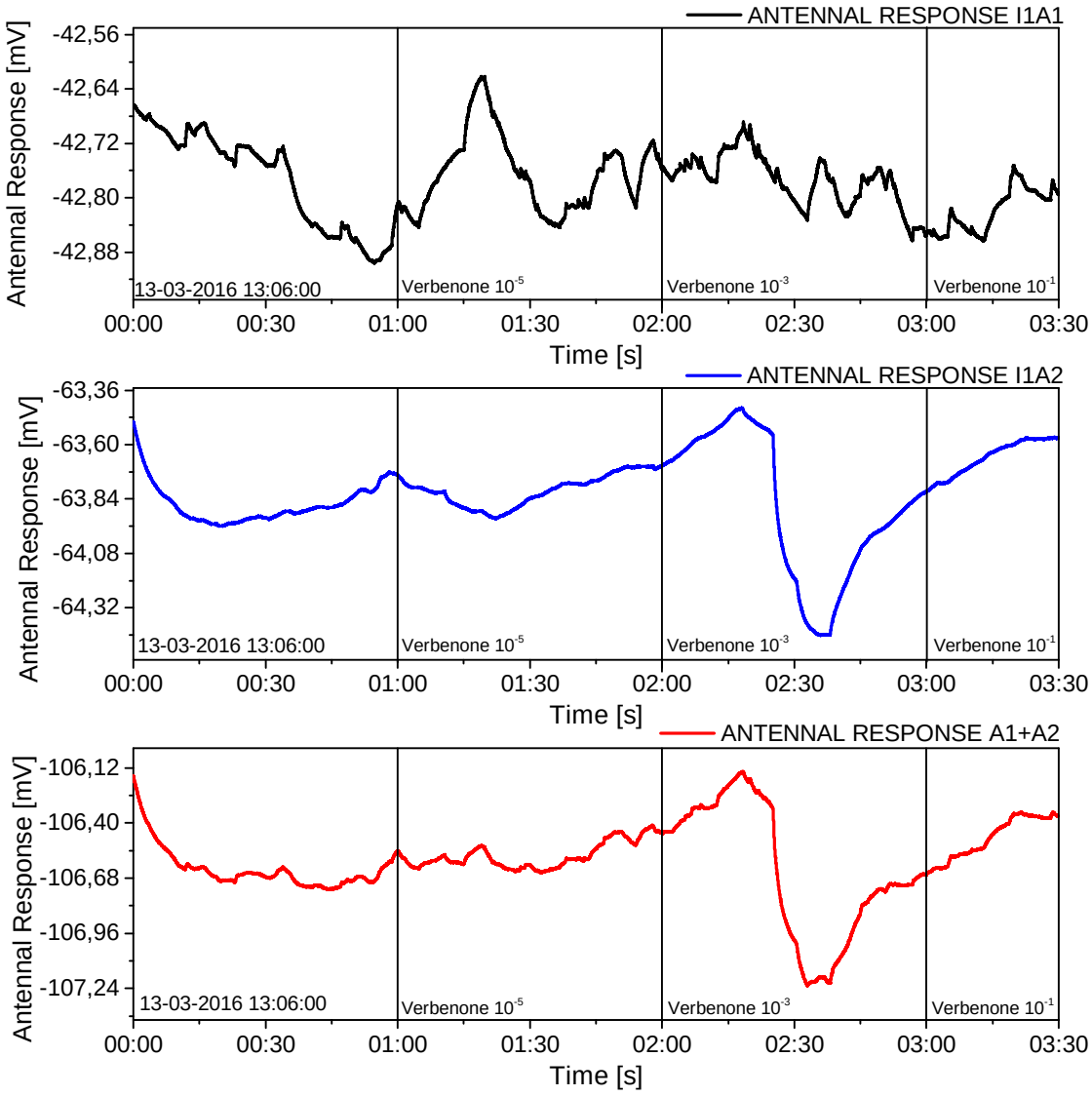

Figure 5.10: Insect 1, 3EC configuration acquisition plots. A1 - Antenna of channel 1, A2 - Antenna of channel 2, A1+A2 - Sum of both plots.

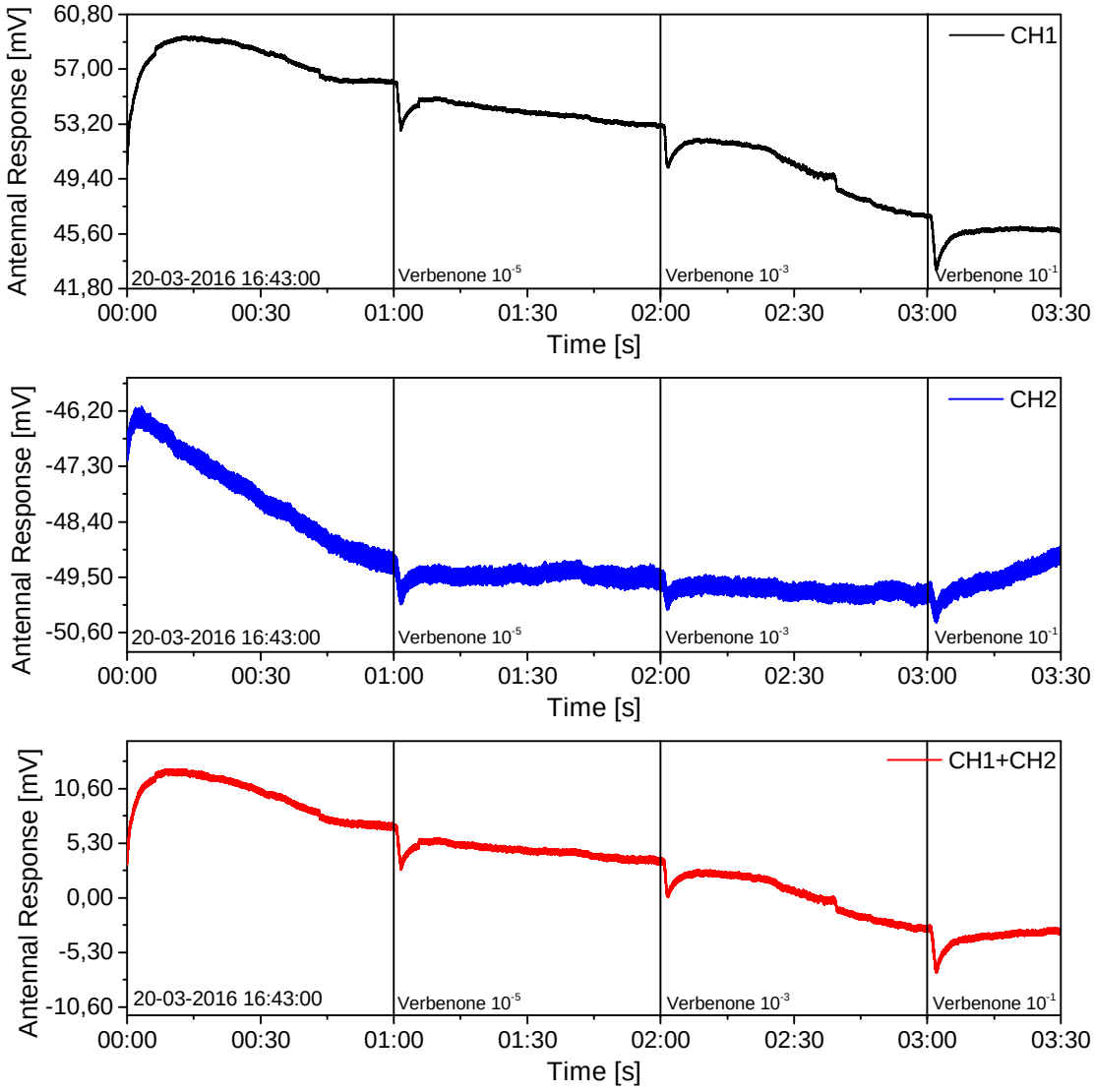

Figure 5.11: 2EC configuration, dual antenna acquisition 18-03-2016, mechanoresponse obtained by squashing stimuli delivery tube.

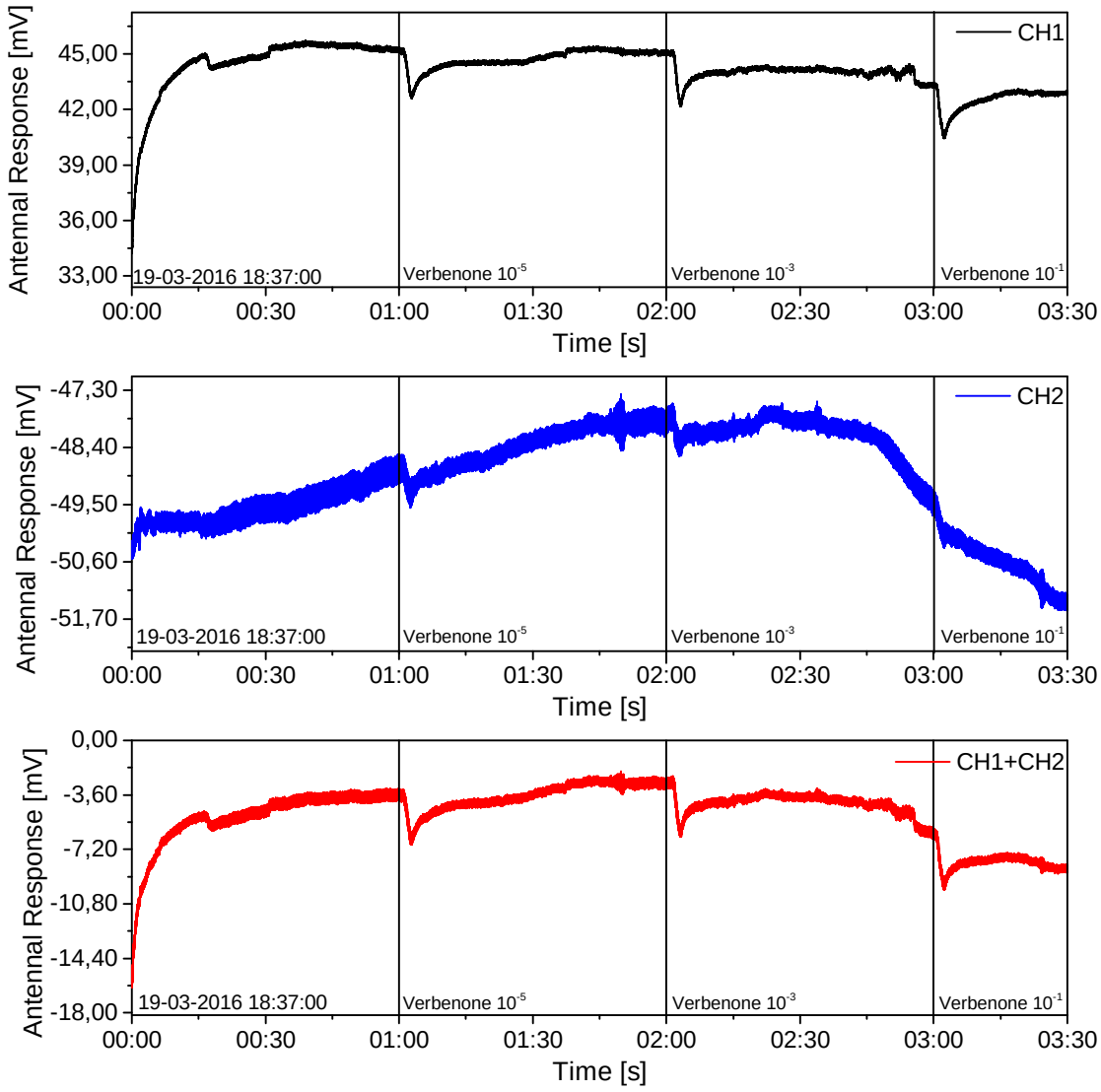

Figure 5.12: 2EC configuration, dual antenna acquisition 19-03-2016, stimuli delivery by aspiration. Dual antennae plot.

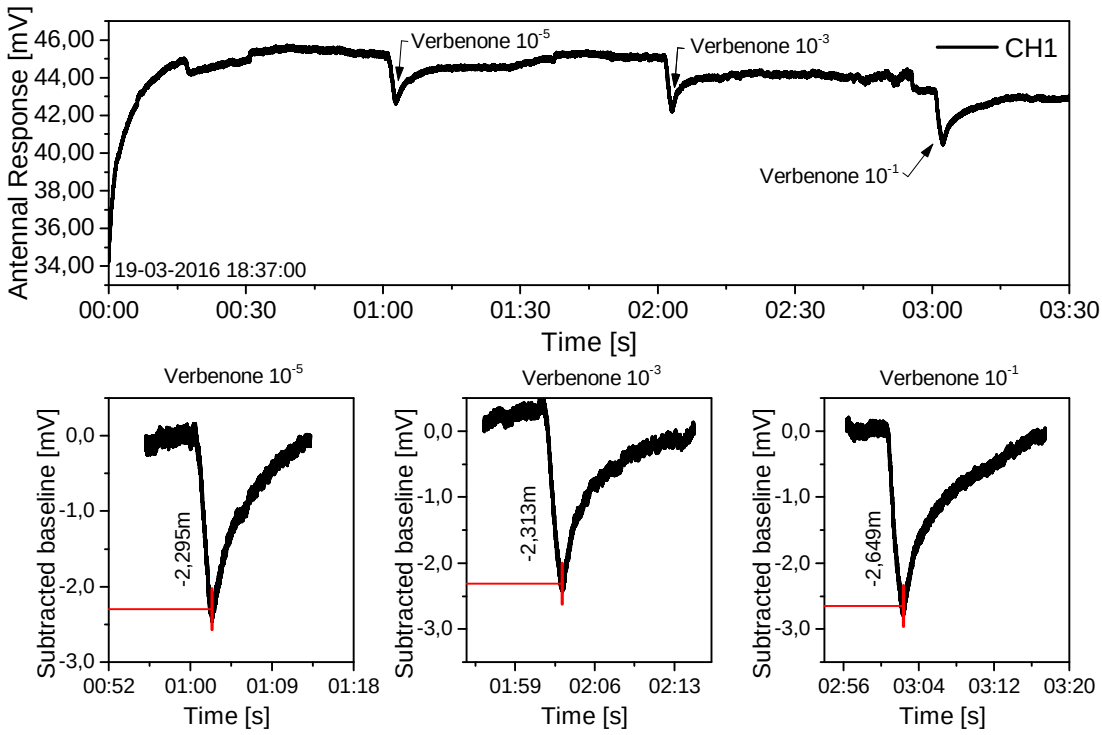

Figure 5.13: 2EC configuration, dual antenna acquisition 19-03-2016, stimuli delivery by aspiration. Peak analysis.

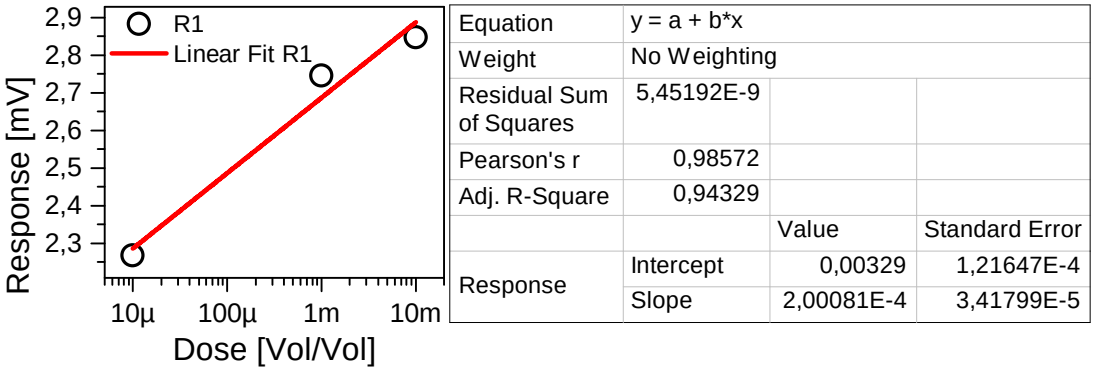

Equation	y = a + b*x		
Weight	No Weighting		
Residual Sum of Squares	5,45192E-9		
Pearson's r	0,98572		
Adj. R-Square	0,94329		
		Value	Standard Error
Response	Intercept	0,00329	1,21647E-4
	Slope	2,00081E-4	3,41799E-5

Figure 5.14: Dose-response plot. Data corresponds to figure 5.13.

Chapter 6

Conclusion

6.1 Concluding notes

This thesis explored the design and development of an electroantennographic recorder. The purpose of this recorder is to allow researchers to perform laboratory and field measurements of the insect responses to semiochemicals. The development is motivated by the evermore use of semiochemical methods to control pests, and the fact that available portable equipment to evaluate insect response is not widely available. Prior to the design of the equipment a series of requirements were established in order to shape and guide the design towards the end result. A design centered on the bio-signal measurement capability of the ADS1299 ADC was devised. Innovative means of antennae support and interfacing were included in the design. Autonomous air pumping and air source selection was also included in the design. The size of the device allows both field use and laboratory use. During the design a CFD simulation of the air flow over the antennae holder was performed showing good indications that the conditions for successful measurements could take place. Initial developments into a first iteration of a final PCB design also started. A prototype of the device was manufactured recurring to SLA printed parts and off the shelf components. Acquisition software was developed for this prototype based on Texas Instruments demonstration software. The functionality of starting and stopping the air pump and switching the distributor valve was added to the software. Due to a limitation of the software it was not possible to switch the distribution valve during an acquisition. An insect antenna simulator was devised in order to characterize the performance of the recorder, and linearity and noise were evaluated. Linearity is good, but the measurement method needs improvement to yield values that can be of calibration use. Input short noise of the device was under 1 µV. Evaluation of the device with *G. platensis* was also conducted. The insect excised

antennae were exposed to ascending dosis of verbenone, a semiochemical known to produce olfactory response. The tests were conducted using two device configurations, namely: 2EC, under this configuration the recording electrode was connected to the clava of the insect antenna and the indifferent and bias electrode to the scape; 3EC, under this configuration the recording electrode was also connected to the clava, the indifferent to the scape and the bias to a third electrode immersed in the electrolyte pool. The latter configuration used RLD noise canceling in order to reduce common-mode noise. Successful olfactory responses were measured with the 2EC configuration and the dose-response dependency was evaluated. The mechano-response response of *G. platensis* sensilla was also measured and several sample delivery strategies were evaluated in order to reduce the disturbance of the antenna. The conclusion of this evaluation was that is better to use the aspiration of the air pump to deliver the stimuli. This method proved to evoke less mechano-response. The author is confident that the performance of the device can even be further improved once the valve distributor is 100% functional and the electronics are totally enclosed in the device.

6.2 Requirements review

The following table presents a final review of the requirements. The requirements were analyzed in terms of accomplishment or compliance.

Table 6.1: Requirements review

Req. nº	**Requirement**	**Concluding notes**
1	EAG recorder shall record antennae signals for a set period of time and send them to the computer	Both the final design and the prototype implement this functionality.
3	EAG recorder shall be able to input a clean air source and a sample source and switch between the two during acquisition to isolate odor sources	The final design will implement this functionality. The valve will be controlled by the MCU allowing valve operation during acquisitions. The awareness of this limitation of the prototype led to a careful stimulus delivery and handling strategy in order to minimize unintended stimulation. (Please read notes of requirements 13 and 3.1)
6	The EAG recorder shall record two antennae independently to allow the simultaneous detection of EAG responses	Both the final design and the prototype implement this functionality.

Continued on next page

Table 6.1: (Continued...)

Req. nº	Requirement	Concluding notes
13	The control software shall be able to start and stop acquisitions, set acquisition total durations and valve opening/closing times	The final control software will implement this functionality. The prototype is able to start and stop acquisitions and the duration of the run. It is not possible to control the valve opening/closing times in the prototype. (Please read note on requirement 3.1)
1.1	The EAG recorder shall communicate through a USB interface.	The EAG recorder communicates through a USB connection. The prototype also uses USB.
2.1	The EAG recorder shall fit in an envelope of 150x150x70 mm.	The overall dimensions of the EAG recorder are 123.02 x 60.5 x 46.4 mm.
3.1	The EAG recorder shall have an internal air distribution valve.	An air distribution valve is included by design. Control of the valve during acquisitions was not implemented in the prototype. Control of the valve is only possible before acquisition begins or after the data is retrieved. This is due to a software limitation.
4.1	The target sensitivity shall be 10 µV p-p.	The linearity test lowest amplitude level of 10 µV was still detectable.
4.2	The EAG recorder shall be able to make differential measurements from 0 to 2 mV amplitude.	The tests showed that the ADS1299 is suitable for the task of measuring antennae potentials. The amplitude of the depolarization peaks can also be successfully detected with a good voltage resolution. Linearity was also evaluated on the 100 µV to 1 mV with good results.
5.1	Input referred noise shall be less than 5 µV p-p.	The measurements of conducted indicated an input referred noise of $\approx$ 1 µV in line with the ADS1299 datasheet.

Continued on next page

Table 6.1: (Continued...)

Req. nº	**Requirement**	**Concluding notes**
6.1	The antenna holder shall be able to record two channels independently.	The antennae holder can record two channels independently. Contact reliability on a first version of the holder was not satisfactory. This issue was solved by a redesign of the 3D printed part which increased the clearance to bottom contact saddles.
7.1	The antennae holder shall be designed in a way that can hold a liquid electrolyte.	The antennae holder can effectively hold liquid electrolytes, however the use of gel is recommended as it allows for a better manipulation of the holder after positioning of the antennae. (Also read note on requirement 8.1 regarding the wetting of the soldered area)
8.1	The EAG recorder shall use AgAgCl electrodes.	The manufacturing process of the AgAgCl electrodes is simple and the results obtained are acceptable, however the portion of the gold plated turrets where the electrode is soldered exhibits a buildup of an unknown white substance. This substance can be due to some unpredicted electrolytic effect. It is recommended that in future design improvements this area is not exposed to the saline solution. A better review of commercially available sintered AgAgCl electrodes should also be considered.

Continued on next page

Table 6.1: (Continued...)

Req. nº	Requirement	Concluding notes
9.1	The antennae support shall be detachable from the main device.	The antennae holder is a detachable part by design. The spring loaded contacts provide a reliable electrical contact between this part and the main unit. Given the results obtained with the three electrode biasing scheme a suggestion is made to modify this part and use the available saddle connection for other purposes (eg. temperature reading for air velocity measurement)
10.1	The antenna holder shall be enclosed by a light tight and air-tight Faraday cage.	The Faraday cage designed effectively insulates the antennae form electrical noise, external light and uncontrolled air sources.
10.2	The EAG recorder electrical ground shall be insulated from the computer ground to minimize USB line noise.	This feature was not implemented on the prototype but will be included in a final design.
10.3	The EAG recorder shall be battery powered to minimize noise.	Batteries were used on the prototype with a significant noise reduction effect, however it was also verified that noise from the USB line was also being introduced. During the tests described in chapter 5 the computer was also disconnected from the mains. The final unit will have a USB insulator to minimize the conducted noise issue (See note on requirement 10.2)
11.1	The air velocity over the antennae shall be in a range of 0 to 2 Km/h.	CFD analysis was performed and the results are within the specified range. Means of measuring flow velocity were not available to evaluate the accuracy of the simulation and are recommended as a future improvement.

Continued on next page

Table 6.1: (Continued...)

Req. nº	Requirement	Concluding notes
12.1	The EAG recorder shall have an internal air pump.	An internal air pump was included in the design. The test results obtained confirm that the pump specifications are suitable for this application. Means of minimizing pump vibration were implemented. No evidence of mechanical coupling noise on acquired signal was found.

6.3 Limitations and further work

Despite the good performance results indicating the device has potential as a research tool, there are some improvements that can be made, namely:

1. **Short term improvements**

    a) **Improvement of the antennae holder**
    The part should be modified in order restrict the electrolyte to the chlorinated portions of the electrodes, to avoid electrolysis.

    b) **Improvement of the prototype software**
    If further testing is to be conducted, the software should be modified to allow actuation of the distributor valve during acquisitions. Acquisition and visualization of the data in real-time would also be a good feature.

    c) **Calibration**
    Calibration of the device with a method similar to the one used, but using a calibrated signal source should be performed in order to validate quantitatively the results obtained.

    d) **Testing of the device with other insects**
    Testing of the device with other insects with other types of antennae should be attempted in order to compare the results obtained with published data.

2. **Medium term improvements**

    a) **Finishing of the on-board electronics**
    The design of the final electronics should be concluded in order to re-evaluate the device with the custom electronics. The finishing of the electronics also imply the development of firmware.

b) **Development of an electroantennography optimized acquisition software**
Dedicated acquisition software would be a good medium term improvement to this design. In fact it is almost unavoidable. Features such as digital filtering, automatic response detection, peak counts, automatic dose-response evaluation, etc. could be implemented.

3. **Long term improvements**

a) **Make the device completely autonomous**
The capability to record and store data internally would allow the use of the EAG recorder as a stand-alone monitoring device.

b) **Add wireless data transfer capability**
Wireless data transfer simplifies the use of the device, especially in outdoor conditions. Besides laptop computers, with the use of wireless data transfer other types of portable devices could also be used to record data (e.g. smartphones and tablets).

c) **Add flow metering capability and temperature sensing**
Flow metering and temperature sensing would be a good addition to the device capabilities, as these are parameters that can affect the results obtained.

d) **Modification to allow recording of live insects**
Extended modifications could also be made to the antennae holder to allow the recording of live insects. No portable equipment was identified with the capability of recording live insects, and its the author opinion that this should be the natural evolution of this device. The recording of live insects have the shortcoming of the undesired mechano-response signal from insect movement, but on the other hand the antennal preparation can last for several days. With this in mind the application of this device as a field monitor is feasible.

This page intentionally left blank.

Bibliography

Acharya, V. (2011). "Improving common-mode rejection using the right-leg drive amplifier." In: *Texas Instruments* July, pp. 1–11.

Arn, H., E. Stadler, and S. Rauscher (1975). "The Electroantennographic Detector — a Selective and Sensitive Tool in the Gas Chromatographic Analysis of Insect Pheromones". In: *Zeitschrift für Naturforsch.* 30, pp. 722–25.

Baigrie, B. (2003). *Taints and Off-Flavours in Food*. Ed. by B. Baigrie. CRC Press.

Beck, J. J., D. M. Light, and W. S. Gee (2012). "Electroantennographic Bioassay as a Screening Tool for Host Plant Volatiles". In: *J. Vis. Exp.* 63, pp. 1–9.

Bouwer, M. C. (2010). "Identification of volatile organic compounds from Eucalyptus detected by Gonipterus scutellatus (Gyllenhal) females by". PhD thesis. University of Pretoria.

Brown, W. L., T. Eisner, R. H. Whittaker, L Brown, and H Whittaker (1970). "Allomones and Kairomones: Transspecific Chemical Messengers". In: *Bioscience* 20.1, pp. 21–22.

Bruyne, M. de and T. C. Baker (2008). "Odor detection in insects: Volatile codes". In: *J. Chem. Ecol.* 34.7, pp. 882–897.

Cardé, R. T. (1995). "Control of Moth Pests by Mating Disruption: Successes and Constraints". In: *Annu. Rev. Entomol.* 40.1, pp. 559–585.

Cork, A., P. S. Beevor, A. J. E. Gough, and D. R. Hall (1990). "Gas Chromatography Linked to Electroantennography: A Versatile Technique for Identifying Insect Semiochemicals". In: *Chromatogr. Isol. Insect Horm. Pheromones*. Boston, MA: Springer US, pp. 271–279.

Damos, P., L.-A. Colomar, and C. Ioriatti (2015). "Integrated Fruit Production and Pest Management in Europe: The Apple Case Study and How Far We Are From the Original Concept?" In: *Insects* 6.3, pp. 626–657.

Dickens, J. C. (1984). "Olfaction in the boll weevil, Anthonomus grandis Boh. (Coleoptera: Curculionidae): Electroantennogram studies". In: *J. Chem. Ecol.* 10.12, pp. 1759–1785.

"Portable Devices for Single Sensillum (SSR) and Electroantennogram (EAG) Recording from Insect Antennae in the Field" (1994). In: *Olfaction Tast. XI*. Ed. by K. K. D.S., N. S. D.S., and D. Hisashi Ogawa M.D. Springer Japan. Chap. 16, p. 846.

Fabre, J.-H. (1916). *The life of the caterpillar / J. Henri Fabre ; translated by Alexander Teixeira De Mattos*. New York: Dodd, Mead and Company, pp. 246–278.

Garcia, A., E. Figueiredo, C. Valente, V. J. Monserrat, and M. Branco (2013). "First record of Thaumastocoris peregrinus in Portugal and of the neotropical predator Hemerobius bolivari in Europe". In: *Bull. Insectology* 66.2, pp. 251–256.

Guerrero, A., R. Murgo, and X. Martorell (1986). "An improved electroantennogram apparatus with a new automatic sample injection system". In: *Physiol. Entomol.* 11.3, pp. 273–277.

Hansson, B. (1999). *Insect Olfaction*. Ed. by B. S. Hansson. Berlin, Heidelberg: Springer Berlin Heidelberg.

Howell, J. F., A. L. Knight, T. R. Unruh, D. F. Brown, J. L. Krysan, C. R. Sell, and P. A. Kirsch (1992). "Control of Codling Moth in Apple and Pear with Sex Pheromone-Mediated Mating Disruption". In: *J. Econ. Entomol.* 85.3, pp. 918–925.

Howse, P. E., I. D. R. Stevens, and O. T. Jones (1998). *Insect Pheromones and their Use in Pest Management*. Dordrecht: Springer Netherlands.

ICNF (2013). *IFN6 - Áreas dos usos do solo e das espécies florestais de Portugal continental em 1995, 2005 e 2010*. Lisboa: Instituto da Conservação da Natureza e das Florestas, p. 34.

Ioriatti, C and G Angeli (2002). "Control of codling moth by attract and kill". In: *Bull. OILB/SROP* 25.9, pp. 129–136.

Jactel, H., P. Menassieu, F. Vétillard, B. Barthélémy, D. Piou, B. Frérot, J. Rousselet, F. Goussard, M. Branco, and a. Battisti (2006). "Population monitoring of the pine processionary moth (Lepidoptera: Thaumetopoeidae) with pheromone-baited traps". In: *For. Ecol. Manage.* 235.1-3, pp. 96–106.

Katsoyannos, B. and E. Boller (1976). "First Field Application of Oviposition-deterring Marking Pheromone of European Cherry Fruit Fly". In: *Environ. Entomol.* 5, pp. 151–152.

Keil, T. A. (1997). "Comparative morphogenesis of sensilla: A review". In: *Int. J. Insect Morphol. Embryol.* 26.3-4, pp. 151–160.

Mapondera, T. S., T. Burgess, M. Matsuki, and R. G. Oberprieler (2012). "Identification and molecular phylogenetics of the cryptic species of the Gonipterus scutellatus complex (Coleoptera: Curculionidae: Gonipterini)". In: *Aust. J. Entomol.* 51.3, pp. 175–188.

Matsumura, F., H. C. Coppel, and A. Tai (1968). "Isolation and Identification of Termite Trail-following Pheromone". In: *Nature* 219.5157, pp. 963–964.

Moorhouse, J. E. (1969). "Method for use in studies of insect chemical communication". In: *Nature* 223, pp. 1174–1175.

Mucignat-Caretta, C. (2014). *Neurobiology ofchemical communication*. Ed. by S. A. Simon. Frontiers. Research and Perspectives in Neurosciences. Berlin, Heidelberg: CRC Press (Verlag), pp. 23–57.

Myrick, a. J., K.-C. Park, J. R. Hetling, and T. C. Baker (2008). "Real-time odor discrimination using a bioelectronic sensor array based on the insect electroantennogram". In: *Bioinspir. Biomim.* 3.4, p. 19.

Nagai, T. (1981). "Electroantennogram response gradient on the antenna of the European corn borer, Ostrinia nubilalis". In: *J. Insect Physiol.* 27.12, pp. 889–894.

Nordlund, D. A. and W. J. Lewis (1976). "Terminology of chemical releasing stimuli in intraspecific and interspecific interactions". In: *J. Chem. Ecol.* 2.2, pp. 211–220.

Page, T. L. and E. Koelling (2003). "Circadian rhythm in olfactory response in the antennae controlled by the optic lobe in the cockroach". In: *J. Insect Physiol.* 49.7, pp. 697–707.

Paiva, M. R., E. Mateus, M. H. Santos, and M. R. Branco (2011). "Pine volatiles mediate host selection for oviposition by Thaumetopoea pityocampa (Lep., Notodontidae)". In: *J. Appl. Entomol.* 135.3, pp. 195–203.

Park, K. C. and T. C. Baker (2002). "Improvement of signal-to-noise ratio in electroantennogram responses using multiple insect antennae". In: *J. Insect Physiol.* 48.12, pp. 1139–1145.

Pasteels, J. and D. Daloze (2002). *Chemoecology of Insect Eggs and Egg Deposition*. Vol. 12. 2, pp. 211–212.

Patlak, M., T. Baker, M. Berenbaum, R. Carde, T. Eisner, J. Meinwald, W. Roelofs, and D. Wood (2003). "Insect Pheromones: Mastering Communication to Control Pests". In: *Beyond Discov. Path from Res. to Hum. Benefit*, pp. 1–9.

Qiu, Y. T. (2005). "Sensory and behavioural responses of the malaria mosquito Anopheles gambiae to human odours". PhD thesis, pp. 1–206.

Reis, A. R., L. Ferreira, M. Tomé, C. Araujo, and M. Branco (2012). "Efficiency of biological control of Gonipterus platensis (Coleoptera: Curculionidae) by Anaphes nitens (Hymenoptera: Mymaridae) in cold areas of the Iberian Peninsula: Implications for defoliation and wood production in Eucalyptus globulus". In: *For. Ecol. Manage.* 270, pp. 216–222.

Rützler, M. and L. J. Zwiebel (2005). "Molecular biology of insect olfaction:recent progress and conceptual models". In: *J. Comp. Physiol. A Neuroethol. Sensory, Neural, Behav. Physiol.* 191.9, pp. 777–790.

Sarton, G. (1931). "A History of Applied Entomology by L. O. Howard Review by : George Sarton". In: *Univ. Chicago Press behalf Hist. Sci. Soc.* 16.1, pp. 169–173.

Sauer, a. E., G Karg, U. T. Koch, J. J. Dekramer, and R Milli (1992). "a Portable Eag System for the Measurement of Pheromone Concentrations in the Field". In: *Chem. Senses* 17.5, pp. 543–553.

Schneider, D. (1999). "Insect pheromone research: Some history and 45 years of personal recollections". In: *IOBC wprs Bull.* 1565.

Schott, M., C. Wehrenfennig, T. Gasch, and A. Vilcinskas (2013). "Insect antenna-based biosensors for in situ detection of volatiles." In: *Adv. Biochem. Eng. Biotechnol.* 136, pp. 101–122.

Šobotník, J., R. Hanus, B. Kalinová, R. Piskorski, J. Cvačka, T. Bourguignon, and Y. Roisin (2008). "(E,E)-α-farnesene, an alarm pheromone of the termite Prorhinotermes canalifrons". In: *J. Chem. Ecol.* 34.4, pp. 478–486.

Suckling, D. M., G Karg, S. J. Bradley, and C. R. Howard (1994). "Field Electroantennogram and Behavioral-Responses of Epiphyas-Postvittana (Lepidoptera, Tortricidae) under Low Pheromone and Inhibitor Concentrations". In: *J. Econ. Entomol.* 87.6, pp. 1477–1487.

SYNTECH (2004). *Electroantennography a practical Introduction*. Hilversum, The Netherlands: Syntech, p. 29.

Takasaki, T., S. Namiki, and R. Kanzaki (2012). "Use of bilateral information to determine the walking direction during orientation to a pheromone source in the silkmoth Bombyx mori". In: *J. Comp. Physiol. A Neuroethol. Sensory, Neural, Behav. Physiol.* 198.4, pp. 295–307.

Texas Instruments (2012). *Low-Noise , 8-Channel , 24-Bit Analog Front-End for Biopotential Measurements ADS1299*.

Van Der Pers, J. N. C. and a. K. Minks (1998). "A portable electroantennogram sensor for routine measurements of pheromone concentrations in greenhouses". In: *Entomol. Exp. Appl.* 87.2, pp. 209–215.

Weissbecker, B., G. Holighaus, and S. Schütz (2004). "Gas chromatography with mass spectrometric and electroantennographic detection: Analysis of wood odorants by direct coupling of insect olfaction and mass spectrometry". In: *J. Chromatogr. A* 1056.1-2 SPEC.ISS. Pp. 209–216.

White, P. R. (1991). "The electroantennogram response: Effects of varying sensillum numbers and recording electrode position in a clubbed antenna". In: *J. Insect Physiol.* 37.2, pp. 145–152.

Whittaker, R. and P. P. Feeny (1971). "Allelochemics: Chemical Interactions between Species". In: *Science (80-.).* 171.3973, pp. 757–770.

Appendix

Antennae simulator test setups

The following figures ilustrate the test setups used for the electrical verification of the EAG recorder.

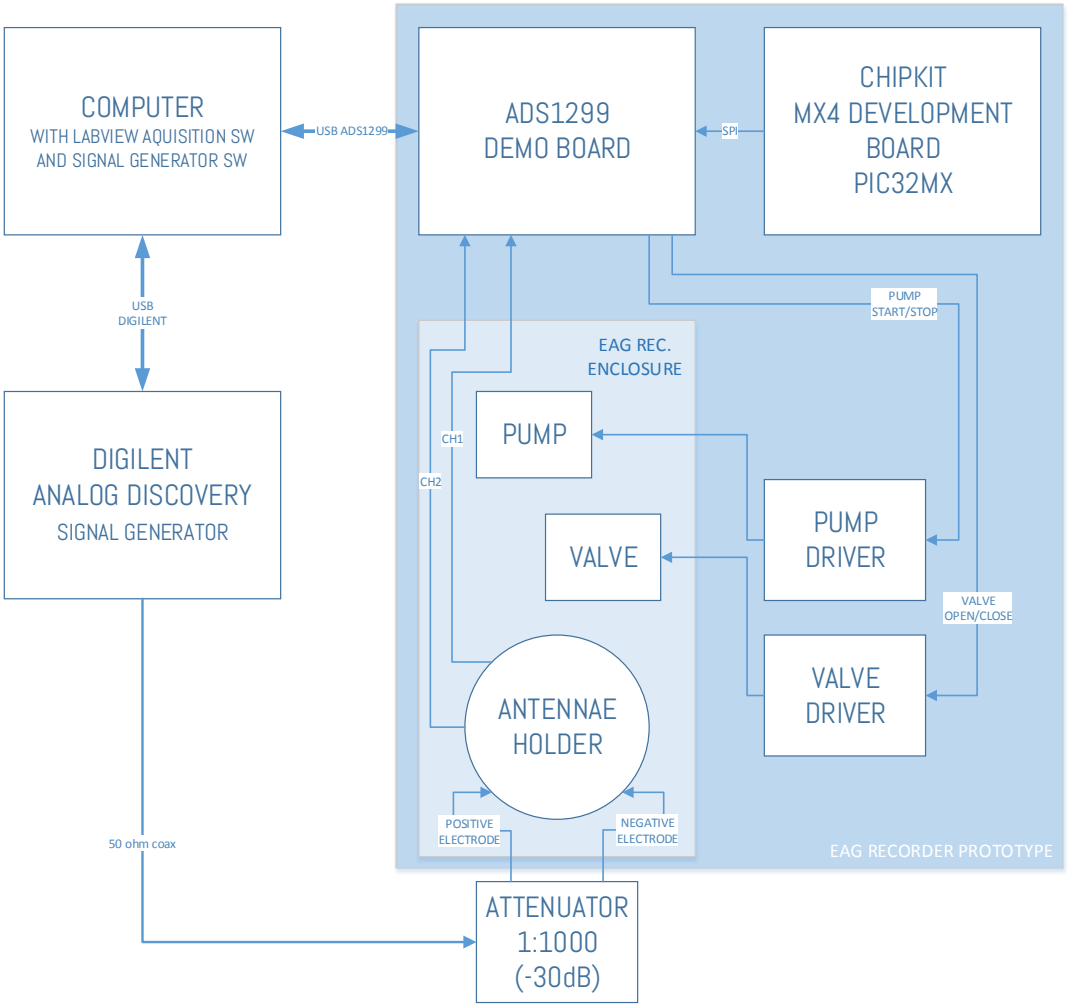

Figure A.1: Test setup for antennae simulation. This test setup is used to evaluate linearity and noise.

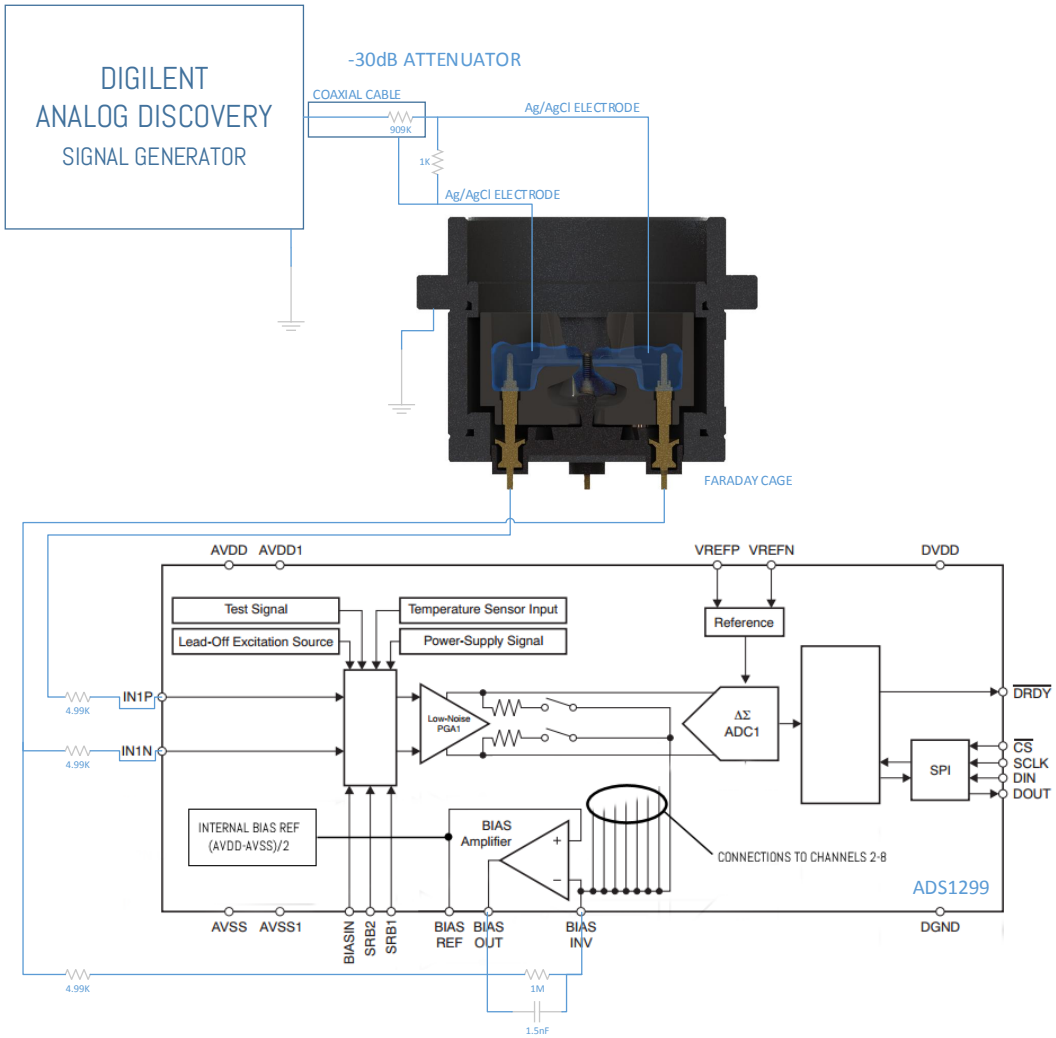

Figure A.2: Test setup used for the 2EC. Reference electrode (bias) is connected to the negative input of the ADC and configured to mid supply voltage.

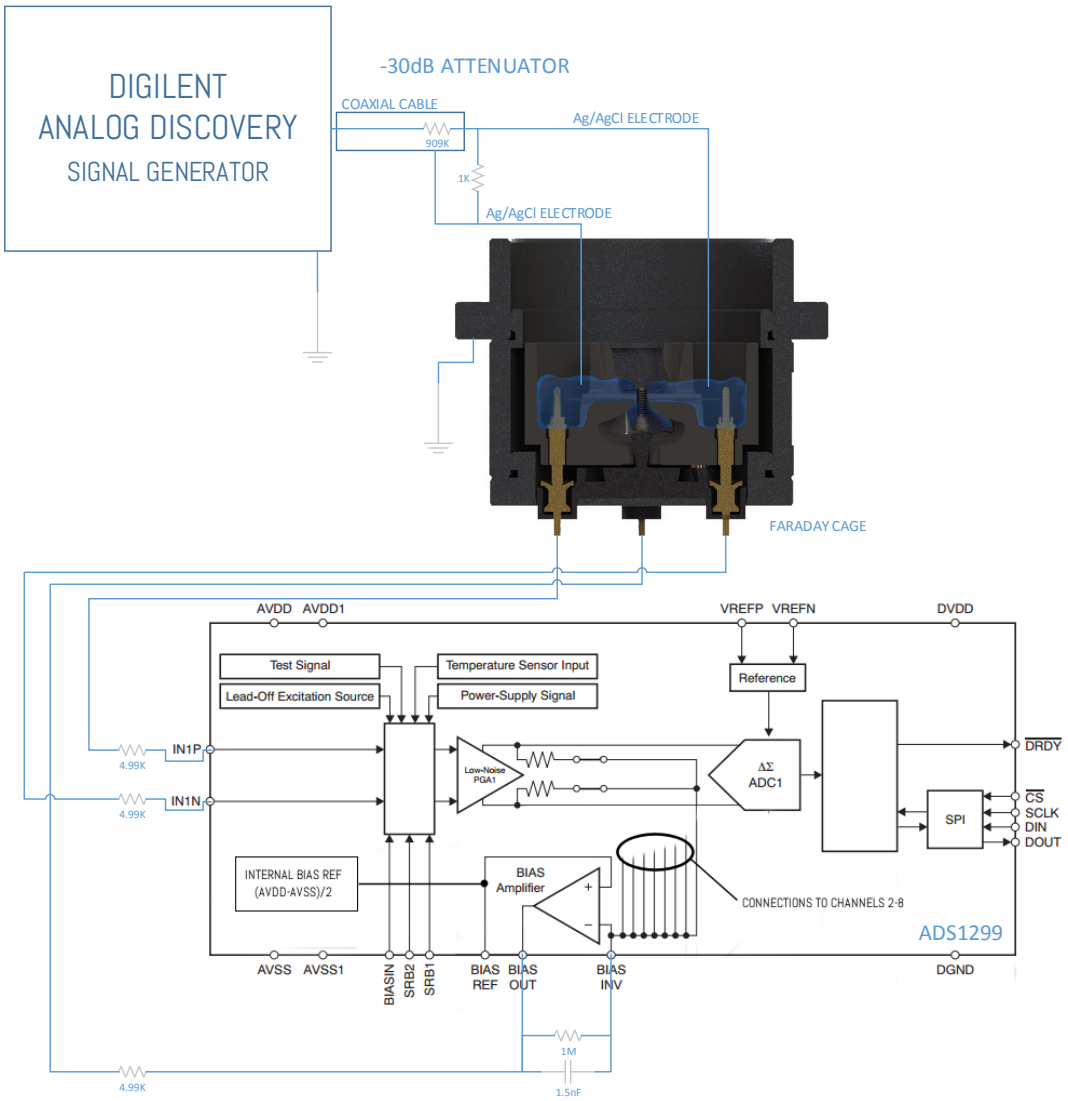

Figure A.3: Test setup used for the 3EC. Reference electrode (bias) of the ADC is connected to the antennae holder reference electrode, or third electrode. RLD feedback is taken from both ADC input electrodes